REPORT

Tonkin+Taylor

Ōpōtiki Coastal Erosion Assessment

Prepared for
Bay of Plenty Regional Council

Prepared by
Tonkin & Taylor Ltd

Date
September 2021

Job Number
1008669.2000

Exceptional thinking together

www.tonkintaylor.co.nz

Document Control

Title: Ōpōtiki Coastal Erosion Assessment					
Date	**Version**	**Description**	**Prepared by:**	**Reviewed by:**	**Authorised by:**
Feb 2020	V1	Draft for client review of methodology	Rebekah Haughey Eddie Beetham	Tom Shand	
Jul 2020	V2	Draft report with methodology review comments addressed	Rebekah Haughey	Tom Shand	
Oct 2020	V3	Final draft report	Rebekah Haughey	Tom Shand	R. Reinen-Hamill
April 2021	V4	Final draft report with additional Ohiwa Spit cell	Rebekah Haughey	Tom Shand	R. Reinen-Hamill
September 2021	V5	Final report	Rebekah Haughey	Tom Shand	R. Reinen-Hamill

Distribution:

Bay of Plenty Regional Council 1 PDF copy

Tonkin & Taylor Ltd (FILE) 1 PDF copy

Table of contents

Executive summary

The Ōpōtiki District coastline is located in the Eastern Bay of Plenty on the east coast of the North Island, New Zealand. The coastline extends approximately 130 km from Ōhiwa spit up to Cape Runaway. The coastline is characterised by a mixture of exposed sandy beaches, small embayments, rocky shore platforms, mixed sand gravel barriers and multiple rivers which supply significant quantities of sediment to the coast.

Tonkin + Taylor Ltd were commissioned by Bay of Plenty Regional Council and Ōpōtiki District Council to undertake coastal erosion hazard assessment for 13 sites within the Ōpōtiki District.

The 13 selected sites can be broadly classified into three different morphological types:

- Sandy beaches
- Mixed sand gravel beaches
  - Wide barriers backed by coastal plains
  - Narrow beaches, perched over rocky shore platforms and backed by higher banks
- River mouth/inlets shorelines

The coastal erosion hazard areas were defined using a probabilistic approach which combines standard and well-tested methods for defining erosion hazard with a stochastic method of combining erosion parameter distributions to allow for inherent statistical variance and uncertainty to be incorporated within results. Results provide a range of potential erosion hazard distances for current and future timeframes (e.g. 2070 and 2130) including different sea level rise scenarios. Erosion distances along the gravel barriers include storm overwash-induced changes in land.

Key conclusions are as follows:

- The Ōhiwa shoreline is largely influenced by significant medium-term fluctuations and spit dynamics with overall long-term stability.
- The Hikuwai to Ōpape coast tends to show an overall trend of long-term erosion.
- Majority of the mixed sand gravel barriers show long-term accretion. This is most likely a result of sediment supply from adjacent river mouths.
- The narrow, mixed sand gravel beaches tend to be more sheltered environments that show long-term stability.
- For several of the mixed sand gravel beaches where there is significant long-term accretion, the impact from long-term accretion is predicted to counteract potential recession due to SLR.
- For the large river mouths, the CEHA have been truncated at the edge of the river as there is high uncertainty in these areas, with the hazard being dominated by river processes which have not been accounted for within this assessment.

1 Introduction

The Ōpōtiki District coastline is located in the Eastern Bay of Plenty on the east coast of the North Island, New Zealand. The coastline extends approximately 130 km from Ōhiwa spit up to Cape Runaway.

Tonkin + Taylor Ltd ("T+T") has been engaged by Bay of Plenty Regional Council ("BOPRC") and Ōpōtiki District Council ("ODC") to undertake coastal erosion hazard assessment for select sites within the Ōpōtiki District. Stage 1 of the assessment included a detailed assessment of Waiōtahe Beach (Tonkin + Taylor, 2020). This report covers Stage 2 of the assessment and includes erosion hazard assessments for 13 selected sites along the Ōpōtiki coast from Ōhiwa to Whangaparaoa Bay (Figure 1.1).

1.1 Study scope

The purpose of the Ōpōtiki Coastal Erosion Hazard Assessment is to identify the magnitude and spatial extent of coastal erosion for select sites in the Ōpōtiki District. The objective is to identify areas of land exposed to coastal erosion over the long term including the impacts of projected SLR. The assessment provides Coastal Erosion Hazard Areas (CEHA) for 13 selected sites along the Ōpōtiki coast (Figure 1.1) and is based on the following scope of works:

- Assess values of components contributing to coastal erosion along the select sites
- Calculate probabilistic coastal erosion distances for the select sites using the T+T stochastic forecast methodology (Shand et al., 2015)
- Apply the coastal erosion methodology for current and future sea level scenarios in accordance with the requirements of:
  - New Zealand Coastal Policy Statement (NZCPS) 2010
  - Natural hazard provisions of the operative Bay of Plenty Regional Policy Statement (RPS) 2016
  - Bay of Plenty Regional Coastal Environment Plan (RCEP) 2019
  - Ministry for the Environment (MfE) Coastal Hazard Guidelines (2017)
- Map coastal erosion distances for present day, 50 year and 100 year timeframe for all SLR scenarios and for 50% and 5% exceedance probabilities
- Produce a technical report describing the methodology and a discussion of the results.

1.2 Report layout

The report is structured as follows:

- Coastal settings are described in Section 2
- Data sources are outlined in Section 3
- Methodologies for deriving coastal erosion hazard are defined in Section 4
- Derivation of components of coastal erosion in Section 5
- Assessment results, mapping and discussion are provided in Section 6
- Summary and recommendations in Section 7

1.3 Datums and coordinates

All elevations (levels) within this report are presented in terms of Moturiki Vertical Datum 1953 (MVD53 or Reduced Level, RL). Coordinates are presented in terms of New Zealand Transverse Mercator (NZTM).

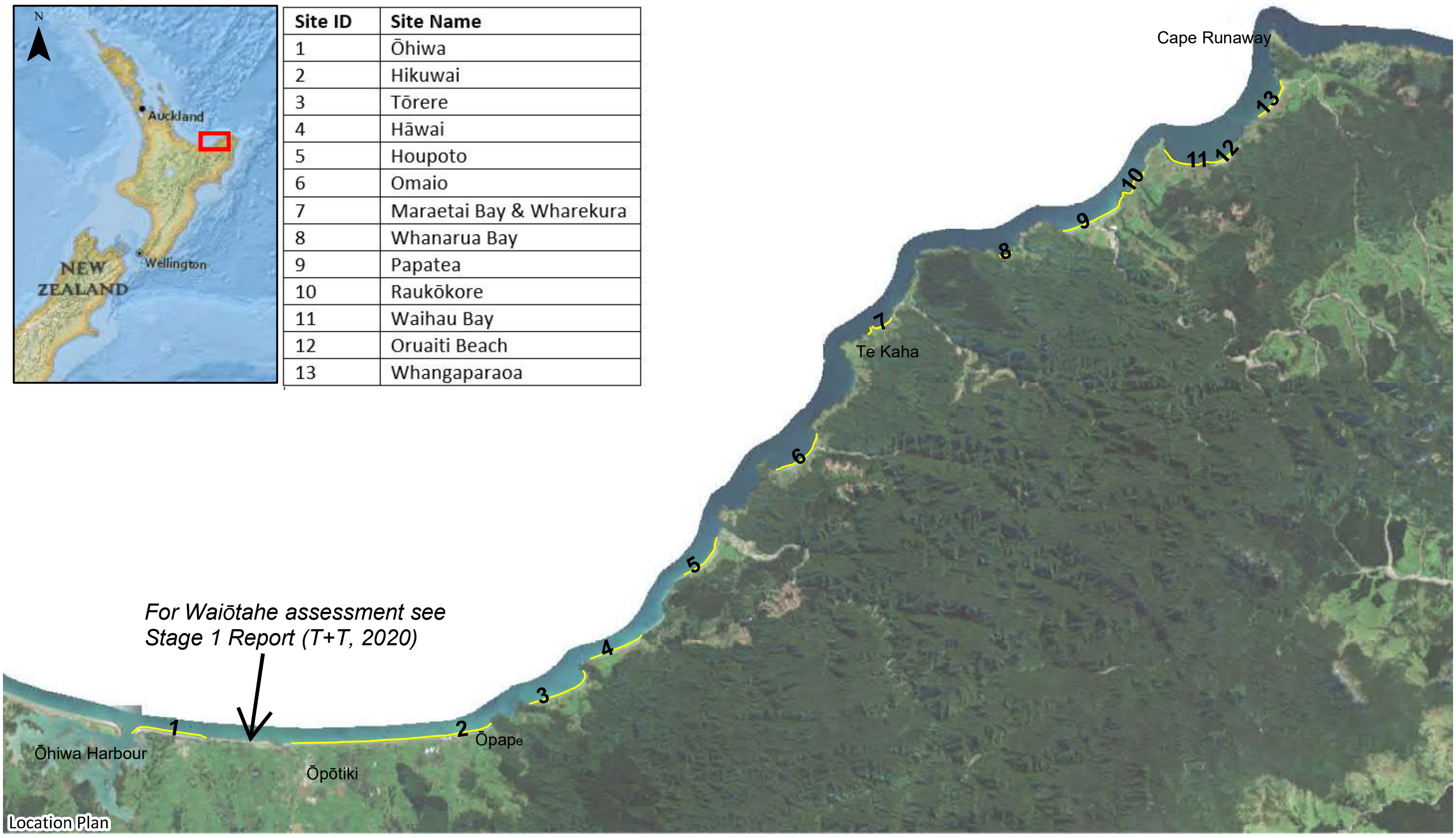

Site ID	Site Name
1	Ōhiwa
2	Hikuwai
3	Tōrere
4	Hāwai
5	Houpoto
6	Omaio
7	Maraetai Bay & Wharekura
8	Whanarua Bay
9	Papatea
10	Raukōkore
11	Waihau Bay
12	Oruaiti Beach
13	Whangaparaoa

Notes:

N

A4 SCALE 1:350,000

0 8 16 (km)

Tonkin+Taylor

105 Carlton Gore Rd, Newmarket, Auckland

www.tonkintaylor.co.nz

DRAWN	RHAU	Jan.20
CHECKED		
APPROVED		
ARCFILE Figure1_1.mxd		
SCALE (AT A4 SIZE) 1:350,000		
PROJECT No. 1008669.2000		

Ōpōtiki Coastal Erosion Assessment

Site Locations

FIGURE No. Figure 1-1

Rev. 0

Path: P:\1008669\1008669.2000\WorkingMaterial\GIS\SiteMaps\Figure1_1.mxd Date: 30/01/2020 Time: 2:45:51 PM

2 Coastal setting

2.1 General characteristics

Ōpōtiki District is located in eastern Bay of Plenty, on the east coast of the North Island, New Zealand. The coastline within the District extends approximately 130 km from Ōhiwa spit up to Cape Runaway (Figure 1.1).

From Ōhiwa Harbour to Ōpape the coastline is mostly characterised by sandy, north-facing beaches. East of Ōpape the coastline gradually curves around to predominately northwest-facing orientation. From Ōpape to Cape Runaway the coastline consists small embayments, rocky shore platforms, mixed sand gravel barriers and multiple rivers which supply significant quantities of sediment to the coast. The coast is largely unpopulated compared with other New Zealand coastal regions however there are multiple small settlements along the coast.

The 13 selected sites can be broadly classified into three different morphological types:

- Sandy beaches (for example, Ōhiwa) (Figure 2.1, A)
- Mixed sand gravel beaches
  - Wide barriers backed by coastal plains (for example, Hāwai) (Figure 2.1, B)
  - Narrow beaches, perched over rocky shore platforms and backed by higher banks (for example, Waihau) (Figure 2.1, C)
- River mouth/inlets shorelines (for example, the Raukōkore River mouth) (Figure 2.1, D)

Figure 2.1: Examples of different shoreline morphology along the Ōpōtiki coastline: (A) Sandy beach, (B) Mixed sand gravel beach, wide barrier, (C) Mixed sand gravel beach, narrow with shore platform, (D) River mouth

2.2 Geology

The headlands and rock outcrops along the Ōpōtiki coast are mostly characterised by Eastern Province sedimentary rocks containing greywacke, argillite and conglomerate. The coastal plains are predominately made of Holocene river and shoreline deposits with some of the higher banks and cliffs are composed of Middle Pleistocene shoreline deposits.

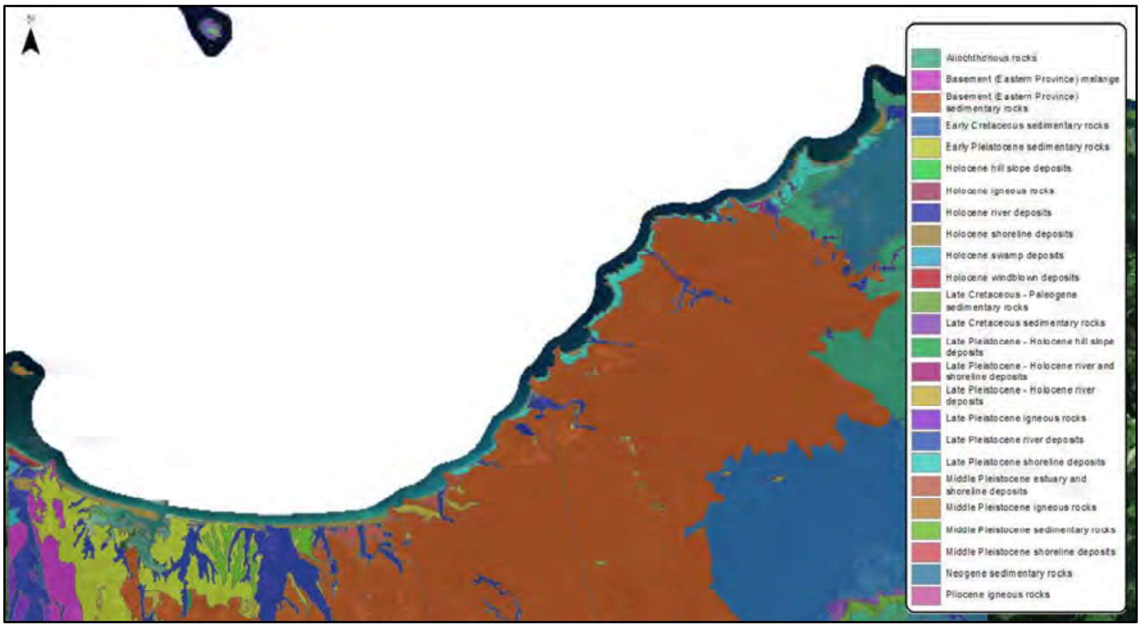

Figure 2.2: Underlying geology for the Ōpōtiki region (based on 1:250 000 Geological Map of New Zealand (QMAP)

2.3 Vertical land movement

The Bay of Plenty is a relatively rapidly deforming area located at the subduction zone of the Pacific and Australian Plates at the Hikurangi trench. Beanland & Berryman (1992) estimated the eastern Bay of Plenty to have tectonic subsidence of 0.4 to 2 mm/yr as it is associated with the Whakatāne Graben.

Beavan and Litchfield (2012) have assessed vertical land movement (VLM) around New Zealand's coastline. They found the land around Ōpōtiki to be subsiding at an average rate of 1.2 mm/yr, measured over approximately 3 years. However, due to the limited length of data we have assumed zero VLM.

2.4 Water levels

Water levels play an important role in determining coastal erosion hazard. Water levels control the amount of wave energy reaching the backshore, causing erosion during storm events and by controlling the mean shoreline position on longer time scales.

Key components that determine water level are:

- Astronomical tide
- Barometric and wind effects, generally referred to as storm surge
- Medium term fluctuations, including El Niño–Southern Oscillation (ENSO) and Interdecadal Pacific Oscillation (IPO) effects
- Long-term changes in sea level due to climate change

- Wave transformation processes through wave setup and run-up.

2.4.1 Astronomical tide

Tidal levels for primary and secondary ports of New Zealand are provided by LINZ based on the average predicted values over the 18.6 year tidal cycle. Tidal conditions within the Bay of Plenty are defined as low mesotidal to microtidal, with spring and neap tide ranges of 1.6 and 1.2 m, respectively. Values for Ōpōtiki Wharf in terms of Chart Datum and Moturiki Vertical Datum 1953 (MVD-53 RL) are presented within Table 2.1. It is assumed that these are representative of the open coast tide levels of the project area.

Table 2.1: Tidal levels given for the Ōpōtiki Wharf (LINZ, 2018)

Tide state	Chart datum (m)	(MVD-53 RL)
Highest Astronomical Tide (HAT)	2.1	1.14
Mean High Water Springs (MHWS)	1.8	0.84
Mean High Water Neaps (MHWN)	1.5	0.54
Mean Sea Level (MSL)	1.0	0.04
Mean Low Water Neaps (MLWN)	0.4	-0.56
Mean Low Water Springs (MLWS)	0.1	-0.86
Lowest Astronomical Tide (LAT)	0.0	-0.96

Source: LINZ New Zealand Nautical Almanac 2018-19

2.4.2 Storm surge

Storm surge results from the combination of barometric setup from low atmospheric pressure and wind set up from winds blowing along or onshore which elevates the water level above the predicted tide (Figure 2.3). Storm-surge applies to the general elevation of the sea above the predicted tide across a region, but excludes nearshore effects of storm waves such as wave setup and wave run-up at the shoreline.

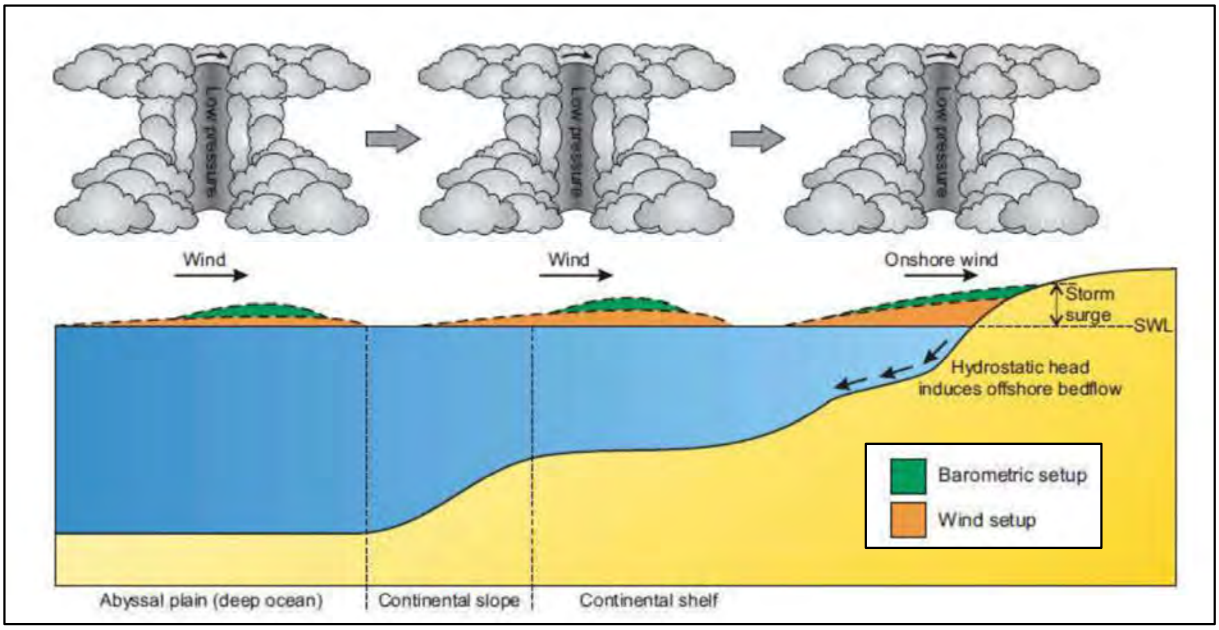

Figure 2.3: Processes causing storm surge (source: Shand, 2010)

2.4.3 Storm tide levels

The combined elevation of the predicted tide, storm surge and medium term fluctuations is known as the storm tide. The NIWA Coastal Calculator (NIWA, 2019) assesses the storm tide and wave hazard for 21 sites along the Bay of Plenty coastline. Extreme storm tide levels predicted for eight sites along the Ōpōtiki coast are shown in Table 2.2. Storm tide levels are relatively consistent across all of the Ōpōtiki sites.

Table 2.2: Extreme storm tide elevations along the Ōpōtiki coast (m above MVD-53) based on the NIWA Coastal Calculator (NIWA, 2019)

Site	Average Recurrence Interval (ARI)			
	5 year ARI	50 year ARI	100 year ARI	200 year ARI
Ōhiwa Harbour Entrance	1.29	1.76	2.06	2.41
Waiōtahe River Mouth	1.29	1.75	2.06	2.41
Ōpōtiki	1.29	1.76	2.08	2.44
Tirohanga Beach	1.29	1.77	2.09	2.45
Hāwai	1.29	1.77	2.08	2.44
Te Kaha	1.29	1.76	2.08	2.44
Papatea Bay	1.29	1.77	2.08	2.41
Whangaparaoa Bay	1.29	1.76	2.08	2.39

2.4.4 Long-term sea levels

Historic SLR in New Zealand has averaged 1.7 ± 0.1 mm/yr with Bay of Plenty exhibiting a slightly higher rate of 1.9± 0.1 mm/yr (Bell and Hannah, 2012). This higher rate may be due to the subsidence associated with the vertical land movement. Climate change is predicted to accelerate this rate of SLR into the future.

The Ministry for the Environment (2017) guideline recommends four SLR scenarios to cover a range of possible sea-level futures. The scenarios are based on the most recent IPCC report (IPCC, 2013) (Figure 2.4). Three of the scenarios (RCP2.6, RCP4.5, RCP8.5) are derived from the median projections of global SLR for the RCPs presented by the IPCC in its Fifth Assessment Report (IPCC, 2013). The fourth scenario, NZRCP8.5H+ is at the upper end of the 'likely range' (83rd percentile) of SLR projections based on RCP8.5. This higher scenario is representative of a situation where more rapid rates of SLR could occur early next century due to dynamic ice sheet processes and instability thresholds that were not fully quantified in the IPCC AR5 projections (MfE, 2017).

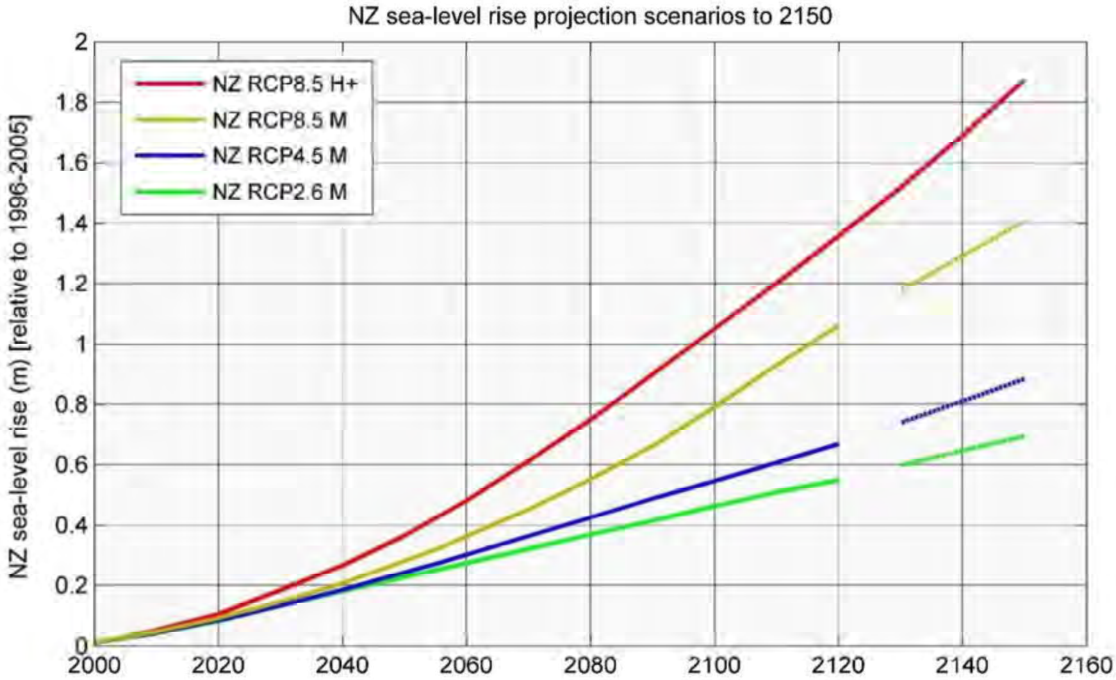

Figure 2.4: Four scenarios of New Zealand-wide regional SLR projections for use with the MfE 2017 guidance, with extensions to 2150 based on Kopp et al (2014) (Source: MfE, 2017)

2.5 Waves

The Ōpōtiki coastline is located on New Zealand's leeward east coast and therefore it is sheltered from the prevailing south-westerly wind and wave climate. Wave energy within eastern Bay of Plenty is dominated by waves from the northerly quarter which are typically associated with tropical cyclones and depressions.

Wave conditions in the Bay of Plenty are moderately influenced by the El Niño Southern Oscillation (ENSO). During La Niña periods there tends to be on average more stormy conditions which are associated with an increase in north-easterlies in the New Zealand region. During El Niño years there is a higher occurrence of south-westerlies and wave conditions in the Bay of Plenty tend to be reduced, although episodic extratopical cyclones still occur (Iremonger, 2011). Extreme significant wave heights based on the NIWA Coastal Calculator are summarised in Table 2.3. Wave heights are largest at the eastern extent of the coastline (Papatea Bay and Whangaparaoa Bay) where the shoreline is most exposed to northeasterly swell from the open ocean.

Table 2.3: Extreme offshore significant wave heights (m) based on the NIWA Coastal Calculator (NIWA, 2019)

Site	Average Recurrence Interval (ARI)			
	5 year ARI	50 year ARI	100 year ARI	200 year ARI
Ōhiwa Harbour Entrance	5.56	7.25	7.80	8.34
Waiōtahe River Mouth	5.56	7.23	7.79	8.34
Ōpōtiki	5.45	7.03	7.57	8.03
Tirohanga Beach	5.44	7.02	7.58	8.00
Hāwai	5.60	7.31	7.89	8.40
Te Kaha	6.45	8.86	9.67	10.38
Papatea Bay	7.04	9.92	10.94	11.82
Whangaparaoa Bay	7.11	10.04	11.01	11.95

2.6 Sediment sources

The Motu River is the largest catchment (total area of 1393 km^2) discharging into the eastern Bay of Plenty and is a major source of sediment to the adjacent coastline (Smith, 1986). Adams (1979) estimated the Motu River to deliver 40,000 to 120,000 m^3 of gravel to the coast annually. Hicks et al. (2011) found the River to have a mean discharge of 91 m^3/s at Houpoto and a suspended sediment yield of 3526 m^3/year. Sediment supply to the coast is likely to vary between years depending on the flow regimes.

The Motu catchment is one of the few remaining major rivers in the North Island whose catchment is relatively undisturbed and forested with native vegetation. The upper Motu catchment however does include high country farms and forestry and has potential for increased dairy farms (Ballantine and Davies-Colley, 2009). Significant changes in the catchment land use could have implications on sediment loads delivered to the coast.

There are an additional nine rivers and multiple small streams that also contribute varying volumes of sediment to the Ōpōtiki coast (Figure 2.5).

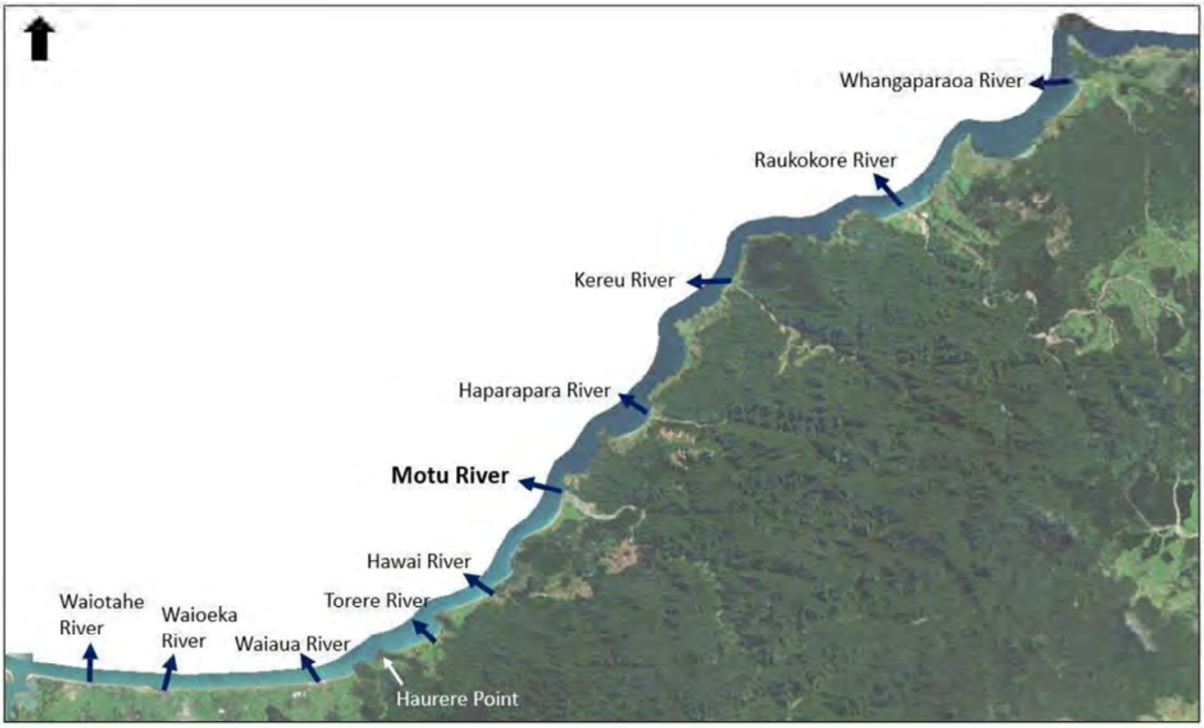

Figure 2.5: Rivers contributing sediment to the Ōpōtiki coastline

2.7 Sediment transport

2.7.1 Longshore transport

Sediment transport is multi directional along the Ōpōtiki coastline. However, there is a net longshore drift to the south-west (Smith, 1986). The dominant north-easterly wave approach is one of the key factors driving the south-westerly longshore drift. Westerly and north-westerly wave conditions occur from time to time, which can cause short-term reversals in sediment drift (Smith, 1986).

The south-westerly longshore drift results in significant volumes of sediment from the Motu River being supplied to the downdrift beaches including Tōrere and Hāwai. Gravel-sized sediment is absent from beaches immediately southwest of Haurere Point, indicating Haurere Point acts a barrier to gravel moving southwest (Ivamy & Kench, 2006). Beyond Haurere Point the beach grain size reduces further with better sorted sands towards the west suggesting longshore drift continues in a westerly direction (Smith, 1986).

While there is longshore drift, many of the gravel beaches are contained within headlands and as a result a significant portion of the sediment supplied by the rivers tends to be trapped within the embayments. Several of the beaches are backed by coastal plains with relic storm ridges which have formed over time as the beach system has prograded seaward.

2.7.2 Cross-shore transport

2.7.2.1 Sandy beaches

Sandy beaches naturally undergo periods of erosion and accretion. Erosion on sandy beaches naturally occurs when super-elevated water levels and waves remove sand offshore from the beach face and dune toe. Removal of sand from the dune toe subsequently results in scarping and instability of the dune face (Figure 2.7). The sand is typically transported offshore and deposited in the surf zone where it forms offshore bars that help absorb storm wave energy. During calmer periods of low swell sand from the offshore bar typically moves back onshore. Wind-blown sand sourced from the dry beach can then be trapped by dune vegetation which gradually results in rebuilding of the dune (Komar, 1998).

During large storms sediment can sometimes be lost from the system, either transported further offshore or alongshore which can lead to a sediment deficit and long-term shoreline erosion.

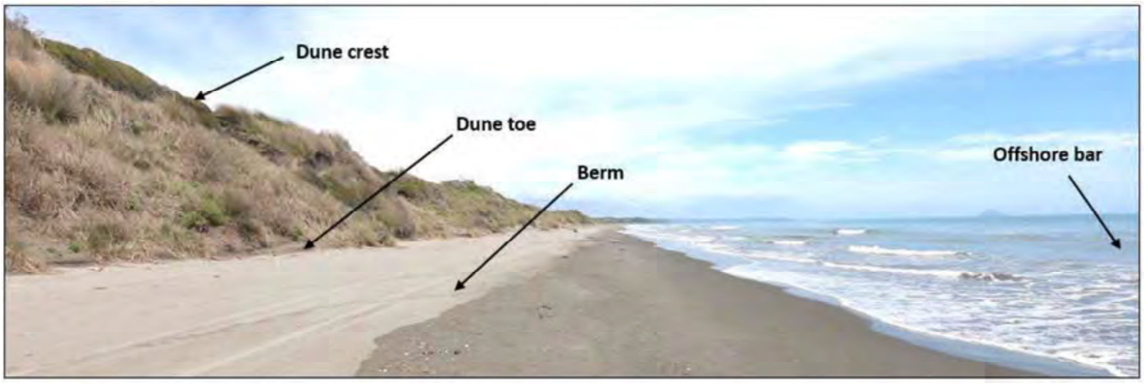

Figure 2.6: Example of key features on sandy beach profile (photo: vegetated dune at Hikuwai Beach)

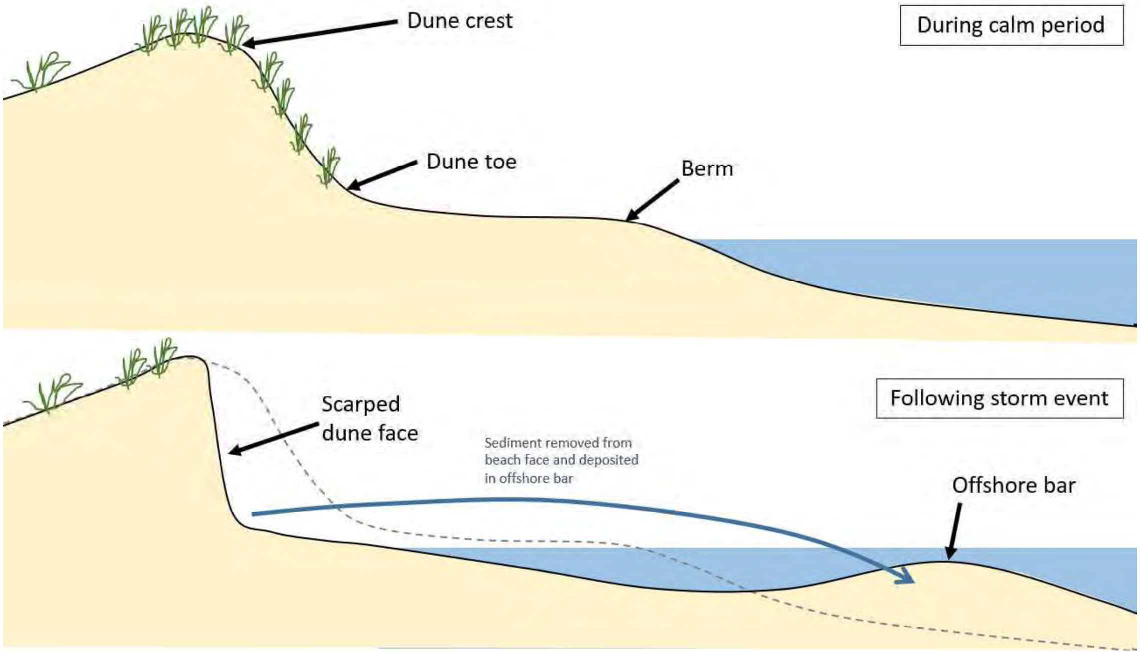

Figure 2.7: Schematic of a typical cross-section of a sandy beach

2.7.2.2 Mixed sand gravel beaches

Due to larger grain size, mixed sand and gravel beaches have different morphological features and erode via slightly different processes to a sandy beach (Figure 2.9 and Figure 2.9). Beach face erosion is less of a significant process on mixed sand and gravel beaches. Instead of beach face erosion the retreat of the shoreline is typically characterised by landward migration of the storm berm through storm-wave overwash.

The higher permeability of gravel increases the infiltration during swash uprush and subsequently the backwash volume and velocities can be considerably reduced. This process leads to the formation a high water mark berm with a steep beach face. The steeper beach face gradient allows waves to break closer onshore. During storm events the super-elevated water levels and waves extend further up the beach face and deposit material further landward, resulting in the formation of a storm berm/ridge. During severe events swash can overtop the storm berm. As the overwash dissipates, sediments are deposited on the landward side of the berm, forming a gentle backslope (Shulmeister and Rouse, 2003). This process of landward migration is the storm-wave overwash which is also sometimes referred to as storm berm "rollover" process (Dahm and Kench, 2007).

In some cases, gravel can be transported offshore by storm waves, however it does not tend to form a bar like sandy beaches but is instead deposited on the beach step. The beach step, also known as the low-tide berm, marks the lower extent of the active beach. Typically, on sand gravel beaches the gravel portion of the shoreface rarely extends below the beach step (Shulmeister and Jennings, 2009). During calm periods gravel can move back up the beach face and form small berms. The extent to which gravel can be transported up the beach face is governed by runup levels reached by waves (NCC, 2007).

Figure 2.8: Example of key features on a gravel barrier (photo: Whangaparaoa Beach)

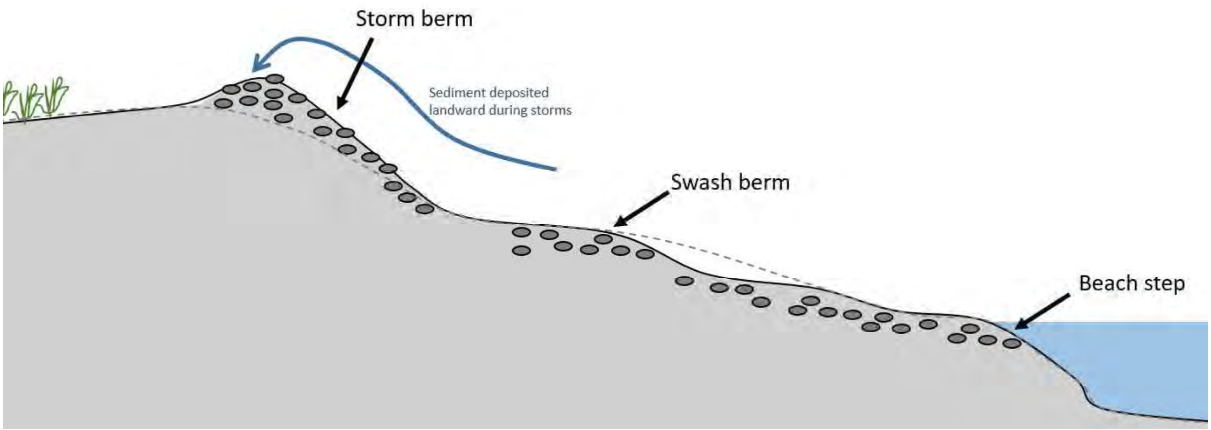

Figure 2.9: Schematic of a typical cross-section of a mixed sand gravel barrier (dashed line shows pre-storm profile, solid line shows storm profile)

2.7.2.3 Narrow mixed sand gravel beaches

The narrow mixed sand gravel beaches along the Ōpōtiki coast are characterised by nearshore rock reef with a narrow band of gravel sediment (typically less than 20 m wide) fronting higher grass embankments comprised of sand and gravel deposits (Figure 2.10).

The narrow mixed sand gravel beaches behave slightly differently to the wide mixed sand gravel barriers. These beaches are typically less dynamic. The nearshore rock reef dissipates a significant amount of the wave energy reaching the shore and sediment supply along the coast is typically less and most of the sediment is retained within the embayment.

The dynamic zone tends to be limited to the narrow gravel beach seaward of the embankments with gravel sediment rarely being washed over the grass banks. It is noted that logs and debris can often be washed over the embankments during large storms, however this is more related to the inundation extent rather than coastal erosion and movement of sediment. Observations do indicate that during large storms there is potential for water levels and waves to undercut the embankments.

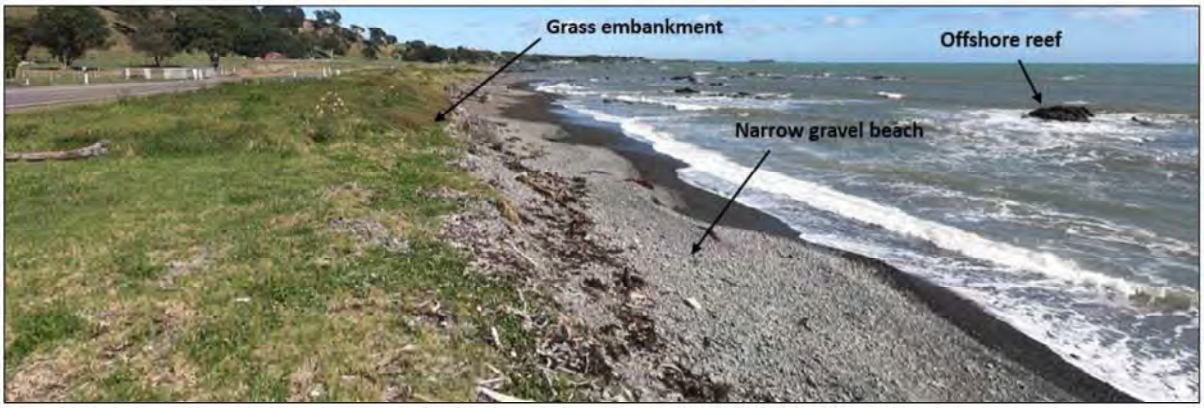

Figure 2.10: Example of key features on a narrow gravel beach (photo: Waihau Bay)

3 Background data

3.1 Previous studies

Previous coastal erosion hazard studies for the Ōpōtiki coastline include Gibb (1994), Dahm and Kench (2007) and Eco Nomos Ltd (2016).

The initial assessment completed by Gibb (1994) was a high level study to identify Areas Sensitive to Coastal Hazards (ASCH). The ASCH line was intended as a screening tool to identify areas where further coastal hazard analysis would be required.

Following the work of Gibb (1994), Dahm and Kench (2007) assessed the coastal erosion hazard in more detail for 13 priority sites. The assessment was undertaken using a combination of field investigations, analysis of historical shoreline data and community consultation. Future shoreline change with sea level rise (SLR) was accounted for in establishing areas potentially vulnerable to coastal erosion over the next 100 years. Due to limited data, Dahm and Kench (2007) adopted a precautionary approach for estimating and mapping the hazard areas with an estimated accuracy of +/- 5 m for hazard lines.

In 2016 Eco Nomos Ltd reviewed the coastal erosion hazard at the 13 priority sites. The worst likely coastal erosion was assessed for planning periods of 50 years (2065), 100 years (2115) and also 200 and 500 years. The assessment also included the potential effects of SLR based on the RCP8.5M scenario. To account for uncertainty around components contributing to coastal erosion, lower, modal and upper bound estimates were assessed for each erosion hazard scenario. The results from the review were generally similar to the Dahm and Kench (2007). Eco Nomos Ltd (2016) found that at most sites the most significant existing coastal erosion hazard is associated with semi-periodic shoreline fluctuations which typically occur over periods of 30 to 50 years. Permanent long term erosion was found to be relatively rare, although likely to increase with future SLR.

3.2 Site inspections

Site inspections were completed for all 13 beaches. Inspections were undertaken by coastal scientists in October 2019. Data collected during the site visits included shoreline observation, photographs, estimates of grain size, slope profiles using a laser level and GPS points to validate current dune toe position and vegetation edge along the shorelines. Appendix A includes the data collected at each of the sites.

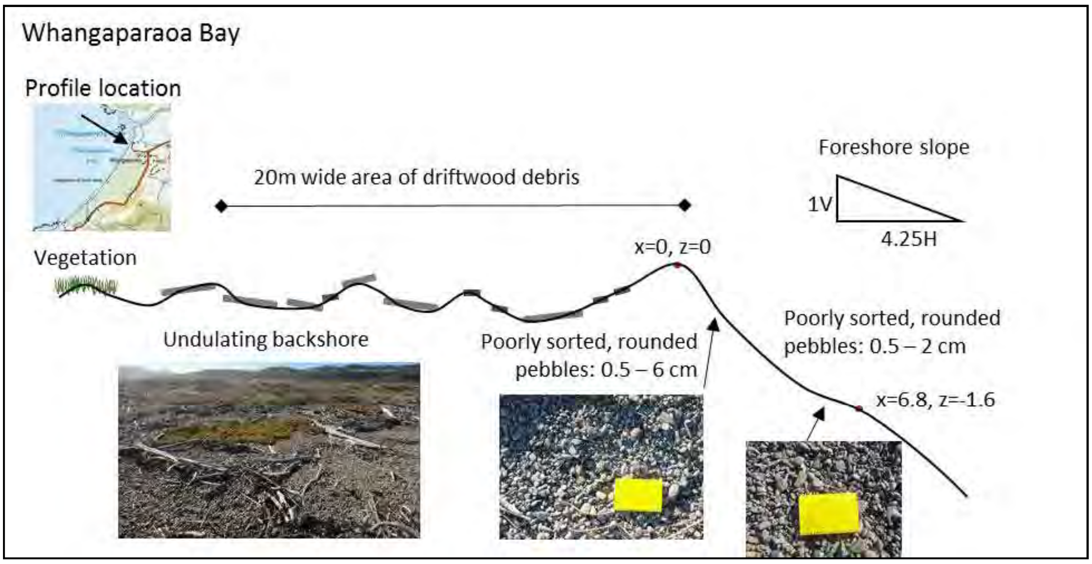

Figure 3.1: Example of beach slope and grain size information collected during site inspections

3.3 Aerial survey

An aerial survey of the Ōpōtiki coastline was undertaken in November 2019. The purpose of this survey was to obtain high resolution oblique photographs of the shorelines. The photographs provide useful information on general site characteristics for the areas of shoreline which were unable to be accessed via foot. The aeroplane was flown at an elevation of roughly 500 ft to 700 ft and typical offshore distance of 500 m. Figure 3.2 shows examples of oblique aerial photographs along the Ōpōtiki coastline during the aerial survey.

Figure 3.2: Examples of oblique aerial survey photographs taken at Ōhiwa (top left), Hāwai (top right), Maraetai (centre left), Houpoto (centre right), Waihau Bay (bottom left), Whangaparaoa (bottom right)

3.4 Topography and bathymetry

Topography has been assessed using LiDAR (Light Detection and Ranging) data sourced from Bay of Plenty Regional Council. For the beaches between Ōhiwa and Ōpape, the most recently available LiDAR data was the 2015 1 m by 1 m DEM (digital elevation model). For the beaches east from

Ōpape the most recently available LiDAR data was 2011 2 m by 2 m DEM (Figure 3.3). Bathymetry sources include the LINZ hydrographic chart (Chart NZ Cuvier Island (Repanga Island) to East Cape).

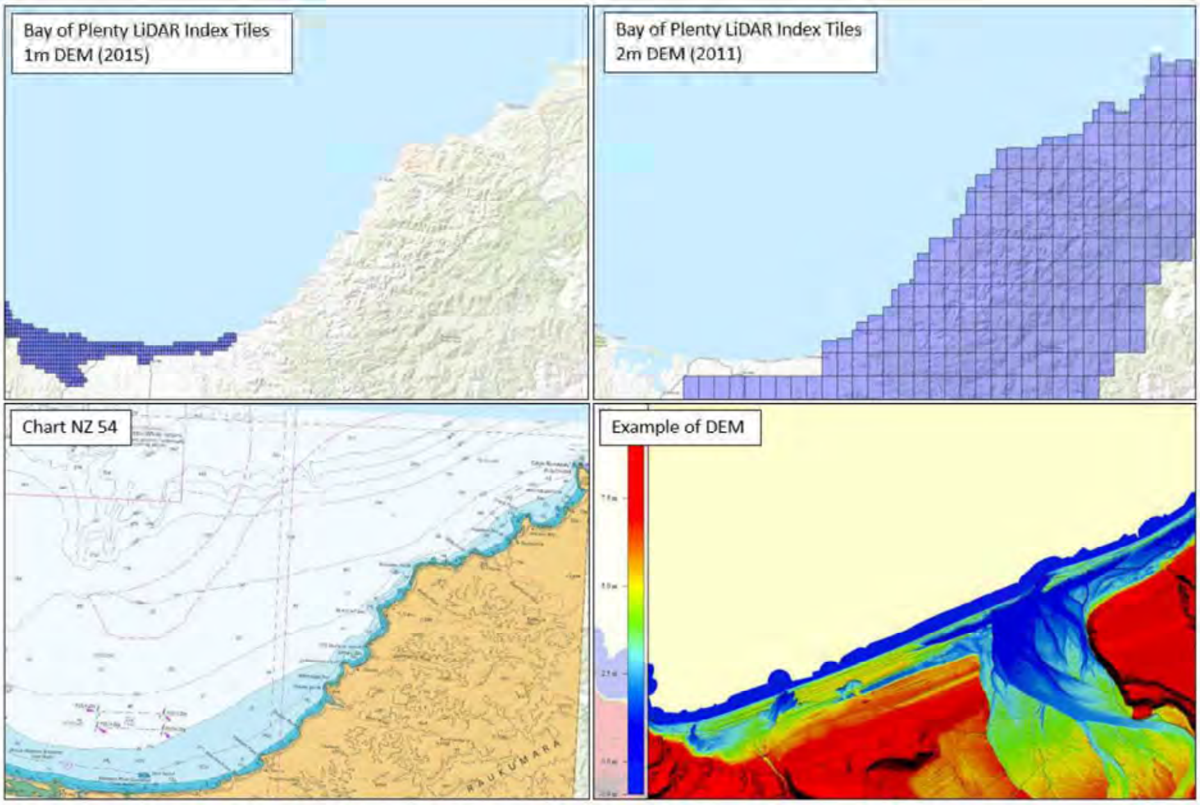

Figure 3.3: Extents and an example of LiDAR and bathymetric data used for assessment

3.5 Historic shorelines

Historic shoreline data exists from multiple sources including Coastal Resource Sheets (CRS), GPS surveys and aerial photographs.

Environment Bay of Plenty's Coastal Resource Sheets (CRS) show various historical shoreline positions fixed by cadastral surveys and mapped from historical aerial photography. The sheets were originally produced by the National Water and Soil Conservation Organisation (NWASCO) using historical shoreline information. The shoreline data typically consists of dune toe/vegetation edge lines for sandy beaches and Mean High Water Mark (MHWM) for gravel beaches.

In addition to the CRS, Environment Bay of Plenty completed a toe of dune survey in 2000 for shoreline from Ōhiwa to Ōpape. A GPS survey also exists for 1994 although there is uncertainty around what the survey represents, particularly on the gravel beaches.

Figure 3.4: Example of historic shorelines provided for Whangaparaoa Beach

The most recently available aerial varies along the coast (Figure 3.5). For Ōhiwa to Ōpape the most recently available aerial is 2015-2017. East of Ōpape to Houpoto the most recent aerial is 2010-2012 and east of Houpoto is the 2019 aerial.

A summary of the shoreline data available for each site is provided in Appendix B.

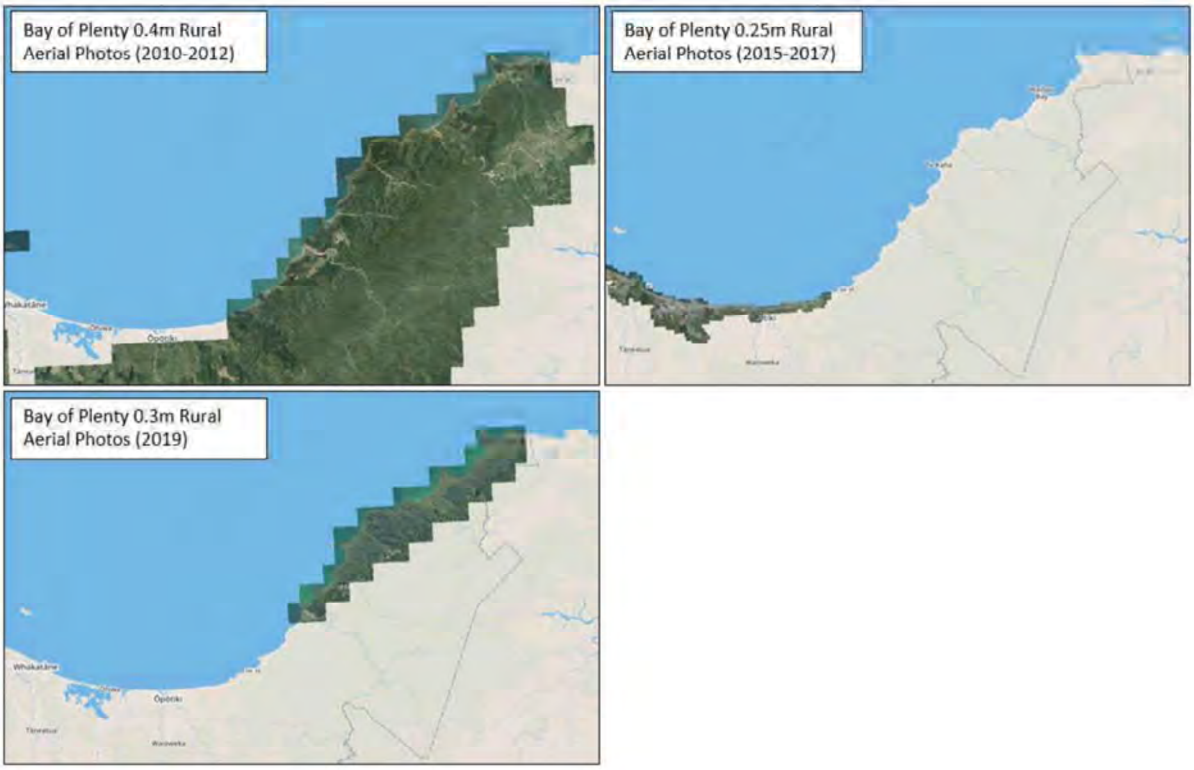

Figure 3.5: Extents of the most recent aerial photographs available for the Ōpōtiki District coastline

3.6 Beach profile data

BOPRC undertake beach profile surveys from the upper dune to approximately the mean sea level contour. BOPRC have eight profile locations between Ōhiwa spit and Ōpape which have been surveyed annually since 1990 (Figure 3.6). Two of the profiles (CCS5 and CCS6) are along Waiōtahe beach which was assessed in Stage 1 (Tonkin + Taylor, 2020). A summary of beach profile data used in this assessment is provided in Table 3.1. Beach profile plots are included in the relevant site assessments (Appendix A).

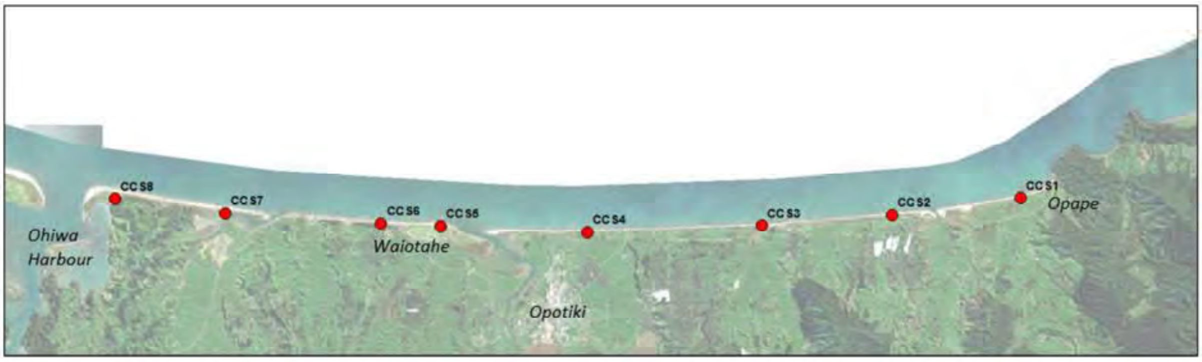

Figure 3.6: Location of beach profiles

Table 3.1: Summary of beach profile data

Profile name	Benchmark location (NZTM)		No. of surveys	Start date	Latest survey date	Years
	Easting	Northing				
CCS1	1987693	5787267	40	5/04/1990	09/01/2020	30
CCS2	1984552	5786851	42	5/04/1990	09/01/2020	30
CCS3	1981387	5786590	39	5/04/1990	09/01/2020	30
CCS4	1977133	5786436	43	5/04/1990	09/01/2020	30
CCS7	1968305	5786895	39	5/04/1990	16/01/2020	30
CCS8	5786895	5786895	34	5/04/1990	30/01/2019	29

4 Methodology

4.1 Statutory considerations

4.1.1 New Zealand Coastal Policy Statement

The New Zealand Coastal Policy Statement 2010 (NZCPS) is a national policy statement under the Resource Management Act 1991. The NZCPS states policies in order to achieve the purpose of the Act in relation to the coastal environments of New Zealand. Regional policy statements and plans must give effect to (be consistent with) the NZCPS.

A number of the objectives and policies of the NZCPS are directly relevant to the assessment of coastal erosion hazard. Relevant policies include:

- Policy 3 - requires a precautionary approach in the use and management of coastal resources potentially vulnerable to effects from climate change so that avoidable social and economic loss and harm to communities does not occur.
- Policy 24 - requires identification of areas in the coastal environment that are potentially affected by coastal hazards (including Tsunami) giving priority to the identification of areas at high risk of being affected. Hazard risks, over at least 100 years, should be assessed having regard to:
  - physical drivers and processes that cause coastal change including SLR
  - short term and long term natural dynamic fluctuations of erosion and accretion
  - geomorphological character
  - cumulative effects of SLR, storm surge and wave height under storm conditions
  - anthropogenic influences
  - extent and permanence of built development
  - effects of climate change on the above matters, on storm frequency and intensity and on natural sediment dynamics.

  These should take into account national guidance and the best available information on the likely effects of climate change for each region.
- Policy 25 - promotes avoiding an increased risk of social, environmental and economic harm in areas potentially affected by coastal hazards over at least the next 100 years.
- Policy 27 - promotes reducing hazard risk in areas of significant existing development likely to be affected by coastal hazards.

4.1.2 Regional Policy Statement

The Bay of Plenty Regional Policy Statement (RPS) outlines the Natural Hazard Policies for the region. The following Policy is relevant to this assessment:

- Policy NH 7A – Identify areas susceptible to natural hazards. Map hazard susceptibility areas (HSA) for the following natural hazards:
  - c) Coastal and marine processes
    - i) coastal erosion
    - ii) coastal inundation
- Policy NH 11B - Incorporate the effects of climate change in natural hazard risk assessment. Authoritative up-to-date projections of changes in sea level, rainfall, temperature, and storm

frequency and severity will be used as updated scientific data become available. Use the following projections as minimum values when undertaking coastal hazard assessments:

a a 100 year timeframe

b a projection of a base SLR of at least 0.6 m (above the 1980–1999 average) for activities/developments which are relocatable

c a projection of a base SLR of 0.9 m (above 1980–1999 average) for activities where future adaptation options are limited, such as regionally significant infrastructure and developments which cannot be relocated

d an additional SLR of 10 mm/annum for activities with life spans beyond 2112.

4.1.3 Operative Regional Coastal Environment Plan

The Bay of Plenty Regional Coastal Environment Plan 2019 (RCEP) manages the natural and physical resources of the Bay of Plenty coastal environment.

Chapter 6 of the RCEP covers coastal hazards and section 6.1.3 specifically details the following policies on coastal hazard for sandy coasts and river mouth shorelines.

- Policy CH 14 - Identify and map erosion and inundation zones over a 100 year timeframe in high priority areas
- Policy CH 15 – apply an appropriate method to identify the erosion extent taking into account best practice guidelines, scientific guidance and relevant components including shoreline response to SLR.

This study maps erosion in accordance with the RCEP policy above and also the RPS requirements for hazard susceptibility areas.

4.1.4 Operative Ōpōtiki District Plan

The Operative Ōpōtiki District Plan (2021) overlaps with the NZCPS as well as the Bay of Plenty RPS and RCEP. Chapter 7 covers natural hazards including coastal erosion. Policies relevant to this assessment include:

- Policy 18.2.3.1 – ensure that all Council databases on natural hazards are kept as current as possible.

4.2 Risk-based approach

A risk-based approach to managing coastal hazard is advocated by the NZCPS and endorsed by BOPRC's RPS, with both the likelihood and consequence of hazard occurrence requiring consideration. For example, the NZCPS suggests consideration of areas both 'likely' to be affected by hazard and areas 'potentially' affected by hazard. The term likely may be related to a likelihood over a defined timeframe based on guidance provided by MfE (2017). This assessment aims to derive a range of hazard zones corresponding to differing likelihoods which may be applied to a risk assessment.

4.3 Stochastic forecast approach

This study combines standard and well-tested approaches for defining coastal erosion hazard zones by addition of component parameters (T+T, 2004; 2017; 2018) over a selected timeframe. However, rather than including single values for each component and a factor for uncertainty, parameter bounds are specified for each parameter and combined by stochastic simulation based on the methods described in Shand et al. (2015). The resulting distribution is a probabilistic forecast of potential hazard zone width over a selected timeframe (Figure 4.1).

The method is based on the premise that uncertainty is inherent in individual components due to an imprecise understanding of the natural processes and due to alongshore variability within individual study cells. Stochastic simulation allows the effect of these uncertainties to be explored simultaneously providing estimates of the combined hazard extent (i.e. the central tendency) and information on potential ranges and upper limit values. This contrasts with deterministic models where the combination of individual conservative parameters with additional factors for uncertainty often result in very conservative products and limited understanding of potential uncertainty range.

The stochastic method is described in Cowell et al. (2006). The methods used to define probability distribution functions (PDFs) for each parameter are described within the parameter descriptions below. Where PDFs are not defined empirically (i.e. based on data or model results), simple triangular distributions have been assumed with bounding (minimum and maximum) and modal parameters. These triangular distributions can be constructed with very little information yet approximate a normal distribution and permit flexibility in defining range and skewed asymmetry.

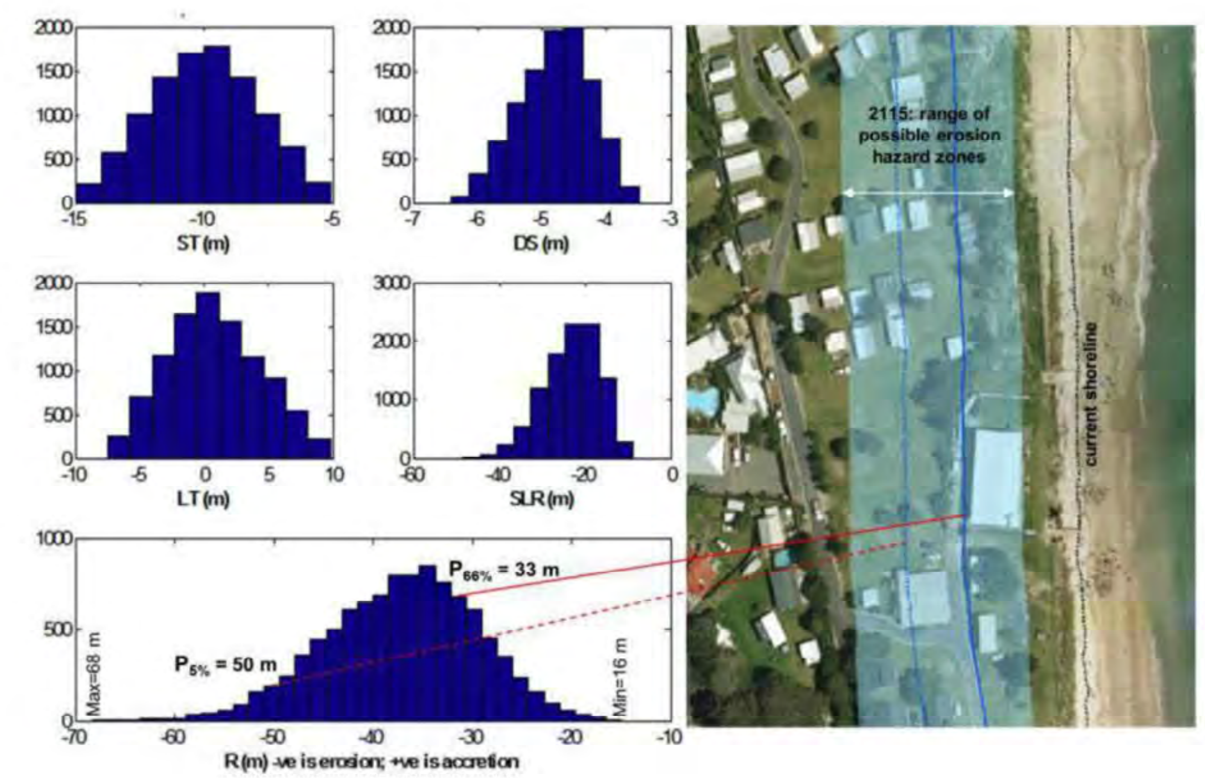

Note: CEHZ components (m): ST, LT = short-term and long-term shoreline change; DS = dune-stability factor; SLR = sea-level rise contribution to shoreline change; R = combined shoreline change used to set a CEHZ. Source: Shand et al (2014)

Figure 4.1: Example of shoreline-change components as histograms in developing a coastal erosion hazard zone (MfE, 2017)

4.4 Coastal erosion hazard methodologies

Coastal erosion hazard methodologies vary depending on shoreline types. The study sites along the Ōpōtiki coastline are characterised by a range of sand beaches, mixed sand and gravel beaches and river inlet shorelines. Large sections of the Ōpōtiki coast are also characterised by rocky shore platforms backed by consolidated banks and cliffs, however, for the purpose of this study consolidated shorelines have not been assessed. The expressions used to define the Coastal Erosion Hazard Areas (CEHAs) for the three major coastal types are presented below.

4.4.1 Sandy beaches

The method for sandy beaches is expressed in Equation 4-1. The CEHA will be established from the cumulative effect of five main parameters (Figure 4.2).

$$CEHA_{Beach} = ST + DS + MT + (LT \times T) + SLR \quad (4\text{-}1)$$

Where:

ST = Short-term changes in horizontal shoreline position related to storm erosion due to singular or a cluster of storms events or fluctuations in sediment supply and demand, beach rotation and cyclical changes in wave climate (m)

DS = Dune stability allowance. This is the horizontal distance from the base of the eroded dune to the dune crest at a stable angle of repose (m)

MT = Medium-term erosion fluctuation of the shoreline (m). This allows for shoreline fluctuations on a decadal timeframe due to ENSO or IPO effects, or changes in sediment budget, which are not included in the long-term changes

LT = Long-term rate of horizontal shoreline movement (m/yr)

T = Timeframe (years)

SLR = Horizontal shoreline retreat due to the effects of increased mean sea level (m).

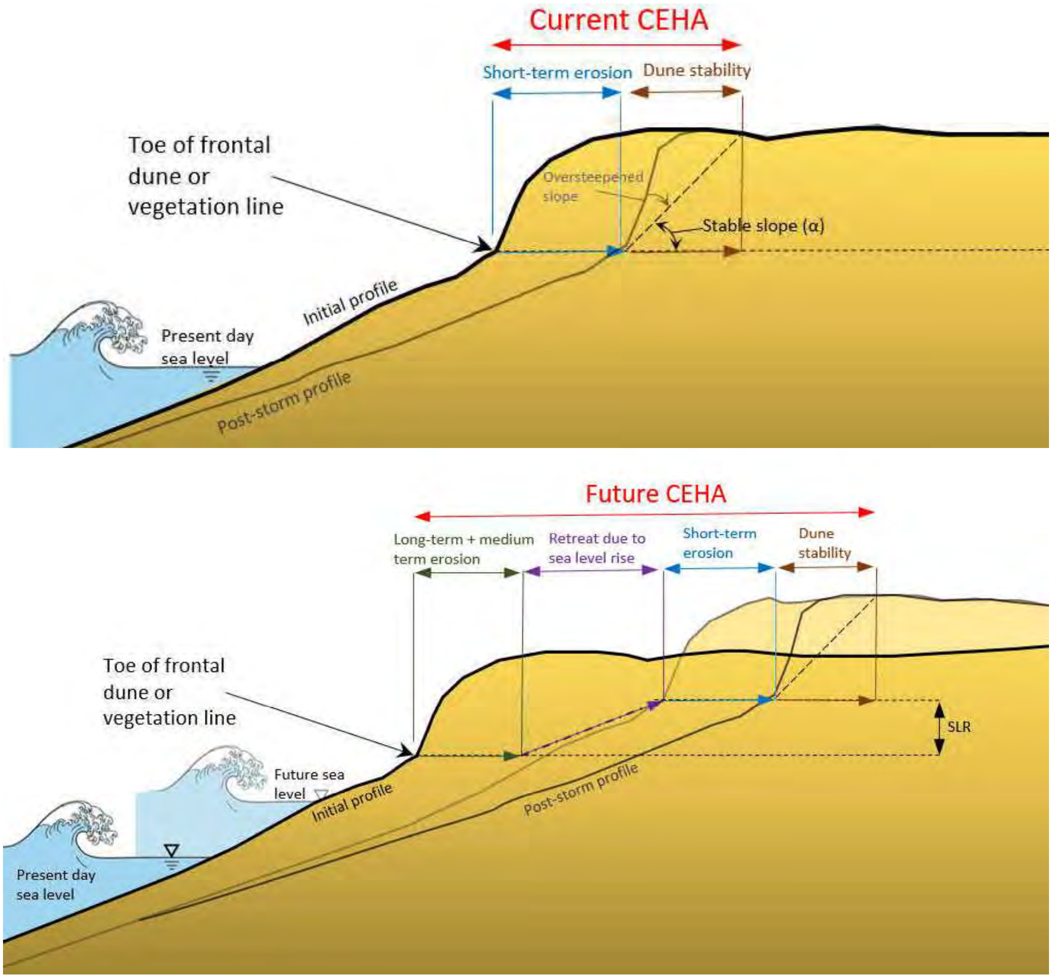

Figure 4.2: Definition sketch for coastal erosion hazard area on open coast sandy beach shoreline

4.4.2 Mixed sand gravel beaches

The methodology used for assessing the erosion hazard on mixed sand gravel shorelines is expressed in Equation 4-2. The CEHA will be established from the cumulative effect of four main parameters (Figure 4.3).

$$CEHA_{Gravel} = DZ + MT + (LT \times T) + SLR \qquad (4\text{-}2)$$

Where:

DZ = The dynamic zone. The landward extent of gravel overwash to occur during a storm event

MT = Medium-term shoreline fluctuations including movement of the storm berm following multiple storm events, potential storm ridge instability and beach rotation.

LT = Long-term rate of horizontal shoreline movement (m/yr)

T = Timeframe (years)

SLR = Roll-over due to SLR (m).

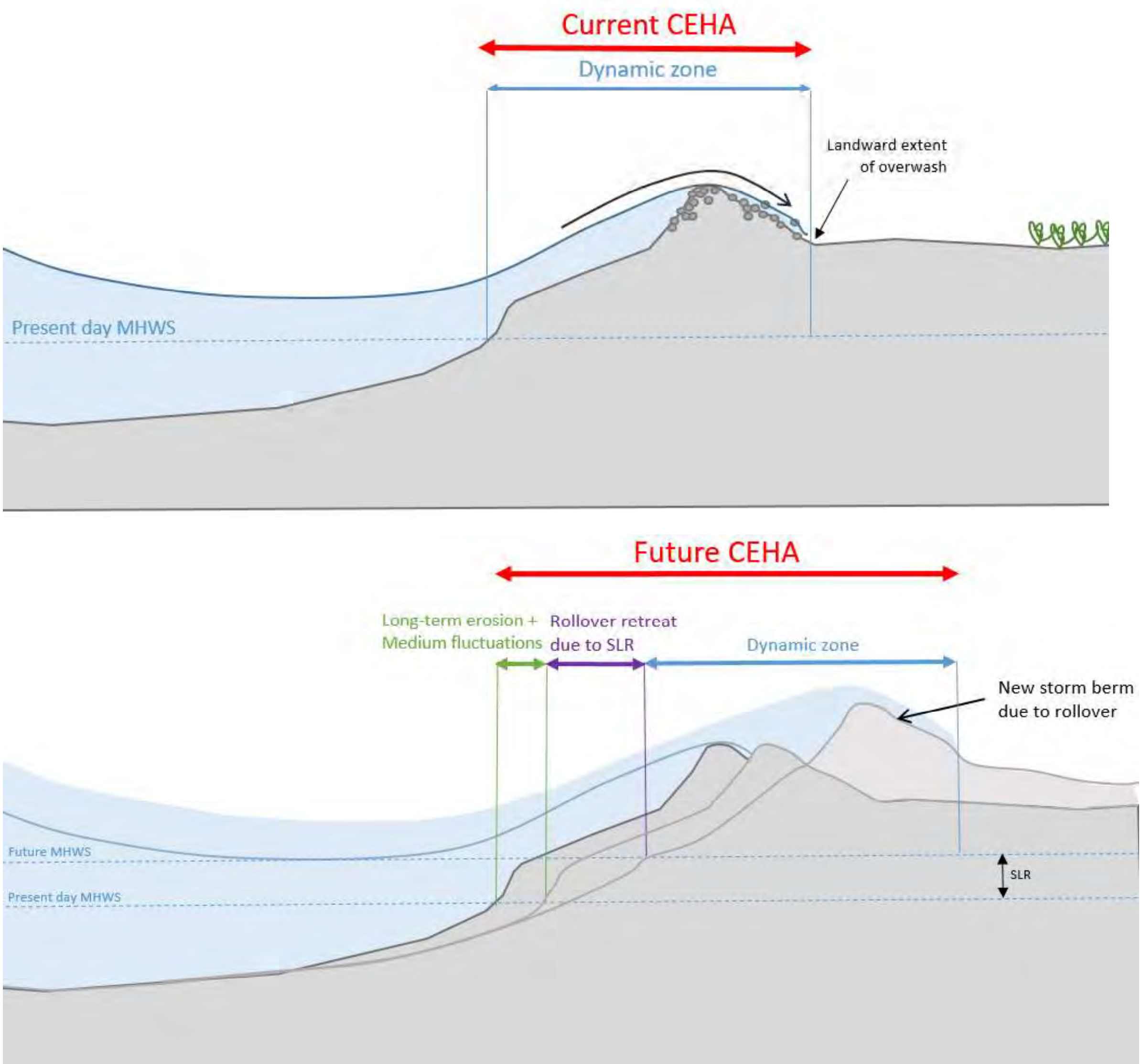

Figure 4.3: Definition sketch for coastal erosion hazard area on a mixed sand gravel beach shoreline

4.4.3 Narrow mixed sand gravel beaches

The method for narrow mixed sand gravel beaches is expressed in Equation 4-3. The CEHA will be established from the cumulative effect of four main parameters (Figure 4.4).

$$CEHA_{Beach} = ST + DS + MT + (LT \times T) + SLR \tag{4-3}$$

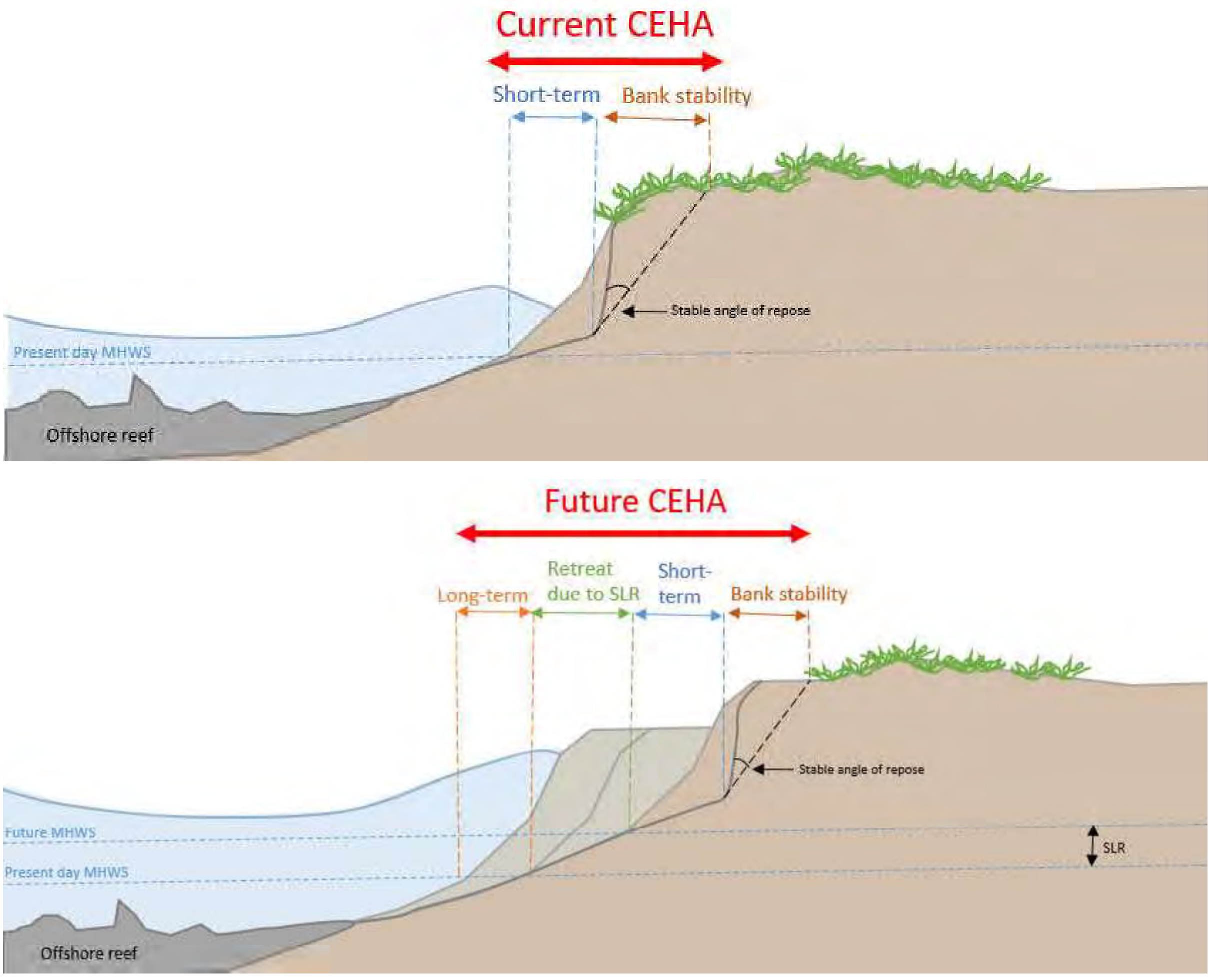

Figure 4.4: Definition sketch for coastal erosion hazard area on a narrow gravel beach shoreline

4.4.4 River/stream mouths

Shoreline movement around river/stream mouths is typically complex and highly variable in both space and time. There can be multiple factors influencing the shoreline position around river and stream mouths, including:

- Alongshore migration of river mouths and stream channels
- Changes in river flows which can either cause
  - enlargement of river mouths during flood events; or
  - contraction of river mouths during periods of sustained low flows
- Upstream channel modifications and changes in sediment loads; and
- Shifts in ebb tidal delta positions due to changes in wave conditions.

For many of the larger river mouths along the Ōpōtiki coast the shoreline directly adjacent to the river mouth is often low, highly dynamic and prone to periodic disturbance by changes in the river dynamics. For the large river mouths the CEHA have been truncated at the edge of the rivers as there is high uncertainty in these areas and the hazard is dominated by river processes (Figure 4.5). For the smaller streams, the erosion hazard has been defined based on the adjacent open coast cells.

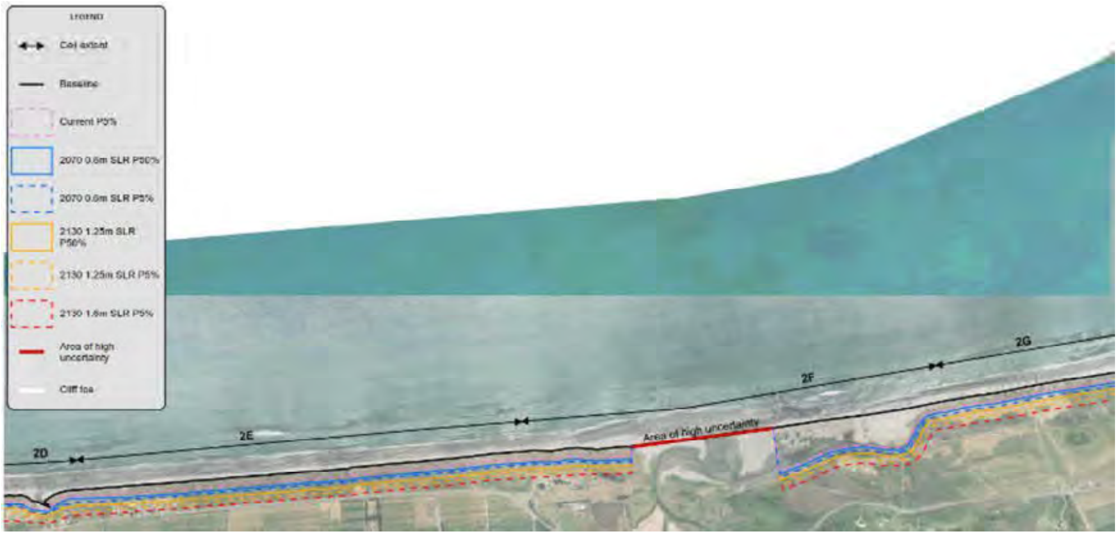

Figure 4.5: Example of CEHA mapped around the Waiaua River mouth

5 Component derivation

5.1 Baseline

The baseline is used to offset the current and future coastal erosion hazard areas. For sandy beaches the baseline is equivalent to the dune toe/seaward edge of vegetation and has been identified using a combination of the 2015-2019 aerials and the most recently available LiDAR, which for the sandy beaches (west of Ōpape) is 2015. For gravel beaches where the methodology differs, the baseline is equivalent to the high water mark as identified from the most recent available aerial which for Tōrere, Hāwai and Houpoto is 2010-2012 and for the remainder of the gravel beaches is 2019. The high water mark identified from the aerials was compared with the MHWS contour derived from the 2011 LiDAR and showed good agreement, For the narrow gravel beaches the baseline is defined as the toe of the embankment/seaward edge of vegetation.

5.2 Coastal cells

Each of the 13 sites has been divided into coastal cells based on shoreline behaviour which can influence the resultant hazard. Factors which may include the behaviour of a cell include:

- Historical shoreline trends
- Cell morphology and lithology
- Profile geometry
- Backshore elevation.

The coastal cell splits for each site and outlined in Appendix A.

5.3 Planning timeframe

Three different planning timeframes have been applied to provide information on current hazards and information at sufficient time scales for planning and accommodating future development:

- Present Day (2020)
- 50 years (2070)
- 110 years (2130).

5.4 Short-term

5.4.1 Sandy beaches (ST)

Sandy beaches undergo short-term cycles of storm-induced erosion (i.e. storm cut) followed by periods of re-building. Where a coast experiences shoreline erosion (i.e. landward movements) due to single or clusters of storms, the short-term erosional component of the cycle needs to be accounted for in any coastal hazard assessment. The post-storm recovery, or accretional part of such cycles, does not need to be accounted for in this short-term (storm cut) component. This is because short-term accretion is not a local coastal hazard. Long-term trends in accretion should already be accounted for in the long-term shoreline trend component (refer to Section 5.7).

The short-term storm cut of the dune toe was assessed using inter-survey erosion distances measured from the beach profiles (see Section 3.6). Based on visual inspection of the beach profiles the dune toe level was estimated to be around 2 m RL. The inter-survey erosion distance is the landward horizontal retreat distance at the dune toe, measured between two consecutive surveys (i.e. distance between excursion distances). An example of the measured excursion distances over time for profile CCS1 at Ōpape (Hikuwai) is provided in Figure 5.1. Figure 5.1 shows that while the beach has experienced net accretion, the shoreline fluctuates over time. The largest inter-survey storm cut measured at CCS1 was 40 m during 2007. In some cases where there are relatively long periods between surveys, the dataset may not represent the largest excursion that may have occurred between the surveys and on the other hand the distances could be a result of multiple storms that occurred within the survey period. However, the data set provides the best source of information to analyse. We note that historically BOPRC have collected post storm surveys and therefore the existing dataset is likely to include some of the largest excursion distances.

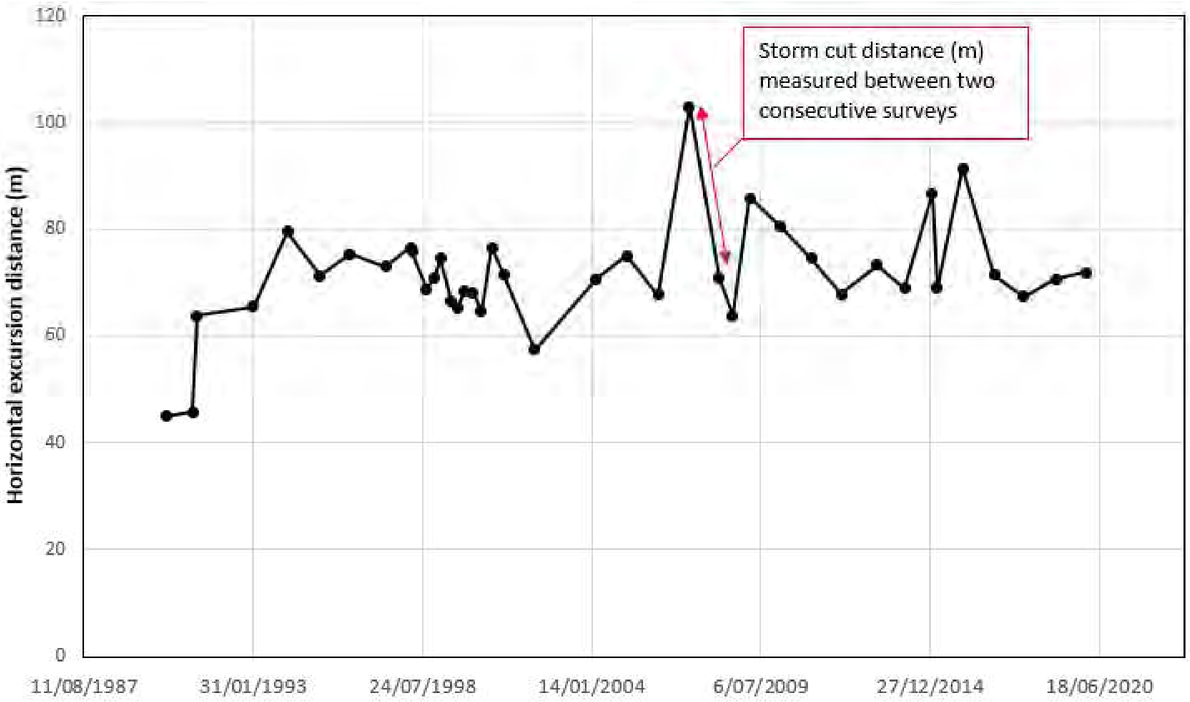

Figure 5.1: Example of excursion distance of dune toe over time at profile CCS1 Ōpape

In order to estimate the short-term erosion distances for larger return periods, which may not be captured within the profile dataset, extreme value analyses were undertaken for each profile location separately by including all the inter-survey erosion distances. Analyses were undertaken using the methods described in Mariani et al. (2012) using toolboxes provided in WAFO (2012). The extreme value curve using the Weibull method was found to reasonably fit the observed datasets and was therefore adopted. Figure 5.2 presents an example of the extreme value curve for profile CCS1.

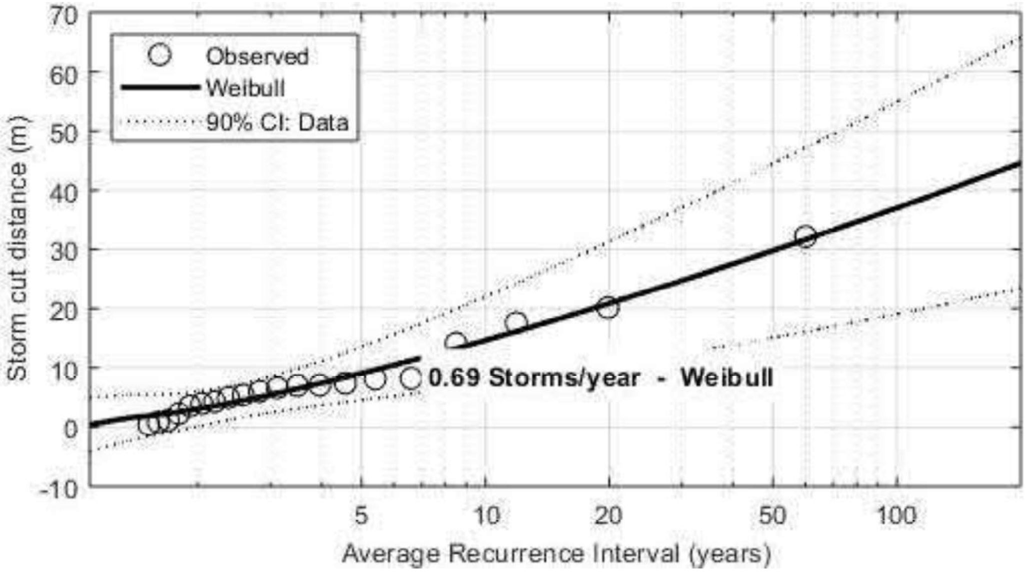

Figure 5.2: Example of extreme value curve for profile CCS1

The short-term storm cut distribution for each coastal cell is based on the erosion distances and related return periods derived from the extreme value curves for each profile. The short-term timeframe for this assessment is taken to be 10 years. Therefore the short-term erosion distances and corresponding Annual Recurrence Intervals (ARIs) have been related to percentages of likelihood and probabilities of exceedance within a 10-year timeframe (Table 5.1).

Table 5.1: Potential storm cut distances (m) and likelihood percentages for Annual Recurrence Interval (ARI) events over a 10-year timeframe

ARI		**5**	**10**	**20**	**50**	**100**	**200**
Probability of event occurrence within 10 years		**87%**	**63%**	**39%**	**18%**	**10%**	**5%**
Ōpape	CCS1	9	15	21	30	37	45
Tirohanga	CCS2	9	13	17	22	25	28
Tirohanga	CCS3	11	15	18	22	25	27
Hikuwai	CCS4	13	18	22	26	30	33
Waiōtahe Spit	CCS7	5	9	13	17	21	25
Ōhiwa Spit	CCS8	17	35	55	86	111	138

The adopted short-term component values for each of the site sandy beach sites is provided in Appendix A. The lower, mode and upper bounds are assumed to equate to 5 year, 50 year and 200 year ARI events (87%, 18% and 5% likelihood of occurring over 10 years).

For the unconsolidated harbour shoreline along Ohiwa Spit, there is no profile data to assess the short-term storm cut. Subsequently a semi-process based numerical model has been used to assess the storm cut along the harbour shoreline. The numerical cross-shore sediment transport and profile change model SBEACH (Storm Induced BEAch CHange) (Larson and Kraus, 1989) has been used to define storm cut volumes and horizontal movement of the dune toe. SBEACH considers sand grain size, the pre-storm beach profile and dune height, plus time series of wave height, wave period and water level in calculating a post-storm beach profile. Model development involved extensive calibration against both large scale wave tank laboratory data and field data. SBEACH has been verified for measured storm erosion on the Australian east coast (Carley, 1992; Carley et al. 1998).

Although this study involves an estuary environment instead of the open coast, the overall processes and input for SBEACH are still applicable.

Model input

A representative cross-shore profile from the beach ridge crest to 400 m offshore was assessed using the 2015 LiDAR. Design storm tide water level time series with a uniform wave height and period were applied at the outer profile boundary. The fetch-limited wave height was calculated based on wind speeds from the New Zealand design wind standards (AS/NZS 1170.2:2011). Based on the 3 km fetch from the south, the fetch-limited wave heights ranged from 0.9 m to 1.1 m for 5 year to 100-year wind speeds. Storm tide levels were based on the extreme sea level estimates from the NIWA Coastal Calculator (Table 5.2). Design storms for 5 year, 50 year and 200 year Average Recurrence Interval (ARI) events were simulated. Grain size characteristics were based on field observations.

Table 5.2: Summary of storm tide levels and wave heights used to assess storm cut along the harbour shoreline at Ohiwa Spit

Average Recurrence Interval (ARI)	Storm tide level (m MVD-53)	Fetch-limited wave height (m)	Fetch-limited wave period (s)	Storm cut (m)
5 year ARI	1.29	0.9	3	1
50 year	1.79	1	3	4
200 year ARI	2.41	1.1	3	6

Model results

SBEACH assumes an equilibrium profile concept which instantly responds to the present wave forcing conditions and calculates an equilibrium profile based on that forcing. Figure 5.3 shows the initial and equilibrium profiles formed due to 5, 50 and 200 year ARI storm conditions along the Ohiwa Harbour shoreline.

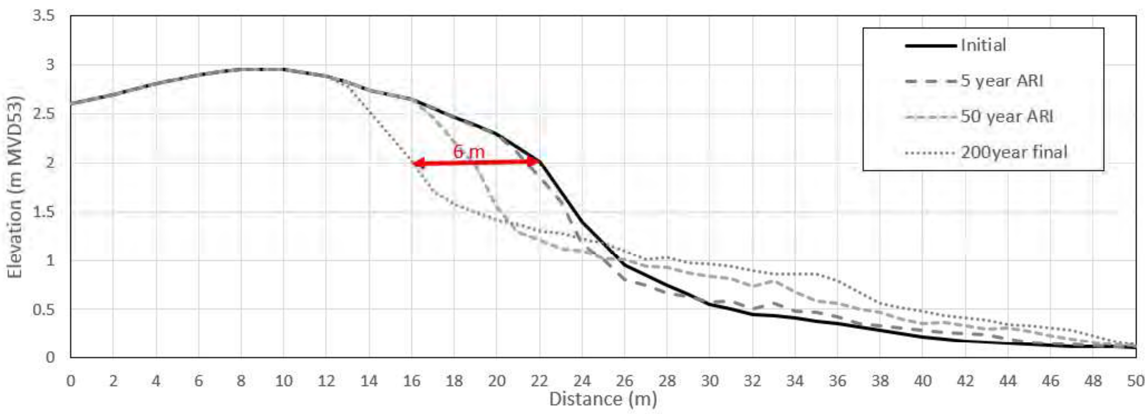

Figure 5.3: Example SBEACH results for the harbour shoreline at Ohiwa Spit. The horizontal distance between the initial profile and the 200 year ARI at the 2 m contour is shown as 6 m.

5.4.2 Mixed sand gravel beaches (DZ)

Mixed sand and gravel beaches can be very dynamic over short time periods with the high tide and storm berms shifting in response to varying tide and wave conditions (Ivamy and Kench, 2006). For this assessment the dynamic zone along the mixed sandy and gravel beaches has been defined as the width of the modern storm barrier which is from the high water mark to the landward extent of storm barrier overwash deposits. We have assessed the width of the dynamic zone using numerical modelling with design storm conditions and have validated against field observations.

The numerical process-based model X-Beach-Gravel (G) has been used to define the extent of gravel overwash. X-Beach-G is intended as a tool to assess the natural coastal response during time-varying storm conditions including beach face erosion, overwash and breaching, by solving the depth averaged non-linear shallow water equations (McCall et al., 2014). These equations are forced by a time-dependent wave action balance that is solved on time-scale of wave groups. In this way the swash motion due to infragravity waves that are forced by the wave group can be simulated. The X-Beach-G model covers in particular grain size, hydraulic conductivity (k), bottom aquifer (d_k) and ground water level (GWL) to accurately simulate the flow through the permeable gravel beach.

Model input

A representative profile for each of the mixed sand gravel beaches was used to assess the extent of overwash. The profiles were derived from a combination of the 2011 LiDAR and LINZ hydrographic charts.

Design storm nearshore time series including wave height, period and water level were applied at the outer profile boundary. The storm tide level and offshore wave heights applied for each site are presented in (Table 5.3). Appendix F provides a summary of the sensitivity analysis completed to determine appropriate water level and wave height combinations based on outputs from the NIWA Coastal Calculator. Design storms have been simulated for 5 year, 50 year and 200 year ARI events.

Table 5.3: Peak storm tide levels and offshore wave heights used to simulate design storm conditions (source NIWA, 2019)

	5 year ARI		**50 year ARI**		**200 year ARI**	
Site	**Storm tide (m MVD-53)**	**Offshore wave height (m)**	**Storm tide (m MVD-53)**	**Offshore wave height (m)**	**Storm tide (m MVD-53)**	**Offshore wave height (m)**
Tōrere	1.05	4.75	1.26	6.23	1.47	7.37
Hāwai	1.05	4.75	1.26	6.23	1.47	7.37
Houpoto	1.05	4.75	1.26	6.23	1.47	7.37
Ōmaio Centre	1.02	5.46	1.26	7.34	1.58	8.74
Ōmaio West (*0.7)	1.02	3.82	1.26	5.14	1.58	6.12
Wharekura	1.02	5.46	1.26	7.34	1.58	8.74
Papatea	1.02	5.87	1.26	8.1	1.47	10.02
Whangaparaoa	1.01	5.95	1.27	8.12	1.57	9.95

Model results

Figure 5.4 provides an example of the outputs from the XBeach-G model for Hāwai. The example shows that for 50 year ARI event the dynamic zone extends approximately 80 m landward of the MHWS.

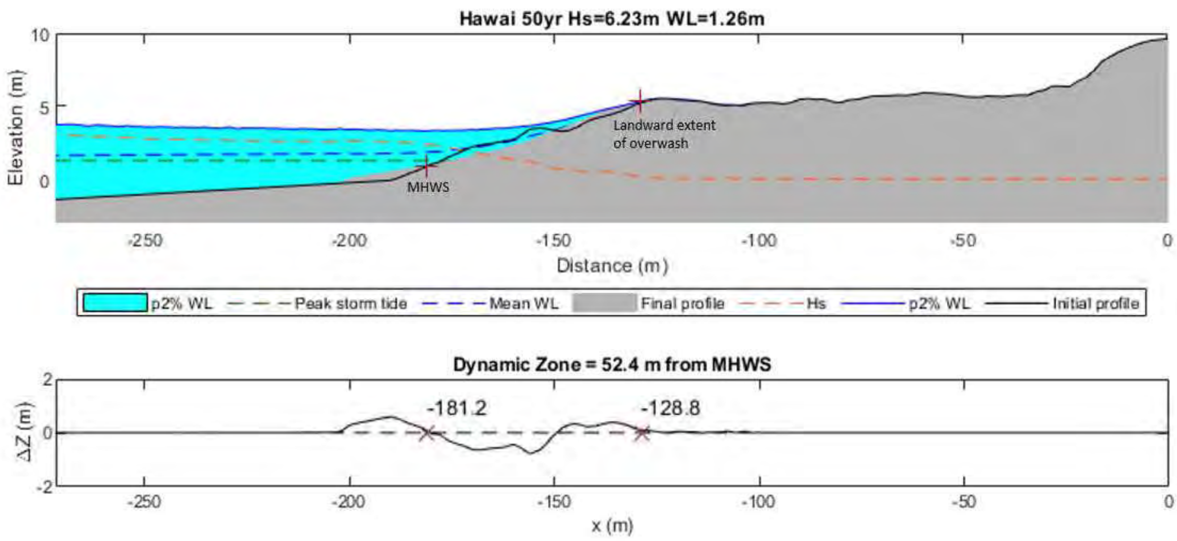

Figure 5.4: Example of XBeach-G model outputs for Hāwai to determine landward extent of overwash during a 50 year ARI event.

Model results for the dynamic zone at each site are presented in Table 5.4. The dynamic zones typically vary from 32 to 80 m for the 5 year to 200 year events. The dynamic zones are larger at Papatea and Whangaparaoa where the offshore wave heights are significantly higher. Due to the more sheltered shoreline along Ōmaio west the dynamic zones are reduced.

Table 5.4: Adopted component values for the dynamic zone (m) across mixed sand gravel beaches

Annual Recurrence Interval (ARI)	**5 year**	**50 year**	**200 year**
Probability of event occurrence within 10 years	**99%**	**45%**	**13%**
Tōrere	45	60	65
Hāwai	43	52	79
Houpoto	32	62	67
Ōmaio	43	60	86
Ōmaio west	21	39	46
Wharekura	67	79	80
Papatea	44	98	120
Whangaparaoa	111	152	191

5.5 Dune stability

The dune stability (DS) factor only applies to sandy beaches where the beach face has potential to become over-steepened. The DS factor delineates the area of potential risk landward of the erosion scarp by buildings and their foundations. The parameter assumes that storm erosion results in an over-steepened scarp which must adjust to a stable angle of repose for loose dune sand. The dune stability width is dependent on the height of the existing backshore and the angle of repose for loose dune sand. This has been obtained from an examination of historic reports, a review of the beach profile data, and our assessment of the beach sediments obtained in this study. The dune stability factor is outlined below:

$$DS = \frac{H_{dune}}{2(\tan \alpha_{sand})} \quad (5\text{-}1)$$

Where H_{dune} is the dune height from the eroded base to the crest and α_{sand} is the stable angle of repose for beach sand (ranging from 30 to 34 deg). In reality, the formation of a talus slope at the toe will allow the scarp to stand at steeper slopes (unless subsequently removed), hence the slope height is divided by 2. Parameter bounds are defined based on the variation in dune height along the coastal behaviour cell and potential range in stable angle of repose.

The adopted dune heights for each coastal cell have be defined based on the most recently available LiDAR for each site and are provided in Appendix A.

5.6 Medium-term

Medium-term fluctuations have been accounted for at the sites where it is appropriate. For many of the wide mixed sand gravel barriers the historic shoreline data indicates long-term dynamic stability. While there may not be any significant long-term accretion or erosion trend the position of the modern storm berm is likely to fluctuate over timescales of several years. Fluctuations in the storm berm position can be associated with multiple storm events, storm berm instability and beach rotation which can occur due to medium-term climatic cycles (such as the IPO) and fluctuations in sediment supply.

For the mixed sand gravel beaches the medium-term component is based on the shoreline change envelop (SCE) calculated from the available historic shoreline data using DSAS. DSAS calculates the SCE as the maximum distance among all the shorelines along each of the defined transects (Figure 5.5).

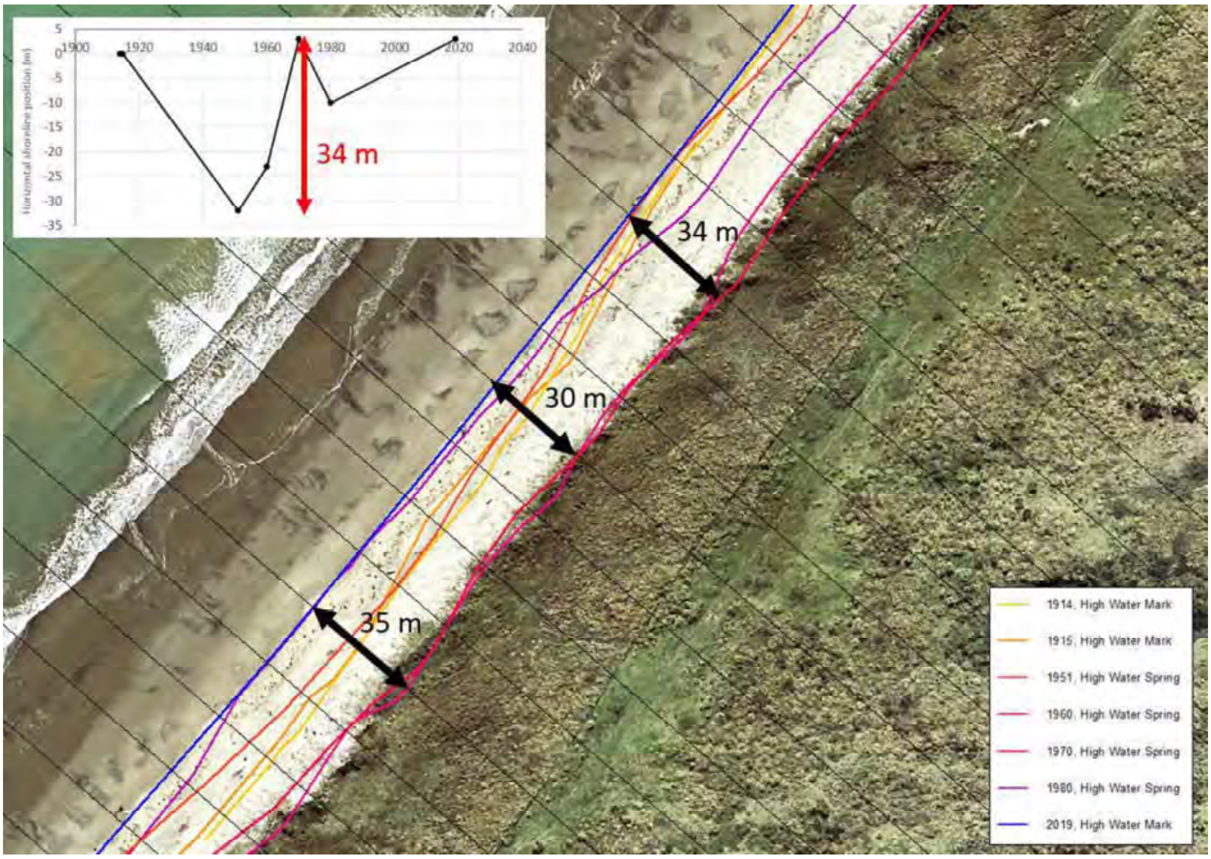

Figure 5.5: Example of Shoreline Change Envelope (SCE) calculated using DSAS

Similarly, on sandy beaches medium-term fluctuations can occur as a result of medium-term climatic cycles (i.e. as reported by de Lange (2001) and Wood (2010) for Coromandel beaches). Medium-term fluctuations can also occur when there are fluctuations in sediment supply or sand-spit migration. For example, historic shorelines and profile data at Ōhiwa spit indicate periods of erosion and progradation occur about once every 50 to 60 years, with periods of erosion and progradation typically lasting 25 to 30 years (Dahm and Kench, 2007). Such fluctuations are likely to be linked with the interactions between the shoreline and adjacent ebb tide delta offshore from the harbour entrance. An example of the medium-term fluctuations evident in profile CCS8 (Ōhiwa spit) is shown in Figure 5.6. The historic shoreline positions indicate a medium-term fluctuation of +/- 150 m over approximately 30 years (Figure 5.6).

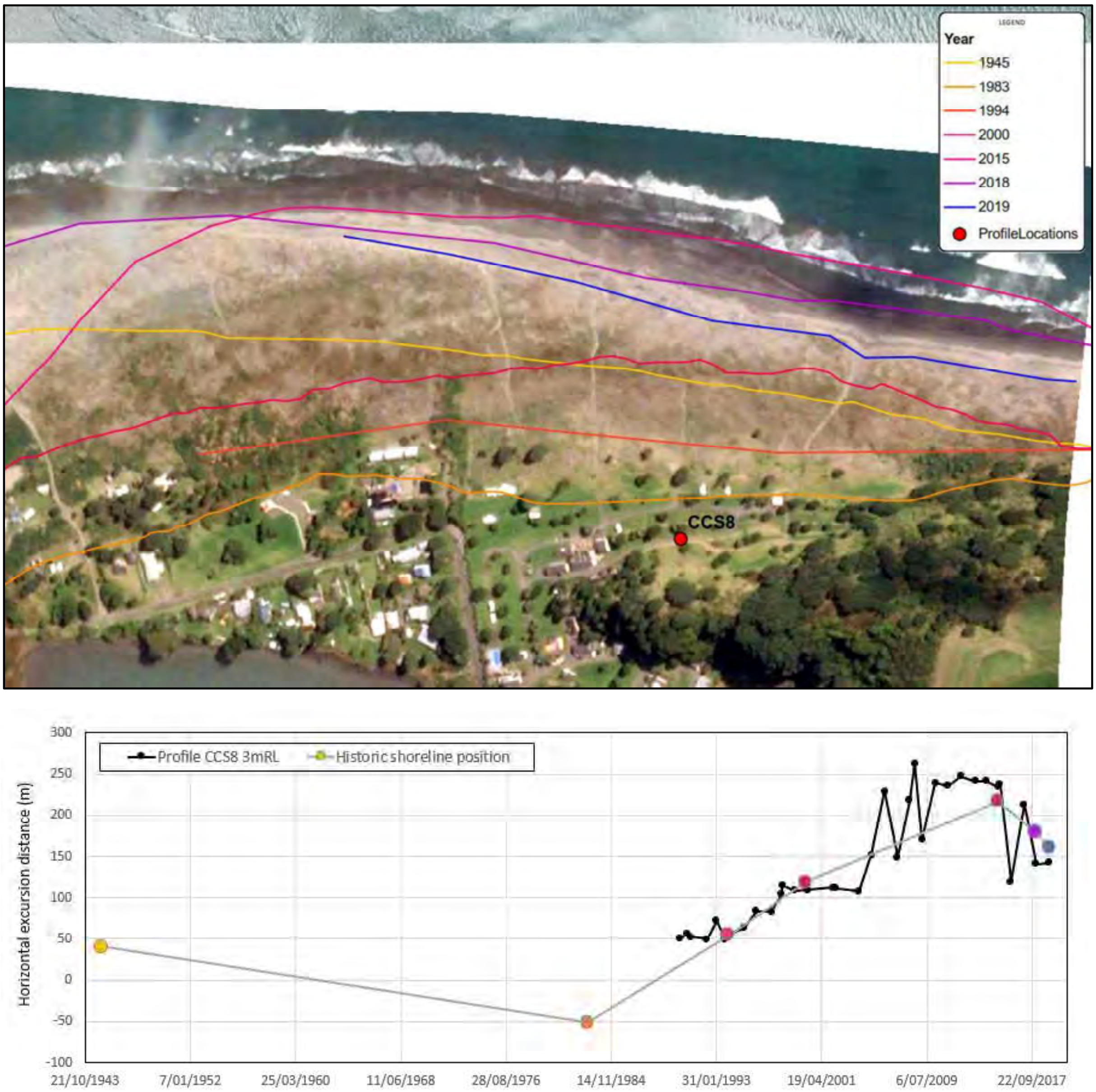

Figure 5.6: Example of medium-term fluctuations at Ōhiwa spit. (Top) Historic shorelines overlaid on 2019 GoogleEarth imagery. (Bottom) Historic shoreline position compared with profile data at CCS8

5.7 Long-term trends

The long-term rate of horizontal coastline movement includes both ongoing trends and long-term cyclical fluctuations. These may be due to changes in sea level or fluctuations in coastal sediment supply. Long-term trends have been derived from a combination of geomorphic evidence and historic shoreline analysis. Beach profiles were also analysed however the limited length of data (1990 to 2019) does not include the significant erosion phase that occurred during the 1970's and therefore does not provide representative long-term trends.

A summary of the shoreline data available for each site is provided in Appendix B. The data available for each site varies with different mapped features including high water mark, dune toe and edge of vegetation. For most of the mixed sand gravel beaches the shoreline data consists of High Water Mark (HWM) and Mean High Water Spring (MHWS). We have assumed these surveys refer to the wet line along the seaward edge of the berm.

The shoreline data has been analysed using the GIS-based DSAS model with shoreline change statistics calculated for comparable features at each site. Linear regression analyses of the shoreline data has been calculated at 20 m intervals along each site (Figure 5.7).

For the sandy beaches the long-term shoreline movement has been assessed based on regression analyses of the dune toe and edge of vegetation. It is assumed that along sandy beaches the edge of vegetation is equivalent to the dune toe. For mixed sand gravel beaches the long-term shoreline movement has been assessed based on linear regression analyses of the HWM and/or MHWS.

A summary of the DSAS results is provided in Table 5.5.

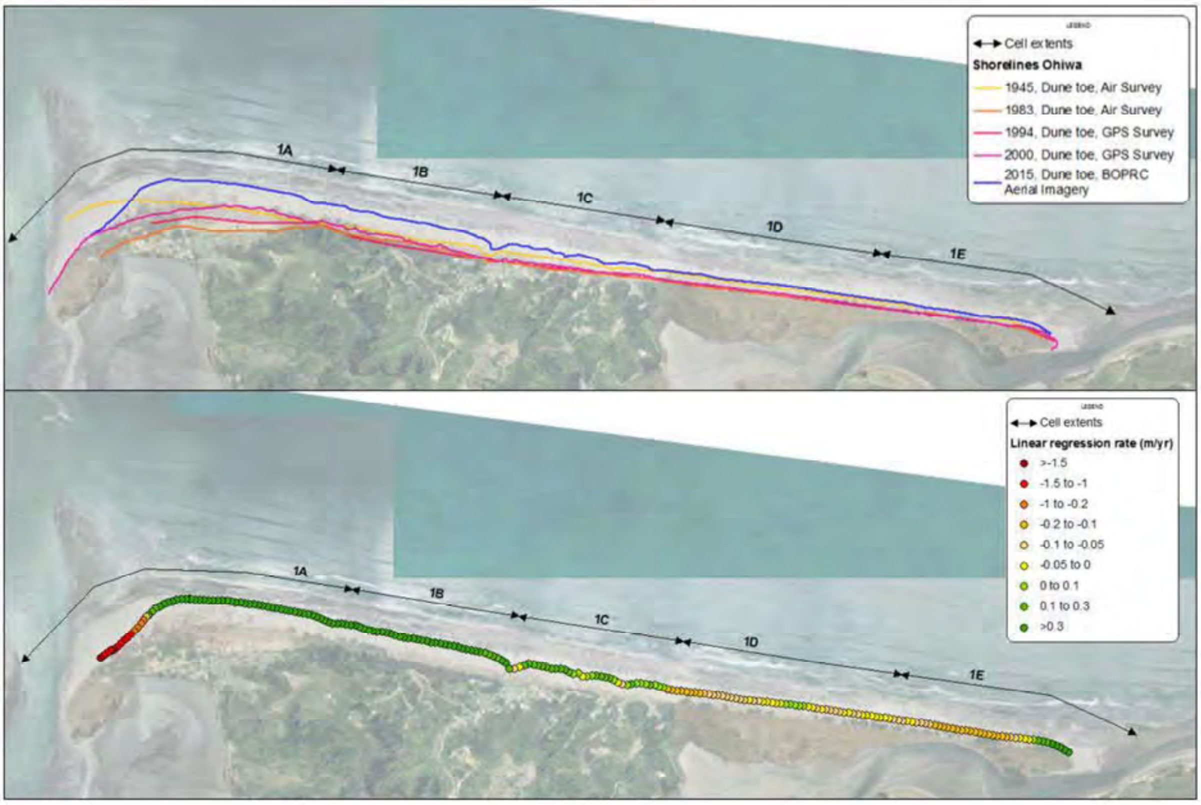

Figure 5.7: Example of DSAS analysis for Ōhiwa

Table 5.5: Summary of dominant long-term trends at each site based on DSAS analysis

Site	Dominant long term trend	Comments
Ōhiwa	Stable/eroding	Large fluctuations around Ōhiwa spit but relatively stable long term
Hikuwai	Eroding	Rates range from -0.05 to -0.27m/yr
Tōrere	Accreting	Increased accretion westward. Slight erosion at eastern extent
Hāwai	Accreting	Increased accretion westward, 0.1 m/yr to 0.5 m/yr
Houpoto	Accreting	High accretion west of the Motu River mouth
Ōmaio	Stable	Relatively stable for most of the beach. Erosion east of Haparapara River mouth, -0.1 to -0.5 m/yr
Maraetai Bay	Stable	Relatively stable, -0.05 to 0.05 m/yr
Wharekura	Stable	Relatively stable, -0.1 to 0.1 m/yr
Whanarua	Stable	
Papatea	Accreting	High accretion west of Raukōkore River mouth
Raukōkore	Stable/eroding	Relatively stable, some erosion along banks
Waihau Bay	Stable/eroding	Relatively stable, some erosion along banks
Oruaiti Beach	Stable	
Whangaparaoa	Stable	Relatively stable with erosion near river mouth

Overall, the historic shorelines show a trend of significant accretion along the large mixed sand gravel barriers adjacent to the river mouths. The accretion is typically highest directly west of the river mouths. Shorelines directly east of the river mouths tend to show an erosional trend, for example at Ōmaio, Tōrere and Hāwai.

The smaller mixed sand gravel beaches fronted with shore platforms are typically located further from the large river mouths and therefore have a reduced sediment supply (i.e. Whanarua and Waihau Bay). The sheltered sections of these beaches appear to be relatively stable while the slightly more exposed sections appear to be eroding (i.e. sections of Raukōkore).

As Haurere Point acts as a barrier to southwest transport of gravel, the beaches west of Ōpape largely depend of sediment supply from the Waiaua, Waioeka and Waiōtahe Rivers. Historic shorelines indicate a general trend of erosion along most of Hikuwai. This is likely due to most of the sediment from the Waioeka and Waiaua Rivers being transported westward towards Waiōtahe.

Ōhiwa beach is largely influence by medium-term fluctuations with overall long-term stability.

Adopted trends for each of the coastal cells is provided in Appendix A.

5.8 Effects of SLR

We have adopted a range of SLR (SLR) values over the two required future timeframes of 2070 and 2130 (i.e. 50 and 110 years respectively). The range of SLR values for each timeframe are based on three RCP scenarios consistent with the guidance provided within MfE (2017). Table 5-6 presents the SLR values used in this present assessment. The 2130 RCP8.5 value of 1.25m SLR is in accordance with the RPS (Policy NH11B).

An average historic rate of SLR of 1.9 mm/year for Tauranga Harbour was subtracted from the adopted SLR values for use in assessment. This approach is required because the existing long term trends and processes already incorporate the response to the historic SLR. Therefore, the historic rate must be subtracted to avoid double counting.

As stated in Section 2.3 the eastern Bay of Plenty is subject to tectonic subsidence. This subsidence is likely to influence the local SLR, however due to the limited data record for the VLM we have not accounted for this local variation and have adopted the national SLR values.

Table 5-6 SLR values (m) utilised in assessment

Year	Timeframe (years)	SLR (m)	RCP Scenario
2070	50	0.4	RCP4.5
2070	50	0.6	RCP8.5(approx.)
2130	110	0.8	RCP4.5
2130	110	1.25	RCP8.5
2130	110	1.6	RCP8.5H+

5.8.1 Sandy beach response

Geometric response models propose that as sea level is raised, the equilibrium profile is moved upward and landward conserving mass and original shape (Figure 5.8). The most well-known of these geometric response models is that of Bruun (Bruun, 1962, 1988) which proposes that with increased sea level, material is eroded from the upper beach and deposited offshore to a maximum depth, termed closure depth. The increase in seabed level is equivalent to the rise in sea level and results in landward recession of the shoreline. The model may be defined by the following equation:

$$SL = \frac{L_*}{B + d_*} S \qquad (5\text{-}2)$$

Where SL is the landward retreat, d_* defines the maximum depth of sediment exchange, L_* is the horizontal distance from the shoreline to the offshore position of d_*, B is the height of the berm/dune crest within the eroded backshore and S is the SLR.

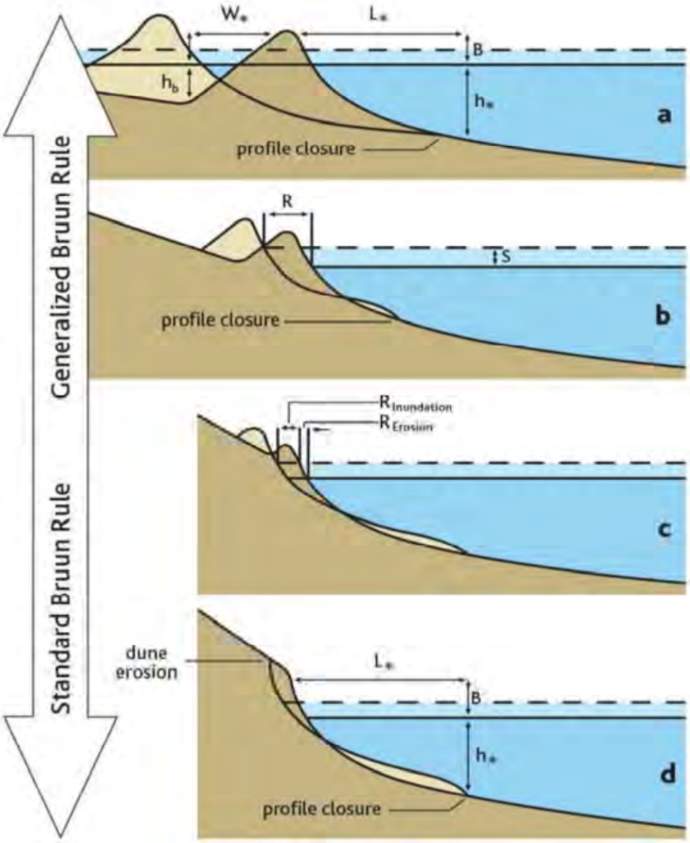

Figure 5.8: Schematic diagrams of the Bruun model modes of shoreline response (after Cowell and Kench, 2001)

The rule is governed by simple, two-dimensional conservation of mass principles and assumes no offshore or onshore losses or gains and an instantaneous profile response following sea level change. The rule assumes an equilibrium beach profile where the beach may fluctuate under seasonal and storm-influences but returns to a statistically average profile (i.e. the profile is not undergoing long-term steepening or flattening). Losses or gains to the system and changes to the equilibrium profile are likely accounted for within the long-term change parameter (LT) (Section 5.7) and therefore are not likely to introduce additional uncertainty. The definition of a closure depth (maximum seaward extent of sediment exchange) and the lag in response of natural systems have been cited as significant limitations in the method (Hands, 1983).

The inner parts of the profile exposed to higher wave energy are likely to respond more rapidly to changes in sea level. For example, Komar (1999) proposes that the beach face slope is used to predict coastal erosion due to individual storms. Deeper definitions of closure including extreme wave height-based definitions (Hallermeier, 1983), sediment characteristics and profile adjustment records (Nicholls et al., 1998) are only affected during infrequent large-wave events and therefore may exhibit response-lag.

Shand et al. (2013) argue that as SLR is expected to be ongoing, then the outer limit of profile adjustment is likely to be ‘left behind’ before it can reach equilibrium. The closure depth can therefore be more realistically defined as the point at which the profile adjustment can ‘keep up’ with sea-level change and becomes a calibration parameter in lieu of an adequate depth-dependent lag parameter. Shand et al. (2013) tested a range of closure depth definitions against a non-equilibrium model calibrated using 30 years of beach data (Ranasinghe et al., 2011). Results show the various definitions of closure to predict Recession/SLR values straddling the entire probabilistic (2 – 99%) range predicted by the Ranasinghe’s probabilistic model.

To define parameter distributions, the Bruun rule has been used to assess the landward retreat of three different active beach slope profiles based on average beach profiles. The three slope profiles include:

1 Active beach face, average dune toe position to low water mark (lower bound)
2 Inner closure slope, average dune crest to inner Hallermeier closure depth (modal value)
3 Outer closure slope, average dune crest to outer Hallermeier closure depth (upper bound).

The Hallermeier closure definitions are defined as follows (Nicholls et al., 1998):

$$d_l = 2.28H_{s,t} - 68.5\left(\frac{H_{s,t}^2}{gT_s^2}\right) \cong 2\ x\ H_{s,t} \quad (5\text{-}2)$$

$$d_i = 1.5\ x\ d_l \quad (5\text{-}3)$$

Where d_l is the closure depth below mean low water spring, $H_{s,t}$ is non-breaking significant wave height exceeded for 12 hours in a defined time period, nominally one year, and T_s is the associated period. For this study the deep water (non-breaking) wave climate parameters of $H_{s,t}$ and T_s were based on the MetOcean View hindcast data (Table 5.7).

Table 5.7: Wave climate parameters based on MetOcean View hindcast data, with inner and outer closure depths based on Equations 5-2 and 5-3

Location	Significant wave height (Hs,t)[1], m	Wave period (Ts), s	Inner closure depth, m	Outer closure depth, m
Ōhiwa	3.0	10.5	7	10.6
Hikuwai	3.0	10.5	7	10.6
Ōpape	2.5	10	6	9.1

[1]non-breaking significant wave height exceeded for 12 hours over one year

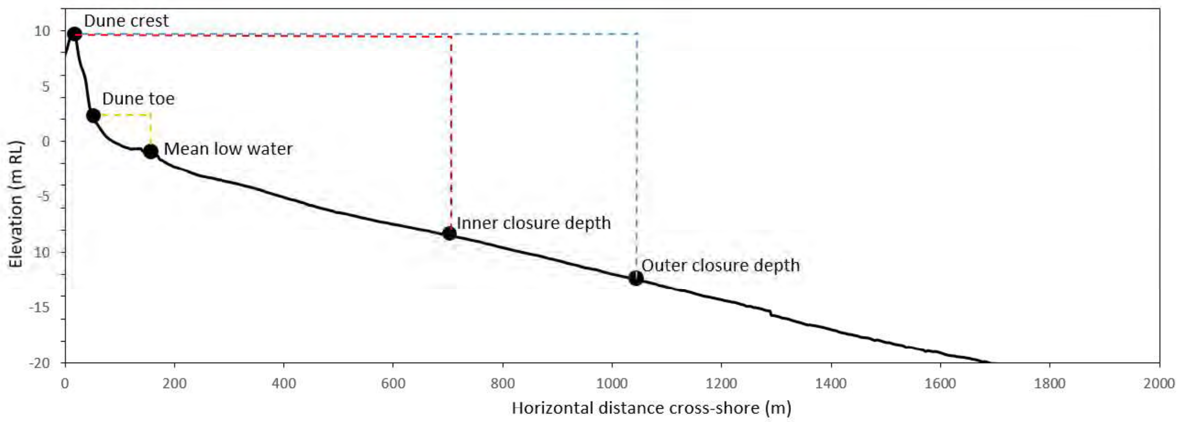

Figure 5.9: Example of extents of active profiles for the Hikuwai shoreline

For the harbour shoreline (i.e. harbour shoreline at Ohiwa Spit), the generalised Brunn Rule is less applicable as harbour sediment lost from the upper beach does not settle on the basin nearshore or bathymetric profile, but is instead lost from the system. In this case, the profile is translated by a modified Bruun principle using the foreshore or beach face slope (β) (Equation 5-4). This is consistent with the principles described in the eShorance estuary shoreline response model, with is considered to be best practice (Stevens and Giles, 2010).

$$SL = tan\beta \quad (5\text{-}4)$$

5.8.2 Mixed sand gravel beach response

For mixed sand gravel beaches, the Bruun Rule is less appropriate. Unlike sandy beaches where sediment tends to be eroded from the beach face and transported offshore, mixed sand gravel beaches tend to retreat in response to SLR via berm rollover.

Barrier rollover is the progressive erosion of the beach face with sediment being transported landward via overwash (Leatherman (1983) (Equation 5-5 and Figure 5.10). It is assumed that the barrier maintains a constant width.

$$Retreat\ due\ to\ SLR = SLR \frac{W}{h_c - h_b} \tag{5-5}$$

Where:

SLR = SLR (m)

W = width of barrier

$h_{c=}$ = closure depth (beach step/offshore location of minimal profile change)

h_b = backshore/lagoon depth

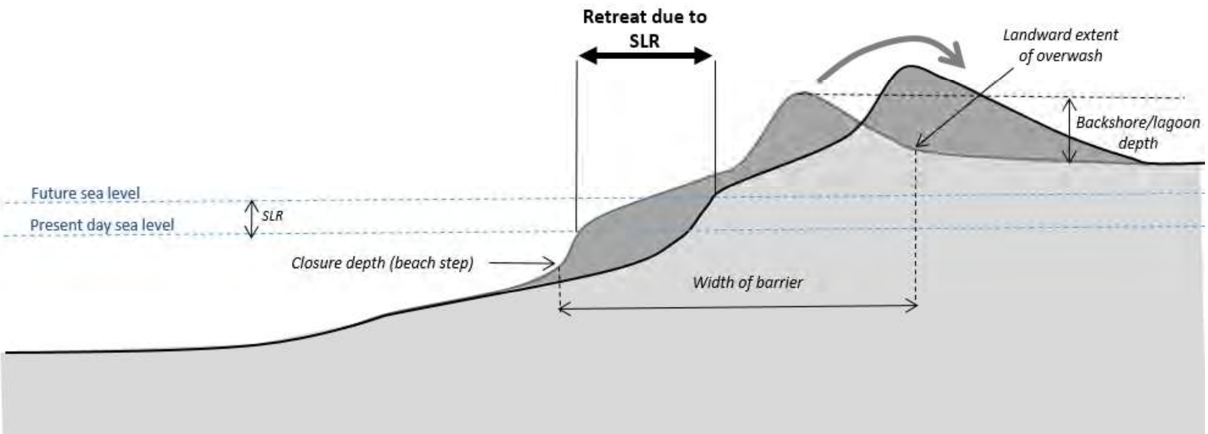

Figure 5.10: Conceptual diagram of barrier rollover model

For the nine mixed sand gravel beaches east of Ōpape we have used one representative profile per site to assess the impact of SLR. The Rollover Model is sensitive to backshore elevations (lagoon depth), with lower backshore elevations resulting in increased shoreline erosion. For most of the Ōpōtiki mixed sand gravel beaches there is no lagoon and the backshore elevation is similar to the berm. The width of the storm barrier is based on landward extent of the overwash as described in Section 5.4.2.

The beach step marks the lower extent of the active beach. Typically on mixed sand gravel beaches the gravel portion of the shoreface rarely extends below the low tide mark (Shulmeister and Jennings, 2009). Ivamy and Kench (2006) assessed morphological changes along Tōrere and found the position of the beach step exhibited little change during the 10-day experimental period but did show mobility during tidal cycles with the beach step moving landward on the rising tide and returned to its initial position at low tide. For this assessment we have assumed the beach step is equivalent to MSL.

The range of parameter bounds are based on the range of barrier widths (Table 5.8).

Table 5.8: Parameter bounds adopted to assess the effects of SLR on mixed sand gravel beaches

Variable	Lower bound	Mode	Upper bound
Barrier width (m)	5 yr ARI overwash extent	50 yr ARI overwash extent	200 yr ARI overwash extent

6 Erosion hazard assessment

6.1 Combination of parameter components to derive CEHA

For each coastal cell, the relevant parameters influencing the CEHA and parameter bounds have been defined according to the methods described above as summarised in Table 6.1 and Table 6.2. Probability distributions constructed for each parameter are randomly sampled and the extracted values used to define a potential CEHA distance. This process is repeated 10,000 times using a Monte Carlo technique and probability distribution of the resultant CEHA width is forecasted.

Table 6.1: Summary of theoretical erosion hazard parameter bounds for sandy beaches

Parameter	Lower bound	Mode	Upper bound
Short-term (m)	5 year ARI storm cut	50 year ARI storm cut	200 year ARI storm cut
Dune Stability (m)	Maximum dune height & minimum stable of repose	Mean dune height & mean stable of repose	Minimum dune height & maximum stable of repose
Medium-term (m)	Site specific values		
Long-term (m/yr)	-95% CI of smallest trend in cell	Mean regression trend	+95% CI of largest trend in cell
SLR effect (m) – (effect for each SLR scenario varies based on closure slopes)	Slope across active beach face to swash excursion	Slope from dune crest to inner Hallermeier closure depth	Slope from dune crest to outer Hallermeier closure depth

Table 6.2: Summary of theoretical erosion hazard parameter bounds for mixed sand gravel beaches

Parameter	Lower bound	Mode	Upper bound
Dynamic zone (m)	5 year ARI storm overwash extent	50 year ARI storm overwash extent	200 year ARI storm overwash extent
Medium-term (m)	Minimum SCE in cell	Average SCE in cell	Maximum SCE in cell
Long-term (m/yr)	-95% CI of smallest trend in cell	Mean regression trend	+95% CI of largest trend in cell
SLR effect (m) - (effect for each SLR scenario varies based on width of barrier)	5 yr ARI overwash extent	50 yr ARI overwash extent	200 yr ARI overwash extent

6.2 Results

Figure 6.1 presents an example of the component histograms and cumulative distribution functions for Cell 4B (Hāwai) at the 2130 planning timeframe. The curved lines represent probability of exceedance by 2130, measured on the right-hand axis. Results show that the possible erosion distances for Cell 4B in 2130 range from -58 to -125 m. Histograms and cumulative distribution function plots for all cells within each site are included in Appendix G.

Table 6.3 presents an example of the tabulated results for Cell 4B (Hāwai). Resultant CEHA tables for each site are included in the site summaries (Appendix A). The assessment output five resultant probabilities or likelihoods of exceedance for each timeframe (i.e. min, P66%, P50%, P5% and max).

The P50% means there is a 50% chance of an erosion distance being exceeded within that timeframe. P66% can be considered a likely scenario and P5% can be considered as a very unlikely scenario.

The future timeframes include a range of SLR scenarios. The highest SLR for the 100 year timeframe is 1.6m, The projected erosion distance for this scenario ranges from -66 to -129 m. Under this scenario, there is a 50% chance of an erosion distance of -94 m (P50%).

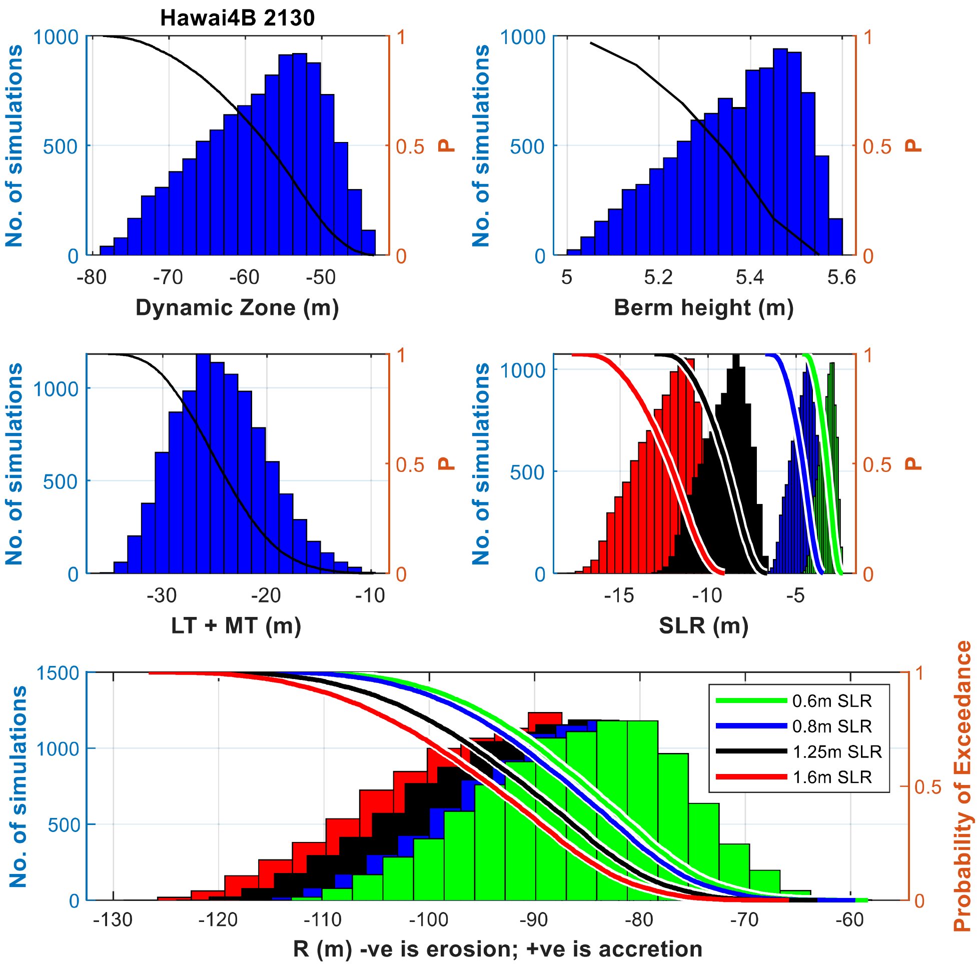

Figure 6.1: Example of histograms and cumulative distribution functions of parameter samples and resultant CEHA distances for cell 4B (Hāwai) in 2130

Table 6.3: Example of CEHA distances for cell 4B Hāwai

Site	Cell	Timeframe	SLR (m)	Approximate RCP scenario	Probability of Exceedance				
					Min	P66%	P50%	P5%	Max
Hāwai	4B	Current (2020)	0.03	N/A	-43	-54	-57	-72	-79
		50yr (2070)	0.4	RCP4.5	-54	-72	-76	-92	-105
			0.6	RCP8.5	-55	-73	-77	-94	-106
		110yr (2130)	0.8	RCP4.5	-59	-83	-86	-104	-118
			1.25	RCP8.5	-63	-87	-91	-109	-124
			1.6	RCP8.5+	-66	-90	-94	-113	-129

6.3 Mapping of the CEHA

Table 6.4 summarises the six scenarios which have been mapped. CEHAs are mapped as offsets to the existing baseline (vegetation edge on sandy beaches, high water mark on mixed sand gravel beaches). Where the hazard values differ between coastal cells, the mapped CEHA is merged over a distance of at least 10 times the differences between values providing smooth transitions. In accretion dominated areas where the future CEHA is seaward of the current CEHA, the future CEHA has been mapped equivalent to the current CEHA.

At some sites, the CEHA distance extends landward of a consolidated cliff. As cliff erosion has been excluded from the scope of this study, the CEHA have been bound along the toe of the cliff and the cliffs have been identified as potentially being at risk to toe instability.

For mapping around river mouths the CEHA have been terminated at the existing river channel. There is high uncertainty in these areas as the hazard is dominated by river processes which have not been accounted for within this assessment.

Table 6.4: Timeframes, likelihood and SLR scenarios for adopted mapping scenarios

Timeframe	SLR scenario	Likelihood of occurring over timeframe (exceedance probability)
Current	N/A	P5%
2070	0.6 m	P50%, P5%
2130	1.25 m	P50%, P5%
2130	1.6 m	P5%

6.4 Discussion

6.4.1 Coastal erosion hazard areas

Resultant CEHA reflect the varying coastal erosion hazard along the Opotiki District coastline which is largely influenced by the varying beach morphologies, wave exposure and sediment supply.

Sandy beaches

The sandy beaches include the relatively exposed coast from Ōhiwa to Ōpape as well as the more sheltered beaches further east such as Maraetai and Orauiti Beach. The Ōhiwa shoreline is influenced by significant medium-term fluctuations and spit dynamics with overall long-term stability. The Hikuwai to Ōpape coast differs, with less medium-term fluctuations and an overall trend of long-term erosion.

Under high future SLR (1.6m) the predicted shoreline retreat varies from -30 m along the most sheltered sandy beaches, such as Oruaiti and Maraetai and is up to -100 m along the exposed beaches such as Hikuwai and Ōpape.

Mixed sand gravel beaches

Overall majority of the mixed sand gravel beaches along the Opotiki District coastline are located on prograding coastal plains and show trends of shoreline advancement. This is largely due to significant sediment supply from nearby rivers. While the barrier systems show overall accretion, they are dynamic and influenced by overwash during storm events and medium-term changes in sediment supply. Current CEHA along the mixed sand gravel beaches typically correlates with the width of the existing gravel deposits. The width of the current CEHA is dependent on the offshore wave exposure and berm elevations. Beaches with larger offshore wave heights and lower berm elevations (i.e. Papatea and Whangaparoa) typically are exposed to greater overwash-induced changes and subsequently have a larger current CEHA.

Shoreline retreat in response to high SLR (1.6 m) is expected to vary from -15 m along the more sheltered barrier systems such as Tōrere, and is up to -40 m along the exposed, low-lying mixed sand gravel barriers such as Papatea and Whangaparoa.

For several of the mixed sand gravel beaches where there is significant long-term accretion (i.e. Houpoto and Papatea), the impact from long-term accretion is expected to balance potential recession due to SLR. It is important to note that if future sediment supply is reduced, the shoreline retreat due to SLR may be exacerbated.

Narrow mixed sand gravel beaches

In general, the CEHA along the narrow, mixed sand gravel beaches tends to be smaller compared with the rest of the assessed coastline. These shorelines are typically more sheltered environments due to the presence of offshore reefs. The data (although limited) also indicates that these shorelines have been relatively stable in the long-term and experience minor storm cut. Shoreline retreat in response to high SLR (1.6 m) is expected to vary from 10 to 30 m.

River mouths

There is high uncertainty within the vicinity of river mouths. The CEHA have been truncated at the edge of the rivers as there is high uncertainty in these areas, with the hazard being dominated by river processes which have not been accounted for within this assessment. Areas of high uncertainty which have not been mapped include:

- Waiōtahe spit
- Waiaua River mouth
- Motu River mouth
- Haparapara River mouth
- Raukōkore River mouth
- Whangaparaoa River mouth

These areas require site-specific assessments which consider the riverine and coastal processes.

6.4.2 Anthropogenic effects

For this coastal erosion hazard assessment, all anthropogenic effects (human influences) have been excluded. However, it is important to note that there are anthropogenic effects which can influence the coastal erosion hazard and should be considered within any detailed site-specific assessments. Such anthropogenic effects include:

- Construction of toe erosion protection works (revetment/seawalls etc.)
- Construction of land stability structures (retaining walls etc.)
- Mining and removal of beach sand, or beach re-nourishment
- Concentration of storm water and surface flows down cliff and bank faces
- Modification of foreshore vegetation
- Land reclamation
- Harbour developments. This assessment does not consider the recent Ōpōtiki harbour development which may influence the CEHA. This site may require reassessment at a later stage once the development is complete and there has been a sufficient period of monitoring.

6.4.3 Uncertainties and limitations

Limitations and uncertainties associated with this study include:

- The size of the coastal cells used to define the erosion hazard. There will always be some alongshore variance within a defined cell, however this can be reduced by splitting the shoreline into continually smaller cells. We consider the cells are refined as far as practical based on the data available and variation in coastal morphology. Residual uncertainty may be allowed for by selecting a lower probability CEHA value.
- Lack of data for short-term storm cut. No beach profile data was available to assess the storm cut along beaches east of Ōpape. Subsequently, the adopted values were estimated based on site observations, geomorphic understanding and findings from previous studies including community observations.
- Lack of data for dynamic zone widths. Some information on peak water levels and debris extents during Cyclone Ivy was available, however there was no specific pre- and post-storm profile data available for validating the XBeach-G model along the mixed sand gravel beaches.
- Long-term trends and medium-term fluctuations are largely based on the historic shoreline data which has been provided by BOPRC. Overall, this study has assessed coastal erosion hazard areas at a local scale and may be superseded by detailed, site-specific assessment undertaken by qualified and experienced practitioners using improved or higher resolution data than presented in this report.

6.4.4 Future changes

Over time there is likely to be an increased understanding around factors such as vertical land movement and SLR projections. Within this assessment the impact of vertical land movement has not been accounted for due to the limited dataset (see Section 2.3). However, as new data becomes available the future erosion hazard should be revised. Depending on the magnitude of vertical land movement the projected erosion hazard areas may change. For example, if the land is subsiding then erosion rates would be expected to increase and vice versa for land uplift.

7 Summary and recommendations

The Ōpōtiki District coastline is in the Eastern Bay of Plenty on the east coast of the North Island, New Zealand. The coastline extends approximately 130 km from Ōhiwa spit up to Cape Runaway. The coastline is characterised by a mixture of exposed sandy beaches, small embayments, rocky shore platforms, mixed sand gravel barriers and multiple rivers which supply significant quantities of sediment to the coast.

Tonkin + Taylor Ltd were commissioned by Bay of Plenty Regional Council and Ōpōtiki District Council to undertake coastal erosion hazard assessment for 13 sites within the Ōpōtiki District.

The 13 selected sites can be broadly classified into three different morphological types:

- Sandy beaches
- Mixed sand gravel beaches
  - Wide barriers backed by coastal plains
  - Narrow beaches, perched over rocky shore platforms and backed by higher banks
- River mouth/inlets shorelines

The coastal erosion hazard areas were defined using a probabilistic approach which combines standard and well-tested methods for defining erosion hazard with a stochastic method of combining erosion parameter distributions to allow for inherent statistical variance and uncertainty to be incorporated within results. Results provide a range of potential erosion hazard distances for current and future timeframes (e.g. 2070 and 2130) including different sea level rise scenarios. Erosion distances along the gravel barriers include storm overwash-induced changes in land.

Key conclusions are as follows:

- The Ōhiwa shoreline is largely influenced by significant medium-term fluctuations and spit dynamics with overall long-term stability.
- The Hikuwai to Ōpape coast tends to show an overall trend of long-term erosion.
- Majority of the mixed sand gravel barriers show long-term accretion. This is most likely a result of sediment supply from adjacent river mouths.
- The narrow, mixed sand gravel beaches tend to be more sheltered environments that show long-term stability.
- For several of the mixed sand gravel beaches where there is significant long-term accretion, the impact from long-term accretion is predicted to counteract potential recession due to SLR.
- For the large river mouths, the CEHA have been truncated at the edge of the river as there is high uncertainty in these areas, with the hazard being dominated by river processes which have not been accounted for within this assessment.
- Areas of high uncertainty which have not been mapped include:
  - Waiōtahe spit
  - Waiaua River mouth
  - Motu River mouth
  - Haparapara River mouth
  - Raukōkore River mouth
  - Whangaparaoa River mouth

Recommendations

For improved understanding of the coastal erosion hazard along the Opotiki coast we recommend the following:

- The collection of additional beach profile information for sites east of Ōpape. This will allow more accurate assessment of short- and long-term coastal change
- The collection of data on overwash extents following significant storm events, and in particular areas where overwash has caused erosion or accretion
- Any changes in vertical land movement being collected under existing programmes are incorporated into any future update
- Any changes in the rates of projected SLR are incorporated into any future update
- Additional assessment for the cliff shorelines which were excluded from this study (particularly the areas with existing or planned development) could be considered.
- Update of this hazard assessment at intervals of no more than 10 years or following significant changes in data availability, or best practice guidance or methods.

This study has assessed coastal erosion hazard areas at a local scale and may be superseded by detailed site-specific assessment undertaken by qualified and experienced practitioner using improved or higher resolution data than presented in this report.

8 Applicability

This report has been prepared for the exclusive use of our client Bay of Plenty Regional Council, with respect to the particular brief given to us and it may not be relied upon in other contexts or for any other purpose, or by any person other than our client, without our prior written agreement.

Tonkin & Taylor Ltd

Report prepared by:

Rebekah Haughey

Coastal Scientist

Eddie Beetham

Coastal Scientist

Authorised for Tonkin & Taylor Ltd by:

Richard Reinen-Hamill

Project Director

Report reviewed by:

Dr Tom Shand

Technical Director of Coastal Engineering

RHAU
t:\tauranga\projects\1008669\1008669.2000\issueddocuments\final v5\r20210702.opotikierosionreportv5.final.docx

9 References

Ballantine, D. J. and Davies-Colley, R. J. (2009). Recommendations for water quality monitoring of a new dairying area – Upper Motu Catchment. NIWA Client Report prepared for Gisborne District Council.

Beanland, S. and Berryman, K. R. (1992). Holocene coastal evolution in a continental rift setting; Bay of Plenty, New Zealand. Quat. Int. 15, 151-158.

Beavan R.J. and Litchfield, N.J. (2012) Vertical land movement around the New Zealand coastline: implications for sea-level rise, GNS Science Report 2012/29. 41p.

Bruun P. (1962) Sea-level rise as a cause of shore erosion. J. Waterways Harbors Div 88:117–130.

Bruun, P. (1988) The Bruun Rule of erosion by SLR: a discussion on large-scale two- and three-dimensional usages. JCR, 4, 627–648.

Buscombe, D. & Masselink, G. (2006). Concepts in gravel beach dynamics. Earth-Science Reviews 79.

Cowell, P.J., Thom, B.G., Jones, R.A., Everts, C.H. and Simanovic, D. (2006) Management of Uncertainty in Predicting Climate-Change Impacts on Beaches. JCR 22(1)232-245.

Dahm, J. and Kench, P. (2007). Ōpōtiki District Coastal Erosion Assessment and Setback Recommendations. Report prepared for Ōpōtiki District Council and Bay of Plenty Regional Council.

Eco Nomos Ltd. (2016). Review of Coastal Erosion Hazard: Selected Beaches of Ōpōtiki District. Report prepared for Ōpōtiki District Council.

Gibb, J. (1994). Initial Assessment of Areas Sensitive to Coastal Hazards for Selected Parts of the Bay of Plenty Coast. Report prepared for Bay of Plenty Regional Council.

Gibb, J. (1977). Late Quaternary sedimentary processes at Ōhiwa Harbour, Eastern Bay of Plenty with special reference to property loss on Ōhiwa Spit. Water and Soil, Technical Publication No. 5.

Iremonger, S. (2011). NERM beach profile monitoring 2011.Bay of Plenty Regional Council.

Ivamy, M. C. and Kench, P. S. (2006). Hydrodynamics and morphological adjustment of a mixed sand and gravel beach, Tōrere, Bay of Plenty, New Zealand.

Hallermeier, R.J. (1983) Sand transport limits in coastal structure designs. Proc. of Conf. on Design,Construction, Maintenance and Performance of Coastal Structures. ASCE, Arlington, pp 703–716.

Hands, E.B. (1983) The Great Lakes as a test model for profile response to SL changes. In: Komar, P.D. (ed.), Handbook of Coastal Processes and Erosion.

Hannah, J. and Bell, R.G. (2012) Regional sea level trends in New Zealand. Journal of Geophysical Research 117: C01004.

Hicks, M. D., Shankar, U., McKerchar, A. I., Basher, L., Jessen, M., Lynn, I. and Page, M. (2011). Suspended sediment yields from New Zealand rivers. Journal of Hydrology (NZ) 50 (1): 81-142.

IPCC (2013). Working Group I contribution to the IPCC 5th Assessment Report "Climate Change 2013: The Physical Science Basis". DRAFT report by Intergovernmental Panel on Climate Change. June, 2013.

Komar, P. D. (1998) Beach Processes and Sedimentation: 2nd edition, Prentice-Hall, Upper Saddle River, New Jersey, 544 pp.

Komar, P.D., McDougal, W.G., Marra, J.J. and Ruggiero, P. (1999). The Rational Analysis of Setback Distances: Application to the Oregon Coast. Shore and Beach Vol. 67 (1) 41-49.

Kopp RE, Horton RM, Little CM, Mitrovica JX, Oppenheimer M, Rasmussen DJ, Strauss BH, Tebaldi C. 2014. Probabilistic 21st and 22nd century sea-level projections at a global network of tide-gauge sites. Earth's Future 2(8): 383–406.

Leatherman, S. (1983). Barrier dynamics and landward migration with Holocene sea-level rise. Nature, volume 301. 3 February 1983.

Ministry for the Environment (2017). Coastal hazards and climate change: guidance for local government.

Nicholls, R.J., Laron, M., Capobianco, M. and Birkemeier, W.A. (1998) Depth of Closure: Improving Understanding and Prediction. ICCE 1998.

NIWA (2019). NIWA Coastal Calculator prepared for Bay of Plenty Regional Council.

NCC (2007). The dynamics of mixed sand and gravel beaches and the Hawke's Bay monitoring programme. Napier City Council

Ranasinghe, R., Callaghan, C. and Stive, M.J.F (2011) Estimating coastal recession due to SLR: beyond the Bruun rule. Climate change June 2010.

Shand, T D, Goodwin, I D, Mole, M A, Carley, J T, Harley, M D and Peirson, W L (2010), NSW Coastal Inundation Hazard Study: Coastal Storms and Extreme Waves, WRL TR2010/16.

Shand, T.D., C Wasko, S Westra, G Smith, J T Carley and W L Peirson (2012) Joint Probability Assessment of NSW Extreme Waves and Water Levels. WRL Technical Report 2011/29. April 2012

Shand, R.D., (2012), Kapiti Coast erosion hazard assessment, 2012 Update report prepared for the Kapiti Coast District Council by Coastal Systems Ltd. Client report No. 2012-8 CRep, August 2012.

Shand, T. D., Shand, R.D., Reinen-Hamill, R., Carley, J.T. and Cos, R.J. (2013). A Review of Shoreline Response Models to Changes in Sea Level. Australasian Coasts and Ports Conference, Sept 2013.

Shulmeister, J. & Jennings, R. (2009). Morphology and morphodynamics of gravel beaches. Coastal Zones and Estuaries.

Shulmeister, J. and Rouse, H. (2003). Gravel and mixed sand and gravel beach systems. The New Zealand Coast: Te Tai O Aotearoa.

Smith, R.K. (1986) Motu river sediments: A source of eastern Bay of Plenty beach material. In Motu River: A description of its catchment, channel, waters and sediments. Miscellaneous Publication 92, Water and Soil Directorate, Ministry of Works and Development, Wellington

Stevens, H. and Giles, G. (2010) eShorance: an online methodology for estimating the response of estuarine shores from SLR. 19th NSW Coast Conf.

Tonkin + Taylor (2004) Hawkes Bay Regional Coastal Hazard Assessment. Report prepared for Hawkes Bay Regional Council.

Tonkin + Taylor (2017) Coastal Hazard Assessment for Christchurch and Banks Peninsula (2017). Technical report prepared for Christchurch City Council.

Tonkin + Taylor (2018) Te Tumu Natural Hazard Assessment – Coastal Hazard. Technical report prepared for Tauranga City Council.

Tonkin + Taylor (2019). Tauranga Harbour Coastal Hazards Study – Coastal Erosion Assessment. Technical report prepared for Bay of Plenty Regional Council.

Tonkin + Taylor (2020). Ōpōtiki Coastal Erosion Hazard Assessment –Stage 1 Waiōtahe. Technical report prepared for Bay of Plenty Regional Council.

Appendix A: Site assessments

Appendix B: Historic shoreline summary

Green shading indicates shorelines used for linear regression analysis

Site	Year	Line Type	Survey Type	Spatial coverage
Ōhiwa	1867	MHWM	Unknown	Partial (Eastern end)
	1911	Edge of vegetation	Cadastral	Partial (western end)
	1945	Toe of dune	Air survey	Complete
	1971	HWM	Air survey	Partial (western end)
	1983	Toe of dune	Air survey	Complete
	1994	Unknown	GPS	Complete
	2015	Toe of dune	Aerial	Complete
Hikuwai	1866	Edge of vegetation	Cadastral	Partial (west and centre)
	1880	Sand ridges	Cadastral	Partial
	1945	Toe of dune	Air survey	Partial (western end)
	1948	Toe of dune	Air survey	Partial (Eastern end)
	1965	Toe of dune	Air survey	Segments
	1974	Toe of dune	Air survey	Partial (centre)
	1981	Toe of dune	Air survey	Partial (centre and east)
	1983	Toe of dune	Air survey	Partial (western end)
	1994	Unknown	GPS	Complete
	2000	Dune toe	GPS	Complete
	2015	Toe of dune	Aerial	Complete
Tōrere	1895	HWM	Cadastral	Partial (western end)
	1895	LDW	Cadastral	Partial (western end)
	1916	HWM	Cadastral	Partial (Eastern end)
	1948	HWS	Air survey	Partial (centre)
	1948	Dune toe	Air survey	Partial (east and west)
	1965	HWS	Air survey	Partial (centre)
	1971	HWS	Air survey	Partial (centre)
	1981	HWS	Air survey	Complete
	2011	Wood debris	Aerial	Partial (Eastern end)
	2011	Edge of vegetation	Aerial	Partial
	2011	MHWS	LiDAR	Complete
	2015	Edge of vegetation	Aerial	Complete
	2015	Wood debris	Aerial	Complete
Hāwai	1910	Edge of vegetation	Cadastral	Complete
	1910	HWM	Cadastral	Complete
	1948	HWS	Air survey	Partial (centre)

Site	Year	Line Type	Survey Type	Spatial coverage
	1948	Dune toe	Air survey	Partial (Eastern end)
	1965	HWS	Air survey	Partial (centre)
	1971	HWS	Air survey	Partial (centre)
	1981	HWS	Air survey	Partial (centre)
	1981	Dune toe	Air survey	Partial
	1994	Unknown	GPS	Complete
	2011	MHWS	LiDAR	Complete
	2015	Edge of vegetation	Aerial	Complete
	2015	Wood debris	Aerial	Complete
Houpoto	1957	HWS	Air survey	Complete
	1971	HWS	Air survey	Partial (Eastern end)
	1981	HWS	Air survey	Complete
	2011	MHWS	LiDAR	Complete
	2015	Edge of vegetation	Aerial	Complete
	2019	High Water Mark	Aerial	Complete
Ōmaio	1913	SWESB	Cadastral	Partial (Eastern end)
	1916	HWM	Cadastral	Partial (western end)
	1957	HWS	Air survey	Complete
	1962	HWS	Air survey	Partial (Eastern end)
	1970	HWS	Air survey	Partial (Eastern end)
	1981	HWS	Air survey	Complete
	2011	MHWS	LiDAR	Complete
	2015	Edge of vegetation	Aerial	Complete
	2015	Wood debris	Aerial	Complete
	2019	High Water Mark	Aerial	Complete
Maraetai	1909	Edge of vegetation	Cadastral	Complete
	1951	HWS	Air survey	Complete
	1980	Toe of cliff	Air survey	Complete
	2011	Edge of vegetation	Aerial	Complete
	2019	Edge of vegetation	Aerial	Complete
Wharekura	1909	Edge of vegetation	Cadastral	Complete
	1951	HWS	Air survey	Complete
	1980	HWS	Air survey	Complete
	2011	Edge of vegetation	Aerial	Complete
	2011	Wood debris	Aerial	Complete
	2011	MHWS	LiDAR	Complete
	2019	High Water Mark	Aerial	Complete
Whanarua	1909	Edge of vegetation	Cadastral	Complete
	1980	Toe of cliff	Air survey	Complete

Site	Year	Line Type	Survey Type	Spatial coverage
	2007	Edge of vegetation	Aerial	Segments
	2007	Wood debris	Aerial	Segments
	2011	Edge of vegetation	Aerial	Partial (western end)
	2011	Wood debris	Aerial	Partial (western end)
	2011	MHWS	LiDAR	Complete
	2019	Edge of vegetation	Aerial	Complete
Papatea	1908	EL	Cadastral	Partial (Eastern end)
	1916	HWM	Cadastral	Partial (western end)
	1918	Edge of vegetation	Cadastral	Partial (western end)
	1918	HWM	Cadastral	Partial (western end)
	1951	HWS	Air Survey	Complete
	1980	HWS	Air Survey	Complete
	2011	Wood debris	Aerial	Partial (Eastern end)
	2011	MHWS	LiDAR	Complete
	2015	Wood debris	Aerial	Partial (western end)
	2015	Edge of vegetation	Aerial	Complete
	2019	High Water Mark	Aerial	Complete
Raukōkore	1914	Edge of vegetation	Cadastral	Complete
	1914	HWM	Cadastral	Partial (centre)
	1951	HWS	Air survey	Segments
	1980	HWS	Air survey	Complete
	2011	MHWS	LiDAR	Complete
	2015	Edge of vegetation	Aerial	Almost complete
	2019	Edge of vegetation	Aerial	Complete
Waihau	1905	Edge of vegetation	Cadastral	Partial (western end)
	1914	Edge of vegetation	Cadastral	Partial (Eastern end)
	1951	HWS	Air Survey	Segments
	1980	HWS	Air Survey	Complete
	2011	MHWS	LiDAR	Complete
	2011	Edge of vegetation	Aerial	Partial (centre)
	2015	Edge of vegetation	Aerial	Partial (western end)
	2019	Edge of vegetation	Aerial	Complete
Oruaiti	1911	Unknown	Cadastral Survey	Partial (Eastern end)
	1914	HWM	Cadastral Survey	Partial (western end)
	1951	HWM	Air Survey	Complete
	1951	Dune toe	Air survey	Complete
	1980	Dune toe	Air Survey	Complete
	2007	Dune toe	Aerial	Partial (Eastern end)
	2015	Edge of vegetation	Aerial	Partial (western end)

Site	Year	Line Type	Survey Type	Spatial coverage
	2019	Edge of vegetation	Aerial	Complete
Whangaparaoa	1914	HWM	Cadastral Survey	Partial
	1915	HWM	Cadastral Survey	Complete
	1951	HWS	Air Survey	Complete
	1960	HWS	Air Survey	Partial (Eastern end)
	1970	HWS	Air Survey	Partial (Eastern end)
	1980	AS Channels	Unknown	River
	1980	HWS	Air Survey	Complete
	2007	Edge of vegetation	Aerial	Complete
	2011	MHWS	LiDAR	Complete
	2015	Edge of vegetation	Aerial	Partial (western end)
	2019	High Water Mark	Aerial	Complete

Appendix C: Historic shoreline maps

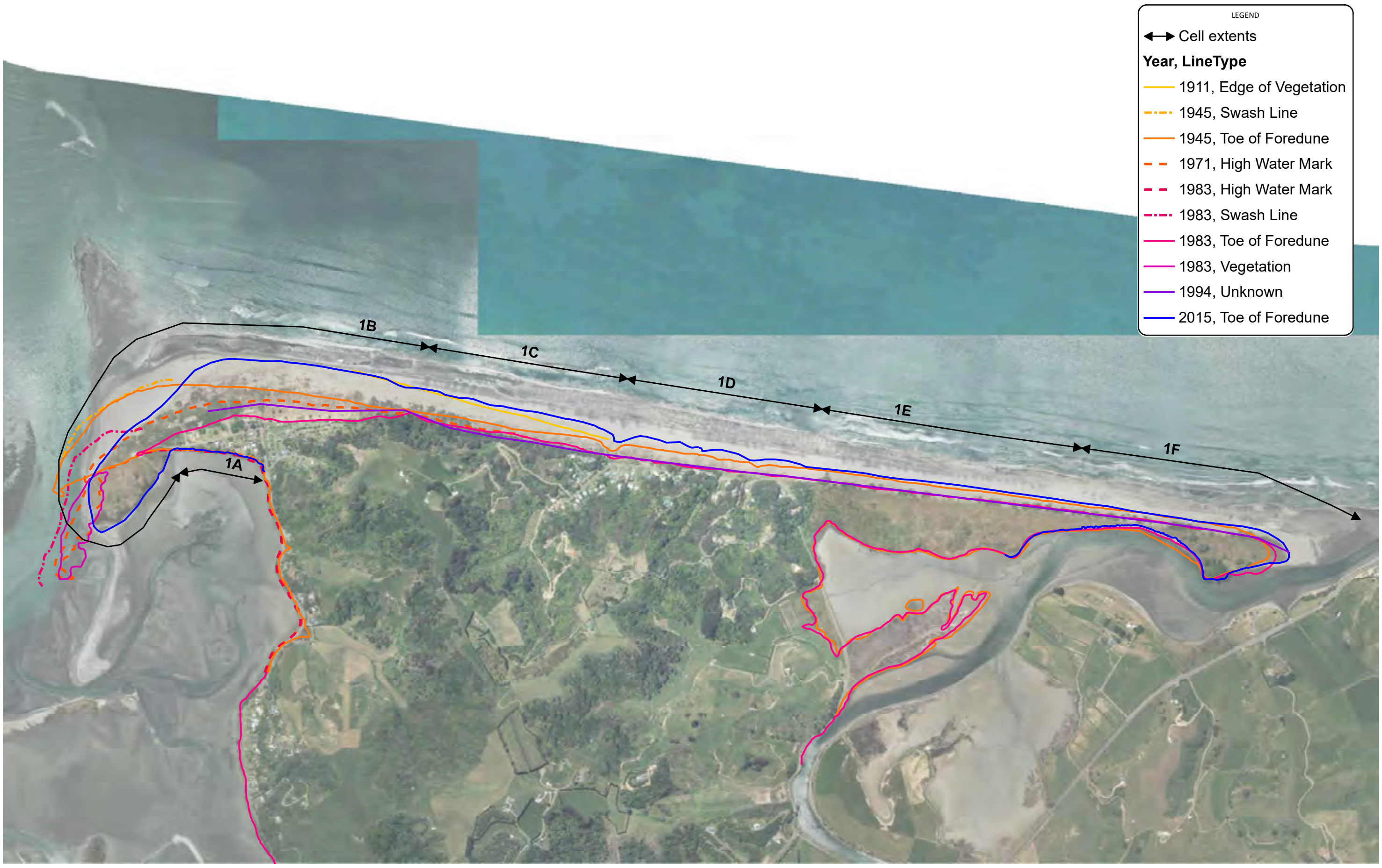

Notes: Aerial photograph (2015) sourced from LINZ Data Service

A3 SCALE 1:13,071

0 0.1 0.2 0.3 0.4 0.5 (km)

N

Location Plan

Tonkin+Taylor

105 Carlton Gore Rd, Newmarket, Auckland
www.tonkintaylor.co.nz

DRAWN	RHAU	Apr.21
CHECKED		
APPROVED		

ARCFILE Shorelines_Ohiwa.mxd

SCALE (AT A3 SIZE) 1:13,071

PROJECT No. 1008669.2000

Opotiki Coastal Erosion Assessment

Historic shorelines

Site: Ohiwa

FIGURE No. Figure 1.

Rev. 0

Path: T:\Tauranga\Projects\1008669\1008669.2000\WorkingMaterial\GIS\Shoreline analysis\Shorelines_Ohiwa.mxd Date: 29/04/2021 Time: 9:11:21 AM

Notes: Aerial photograph (2015) sourced from LINZ Data Service

A3 SCALE 1:10,000

0 0.1 0.2 0.3 0.4 0.5 (km)

Location Plan

Tonkin+Taylor

105 Carlton Gore Rd, Newmarket, Auckland
www.tonkintaylor.co.nz

DRAWN	RHAU	Jul.20
CHECKED		
APPROVED		
ARCFILE Shorelines_Hikuwai.mxd		
SCALE (AT A3 SIZE) 1:10,000		
PROJECT No. 1008669.2000		

Opotiki Coastal Erosion Assessment

Historic shorelines

Site: Hikuwai

FIGURE No. Figure 2

Rev. 0

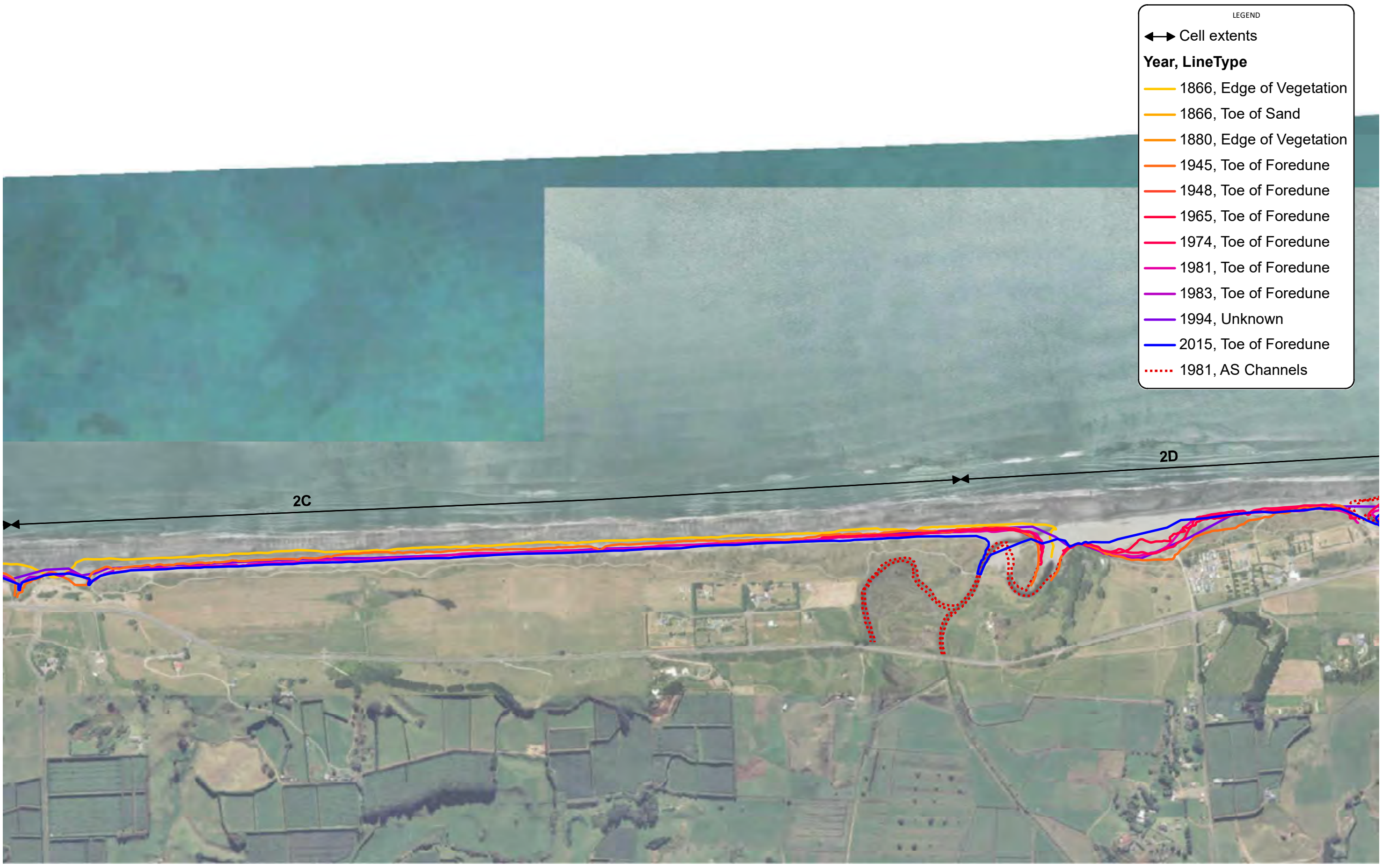

Notes: Aerial photograph (2015) sourced from LINZ Data Service

A3 SCALE 1:10,000

0 0.1 0.2 0.3 0.4 0.5 (km)

Tonkin+Taylor

105 Carlton Gore Rd, Newmarket, Auckland

www.tonkintaylor.co.nz

DRAWN	RHAU	Jul.20
CHECKED		
APPROVED		
ARCFILE Shorelines_Hikuwai.mxd		
SCALE (AT A3 SIZE) 1:10,000		
PROJECT No. 1008669.2000		

Opotiki Coastal Erosion Assessment

Historic shorelines

Site: Hikuwai

FIGURE No. Figure 3

Rev. 0

Path: T:\Tauranga\Projects\1008669\1008669.2000\WorkingMaterial\GIS\Shoreline analysis\Shorelines_Hikuwai.mxd Date: 13/07/2020 Time: 8:53:00 AM

Notes: Aerial photograph (2015) sourced from LINZ Data Service

A3 SCALE 1:10,000

0 0.1 0.2 0.3 0.4 0.5 (km)

Location Plan

Tonkin+Taylor

105 Carlton Gore Rd, Newmarket, Auckland
www.tonkintaylor.co.nz

DRAWN	RHAU	Jul.20
CHECKED		
APPROVED		
ARCFILE Shorelines_Hikuwai.mxd		
SCALE (AT A3 SIZE) 1:10,000		
PROJECT No. 1008669.2000		

Opotiki Coastal Erosion Assessment
Historic shorelines
Site: Hikuwai

FIGURE No. Figure 4 Rev. 0

Path: T:\Tauranga\Projects\1008669\1008669.2000\WorkingMaterial\GIS\Shoreline analysis\Shorelines_Hikuwai.mxd Date: 13/07/2020 Time: 8:53:30 AM

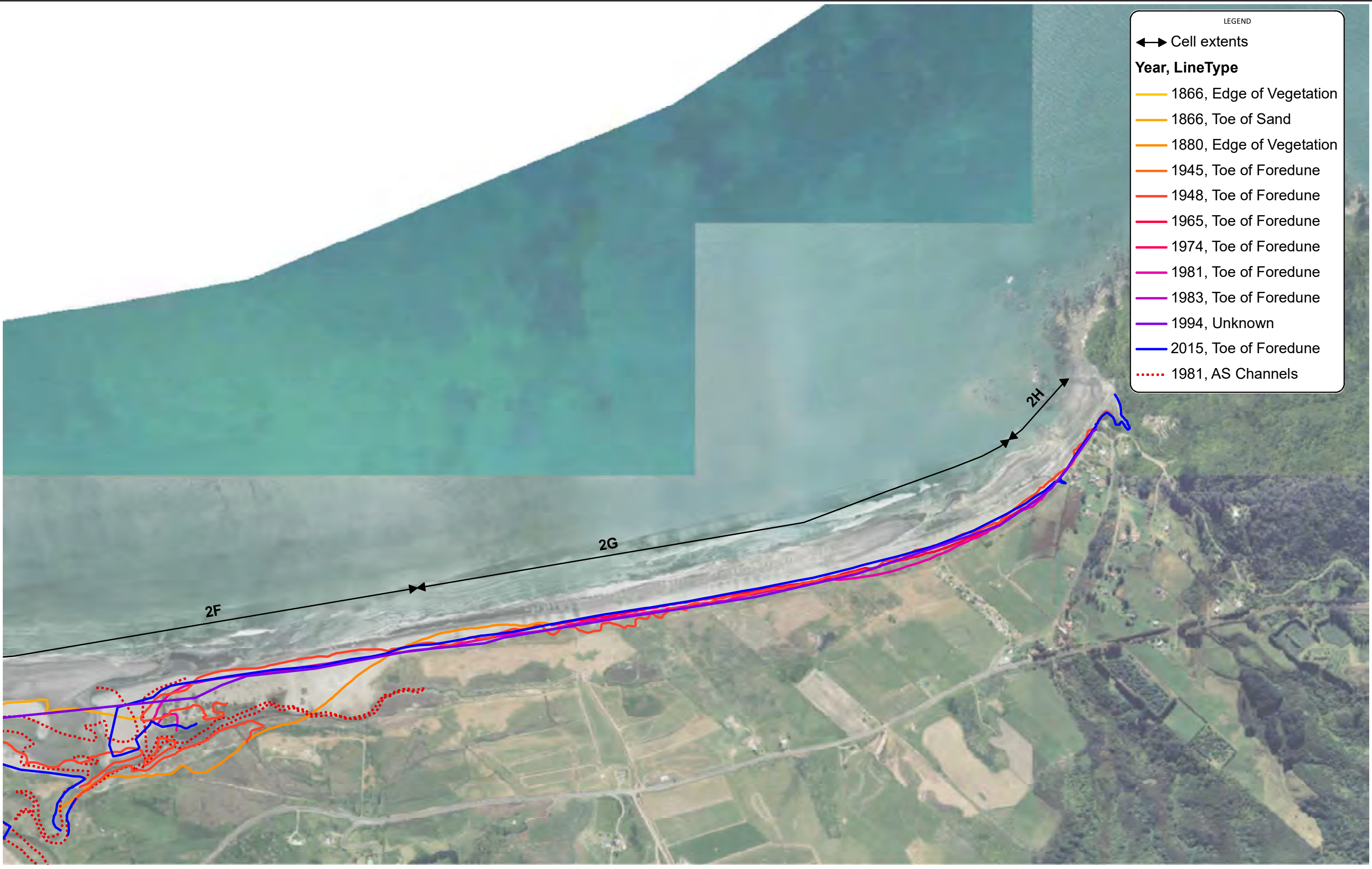

Notes: Aerial photograph (2015) sourced from LINZ Data Service

A3 SCALE 1:10,000

0 0.1 0.2 0.3 0.4 0.5 (km)

Tonkin+Taylor
105 Carlton Gore Rd, Newmarket, Auckland
www.tonkintaylor.co.nz

DRAWN	RHAU	Jul.20
CHECKED		
APPROVED		
ARCFILE Shorelines_Hikuwai.mxd		
SCALE (AT A3 SIZE) 1:10,000		
PROJECT No. 1008669.2000		

Opotiki Coastal Erosion Assessment
Historic shorelines
Site: Hikuwai

FIGURE No. Figure 5 Rev. 0

Path: T:\Tauranga\Projects\1008669\1008669.2000\WorkingMaterial\GIS\Shoreline analysis\Shorelines_Hikuwai.mxd Date: 13/07/2020 Time: 8:54:33 AM

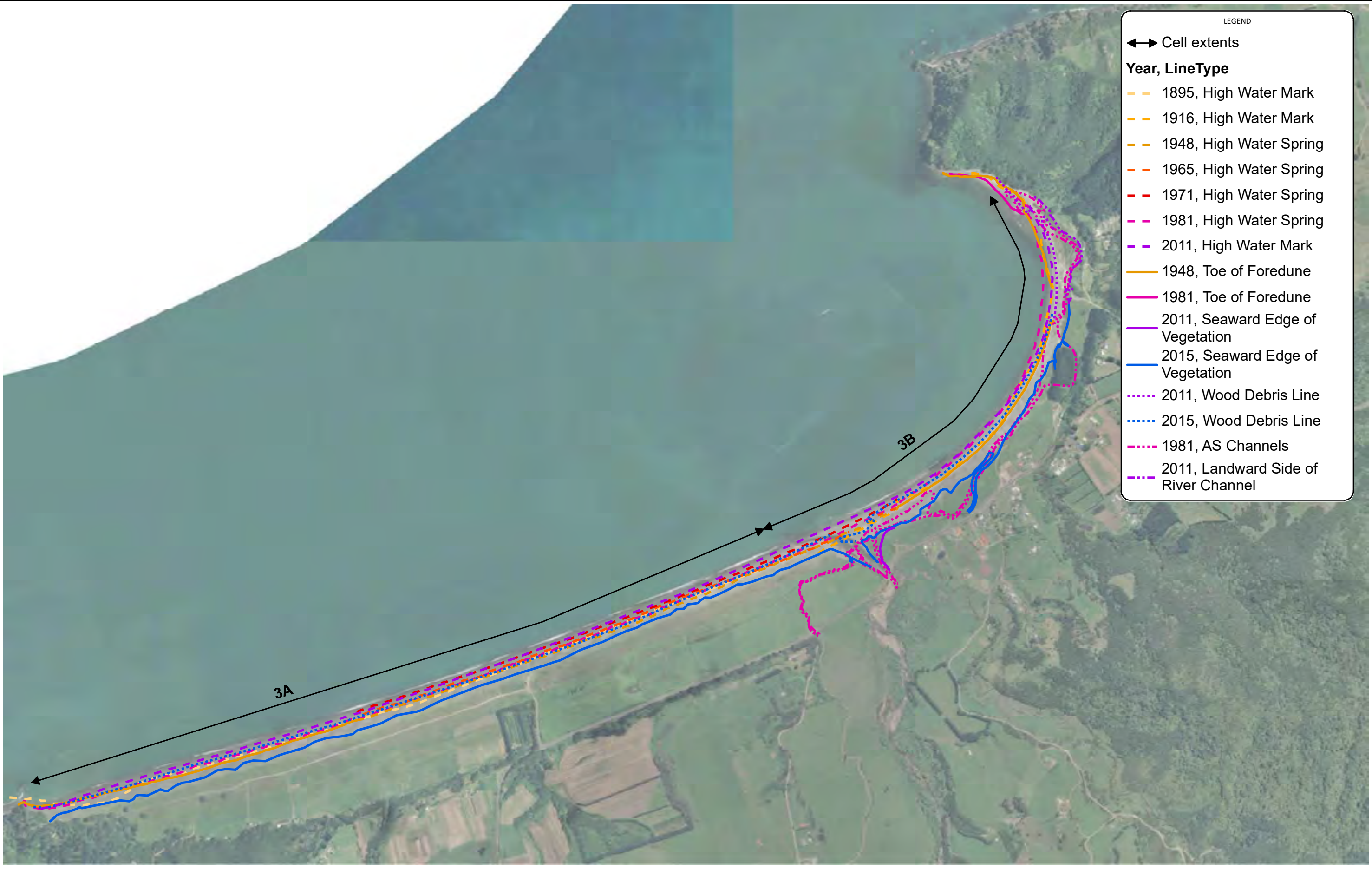

Notes: Aerial photograph (2011) sourced from LINZ Data Service

A3 SCALE 1:13,000

0 0.15 0.3 0.45 0.6 0.75 (km)

Tonkin+Taylor

105 Carlton Gore Rd, Newmarket, Auckland

www.tonkintaylor.co.nz

DRAWN	RHAU	Jul.20
CHECKED		
APPROVED		
ARCFILE Shorelines_Torere.mxd		
SCALE (AT A3 SIZE) 1:13,000		
PROJECT No. 1008669.2000		

Opotiki Coastal Erosion Assessment

Historic shorelines

Site: Torere

FIGURE No. Figure 6

Rev. 0

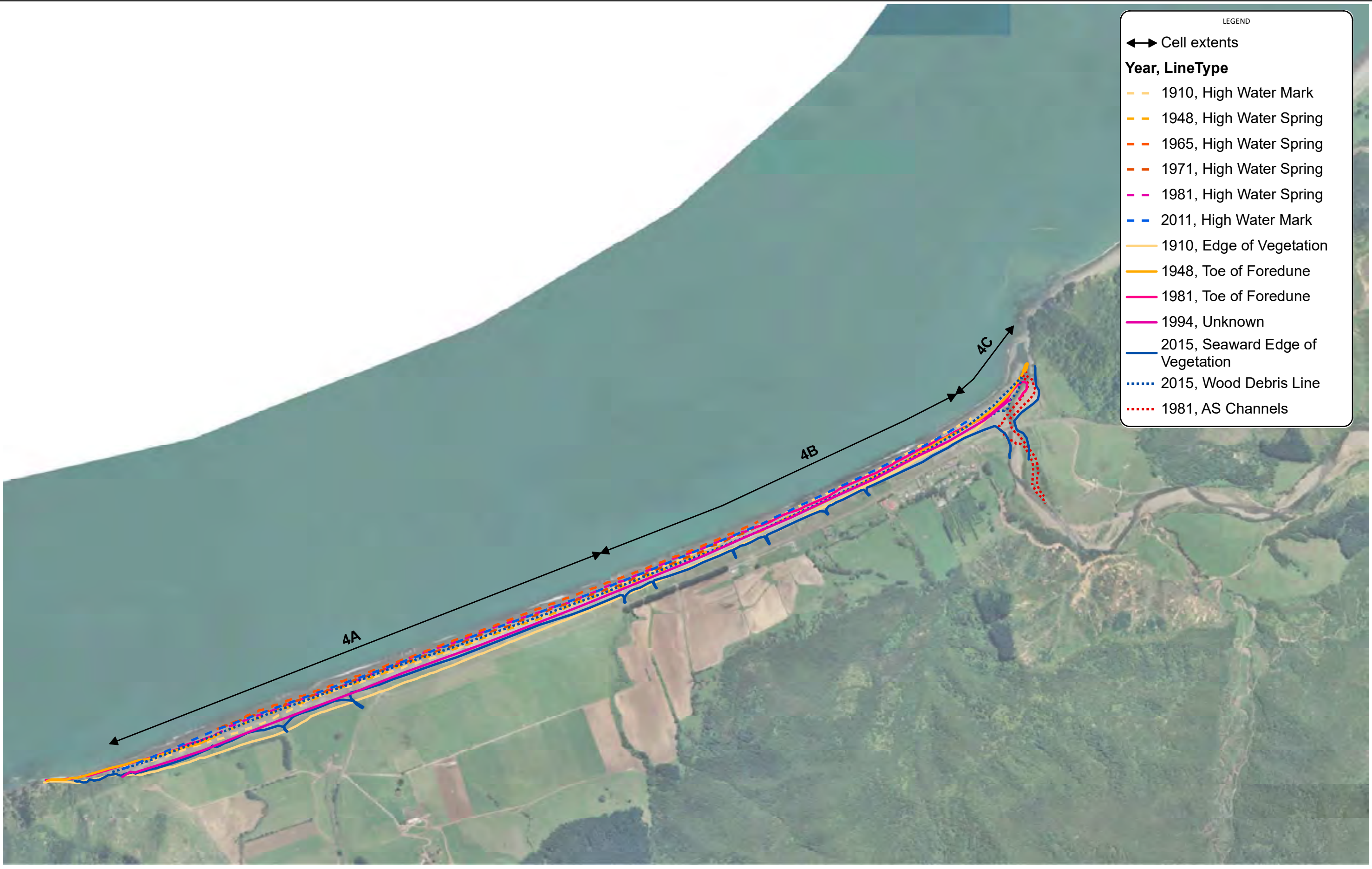

Notes: Aerial photograph (2011) sourced from LINZ Data Service

A3 SCALE 1:13,000

0 0.15 0.3 0.45 0.6 0.75 (km)

N

Tonkin+Taylor

105 Carlton Gore Rd, Newmarket, Auckland
www.tonkintaylor.co.nz

DRAWN	RHAU	Jul.20
CHECKED		
APPROVED		
ARCFILE Shorelines_Hawai.mxd		
SCALE (AT A3 SIZE) 1:13,000		
PROJECT No. 1008669.2000		

Opotiki Coastal Erosion Assessment

Historic shorelines

Site: Hawai

FIGURE No. Figure 7

Rev. 0

Path: T:\Tauranga\Projects\1008669\1008669.2000\WorkingMaterial\GIS\Shoreline analysis\Shorelines_Hawai.mxd Date: 8/07/2020 Time: 9:25:17 AM

Notes: Aerial photograph (2011) sourced from LINZ Data Service

A3 SCALE 1:16,000

0 0.15 0.3 0.45 0.6 0.75 (km)

Location Plan

Tonkin+Taylor
105 Carlton Gore Rd, Newmarket, Auckland
www.tonkintaylor.co.nz

DRAWN	RHAU	Jul.20
CHECKED		
APPROVED		
ARCFILE Shorelines_Houpoto.mxd		
SCALE (AT A3 SIZE) 1:16,000		
PROJECT No. 1008669.2000		

Opotiki Coastal Erosion Assessment
Historic shorelines
Site: Houpoto

FIGURE No. Figure 8

Rev. 0

Path: T:\Tauranga\Projects\1008669\1008669.2000\WorkingMaterial\GIS\Shoreline analysis\Shorelines_Houpoto.mxd Date: 8/07/2020 Time: 9:09:21 AM

Notes: Aerial photograph (2019) sourced from LINZ Data Service

A3 SCALE 1:11,000

0 0.1 0.2 0.3 0.4 0.5 (km)

Tonkin+Taylor

105 Carlton Gore Rd, Newmarket, Auckland

www.tonkintaylor.co.nz

DRAWN	RHAU	Jul.20
CHECKED		
APPROVED		
ARCFILE DSAS_Omaio.mxd		
SCALE (AT A3 SIZE) 1:11,000		
PROJECT No. 1008669.2000		

Opotiki Coastal Erosion Assessment

Historic shorelines

Site: Omaio

FIGURE No. Figure 9

Rev. 0

Path: T:\Tauranga\Projects\1008669\1008669.2000\WorkingMaterial\GIS\Shoreline analysis\DSAS_Omaio.mxd Date: 8/07/2020 Time: 8:57:55 AM

Notes: Aerial photograph (2019) sourced from LINZ Data Service

A3 SCALE 1:6,000

0 0.065 0.13 0.195 0.26 0.325 (km)

Location Plan

Tonkin+Taylor

105 Carlton Gore Rd, Newmarket, Auckland

www.tonkintaylor.co.nz

DRAWN	RHAU	Jul.20
CHECKED		
APPROVED		
ARCFILE	Shorelines_Wharekura.mxd	
SCALE (AT A3 SIZE)	1:6,000	
PROJECT No.	1008669.2000	

Opotiki Coastal Erosion Assessment

Historic shorelines

Site: Maraetai Bay and Wharekura

FIGURE No. Figure 10

Rev. 0

Path: T:\Tauranga\Projects\1008669\1008669.2000\WorkingMaterial\GIS\Shoreline analysis\Shorelines_Wharekura.mxd Date: 8/07/2020 Time: 8:45:59 AM

Notes: Aerial photograph (2019) sourced from LINZ Data Service

A3 SCALE 1:3,000

0 0.03 0.06 0.09 0.12 0.15 (km)

Tonkin+Taylor
105 Carlton Gore Rd, Newmarket, Auckland
www.tonkintaylor.co.nz

DRAWN	RHAU	Jul.20
CHECKED		
APPROVED		
ARCFILE Shorelines_Whanarua.mxd		
SCALE (AT A3 SIZE) 1:3,000		
PROJECT No. 1008669.2000		

Opotiki Coastal Erosion Assessment

Historic shorelines

Site: Whanarua Bay

FIGURE No. Figure 11

Rev. 0

Path: T:\Tauranga\Projects\1008669\1008669.2000\WorkingMaterial\GIS\Shoreline analysis\Shorelines_Whanarua.mxd Date: 8/07/2020 Time: 8:17:39 AM

Notes: Aerial photograph (2019) sourced from LINZ Data Service

A3 SCALE 1:11,000

0 0.1 0.2 0.3 0.4 0.5 (km)

Location Plan

Tonkin+Taylor
105 Carlton Gore Rd, Newmarket, Auckland
www.tonkintaylor.co.nz

DRAWN	RHAU	Jul.20
CHECKED		
APPROVED		
ARCFILE Shorelines_Papatea.mxd		
SCALE (AT A3 SIZE) 1:11,000		
PROJECT No. 1008669.2000		

Opotiki Coastal Erosion Assessment
Historic shorelines
Site: Papatea

FIGURE No. Figure 12 Rev. 0

Path: T:\Tauranga\Projects\1008669\1008669.2000\WorkingMaterial\GIS\Shoreline analysis\Shorelines_Papatea.mxd Date: 8/07/2020 Time: 8:05:19 AM

Notes: Aerial photograph (2019) sourced from LINZ Data Service

A3 SCALE 1:8,000
0 0.09 0.18 0.27 0.36 0.45 (km)

Location Plan

Tonkin+Taylor
105 Carlton Gore Rd, Newmarket, Auckland
www.tonkintaylor.co.nz

DRAWN	RHAU	Jul.20
CHECKED		
APPROVED		
ARCFILE Shorelines_Raukokore.mxd		
SCALE (AT A3 SIZE) 1:8,000		
PROJECT No. 1008669.2000		

Opotiki Coastal Erosion Assessment
Historic shorelines
Site: Raukokore

FIGURE No. Figure 13

Rev. 0

Path: T:\Tauranga\Projects\1008669\1008669.2000\WorkingMaterial\GIS\Shoreline analysis\Shorelines_Raukokore.mxd Date: 7/07/2020 Time: 3:28:25 PM

Notes: Aerial photograph (2019) sourced from LINZ Data Service

A3 SCALE 1:10,000
0 0.1 0.2 0.3 0.4 0.5 (km)

Location Plan

Tonkin+Taylor
105 Carlton Gore Rd, Newmarket, Auckland
www.tonkintaylor.co.nz

DRAWN	RHAU	Jul.20
CHECKED		
APPROVED		
ARCFILE Shorelines_Waihau.mxd		
SCALE (AT A3 SIZE) 1:10,000		
PROJECT No. 1008669.2000		

Opotiki Coastal Erosion Assessment
Historic shorelines
Site: Waihau Bay

FIGURE No. Figure 14

Rev. 0

Path: T:\Tauranga\Projects\1008669\1008669.2000\WorkingMaterial\GIS\Shoreline analysis\Shorelines_Waihau.mxd Date: 8/07/2020 Time: 8:06:53 AM

Notes: Aerial photograph (2019) sourced from LINZ Data Service

A3 SCALE 1:5,000

0 0.055 0.11 0.165 0.22 0.275 (km)

Location Plan

Tonkin+Taylor
105 Carlton Gore Rd, Newmarket, Auckland
www.tonkintaylor.co.nz

DRAWN	RHAU	Jul.20
CHECKED		
APPROVED		
ARCFILE Shorelines_Oruaiti.mxd		
SCALE (AT A3 SIZE) 1:5,000		
PROJECT No. 1008669.2000		

Opotiki Coastal Erosion Assessment
Historic shorelines
Site: Oruaiti

FIGURE No. Figure 15

Rev. 0

Path: T:\Tauranga\Projects\1008669\1008669.2000\WorkingMaterial\GIS\Shoreline analysis\Shorelines_Oruaiti.mxd Date: 8/07/2020 Time: 7:56:39 AM

Notes: Aerial photograph (2019) sourced from LINZ Data Service

Tonkin+Taylor
105 Carlton Gore Rd, Newmarket, Auckland
www.tonkintaylor.co.nz

DRAWN	RHAU	Jul.20
CHECKED		
APPROVED		
ARCFILE	Shorelines_Whangaparaoa.mxd	
SCALE (AT A3 SIZE)	1:10,000	
PROJECT No.	1008669.2000	

Opotiki Coastal Erosion Assessment
Historic shorelines
Site: Whangaparaoa

FIGURE No. Figure 16
Rev. 0

Path: T:\Tauranga\Projects\1008669\1008669.2000\WorkingMaterial\GIS\Shoreline analysis\Shorelines_Whangaparaoa.mxd Date: 7/07/2020 Time: 2:25:23 PM

Appendix D: DSAS plots

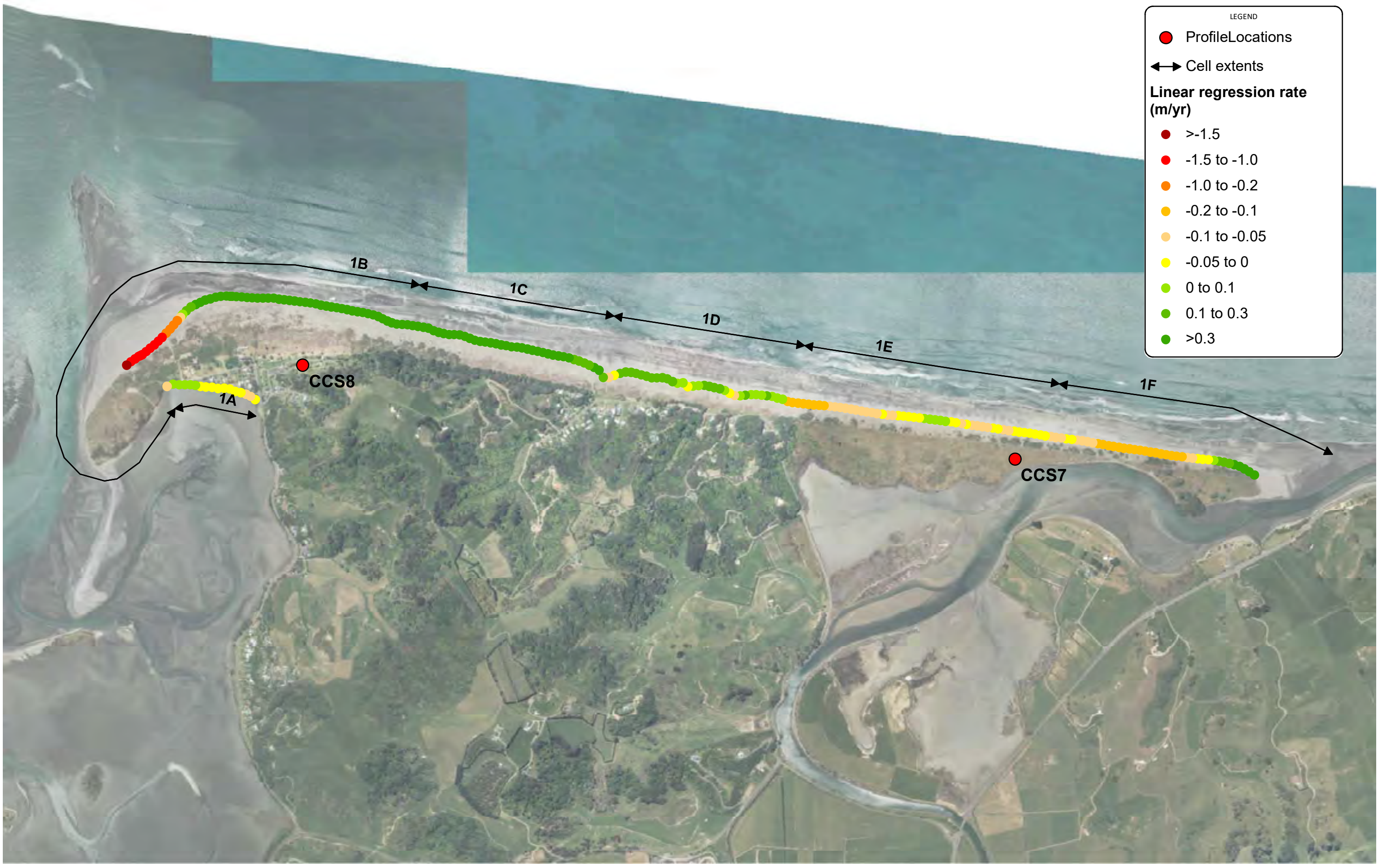

Notes: Aerial photograph (2015) sourced from LINZ Data Service

A3 SCALE 1:13,302

0 0.15 0.3 0.45 0.6 0.75 (km)

Tonkin+Taylor
105 Carlton Gore Rd, Newmarket, Auckland
www.tonkintaylor.co.nz

DRAWN	RHAU	Mar.21
CHECKED		
APPROVED		
ARCFILE Shorelines_Ohiwa.mxd		
SCALE (AT A3 SIZE) 1:13,302		
PROJECT No. 1008669.2000		

Opotiki Coastal Erosion Assessment
Historic shorelines
Site: Ohiwa

FIGURE No. Figure 1. Rev. 0

Path: T:\Tauranga\Projects\1008669\1008669.2000\WorkingMaterial\GIS\Shoreline analysis\Shorelines_Ohiwa.mxd Date: 31/03/2021 Time: 12:00:58 PM

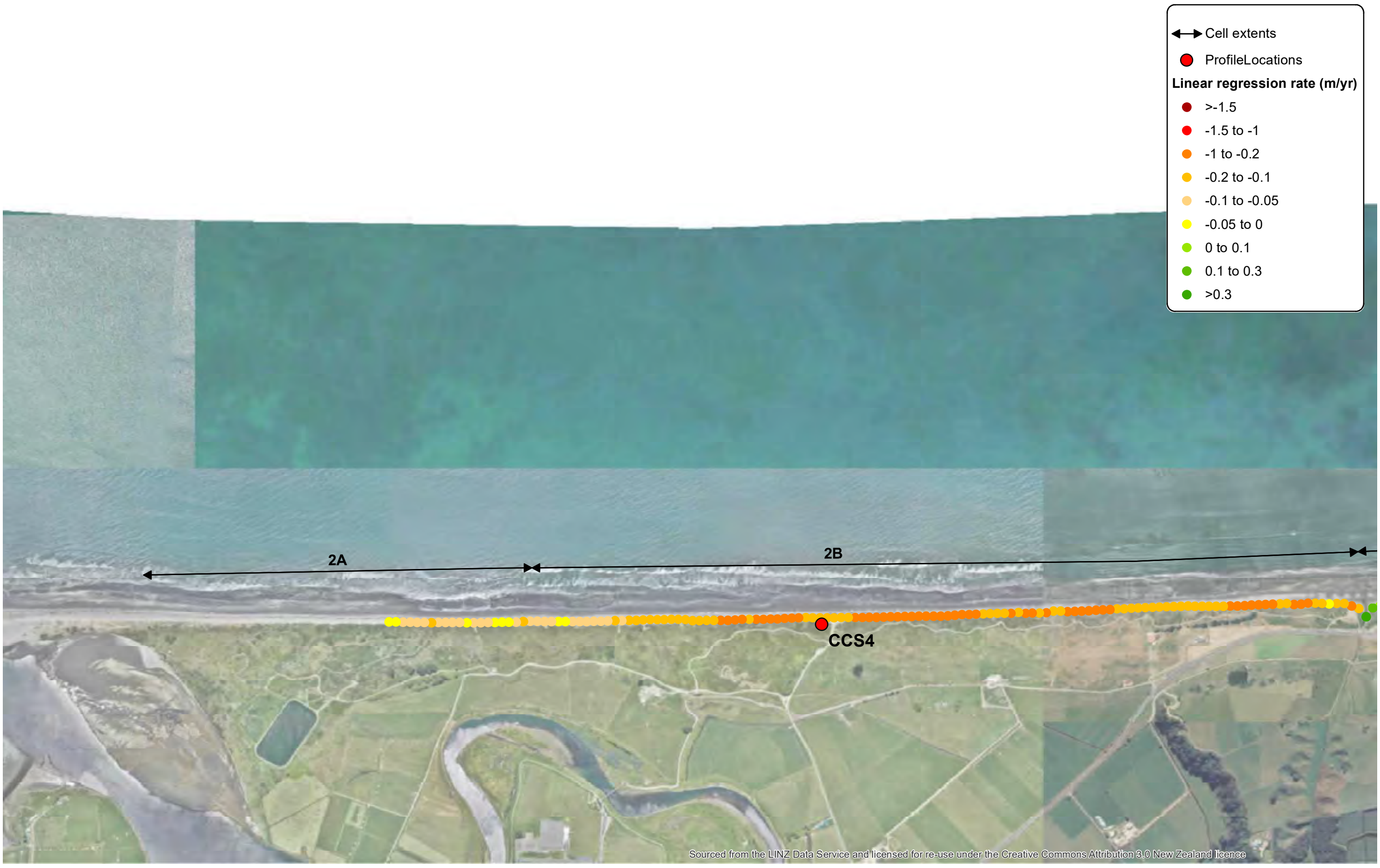

Notes: Aerial photograph (2015-2017) sourced from BOPLASS GIS server

A3 SCALE 1:10,000

0 0.1 0.2 0.3 0.4 0.5 (km)

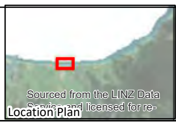

Tonkin+Taylor
105 Carlton Gore Rd, Newmarket, Auckland
www.tonkintaylor.co.nz

DRAWN	RHAU	Jun.20
CHECKED		
APPROVED		
ARCFILE	DSAS_Maps_2.mxd	
SCALE (AT A3 SIZE)	1:10,000	
PROJECT No.	1008669.2000	

Opotiki Coastal Erosion Assessment
DSAS Analysis
Site: Hikuwai

FIGURE No. Figure 2

Rev. 0

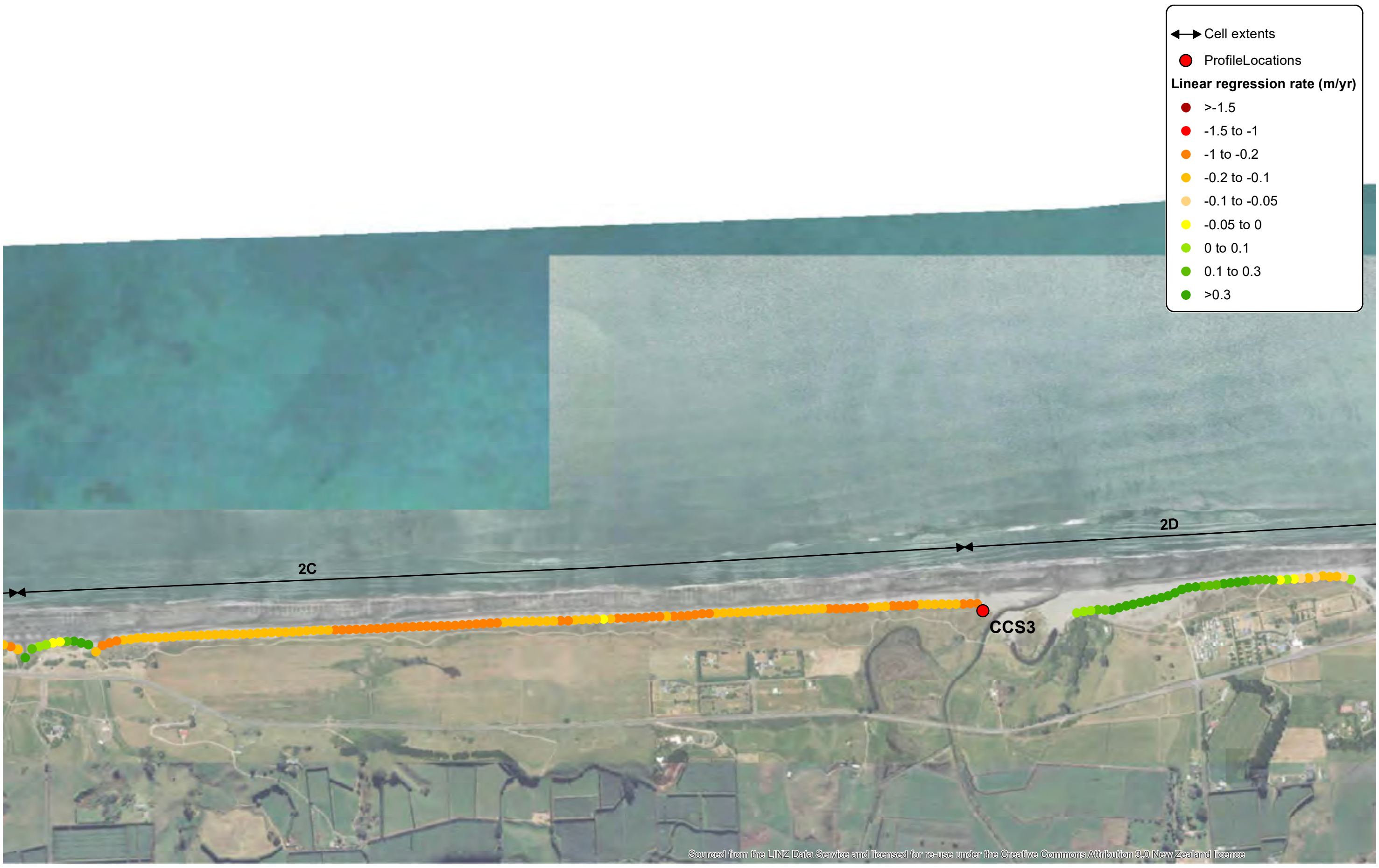

Notes: Aerial photograph (2015-2017) sourced from BOPLASS GIS server

A3 SCALE 1:10,000

0 0.1 0.2 0.3 0.4 0.5 (km)

N

Tonkin+Taylor
105 Carlton Gore Rd, Newmarket, Auckland
www.tonkintaylor.co.nz

DRAWN	RHAU	Jun.20
CHECKED		
APPROVED		
ARCFILE DSAS_Maps_2.mxd		
SCALE (AT A3 SIZE) 1:10,000		
PROJECT No. 1008669.2000		

Opotiki Coastal Erosion Assessment

DSAS Analysis

Site: Hikuwai

FIGURE No. Figure 3

Rev. 0

Path: T:\Tauranga\Projects\1008669\1008669.2000\WorkingMaterial\GIS\Shoreline analysis\DSAS\DSAS_Maps_2.mxd Date: 19/06/2020 Time: 6:54:01 AM

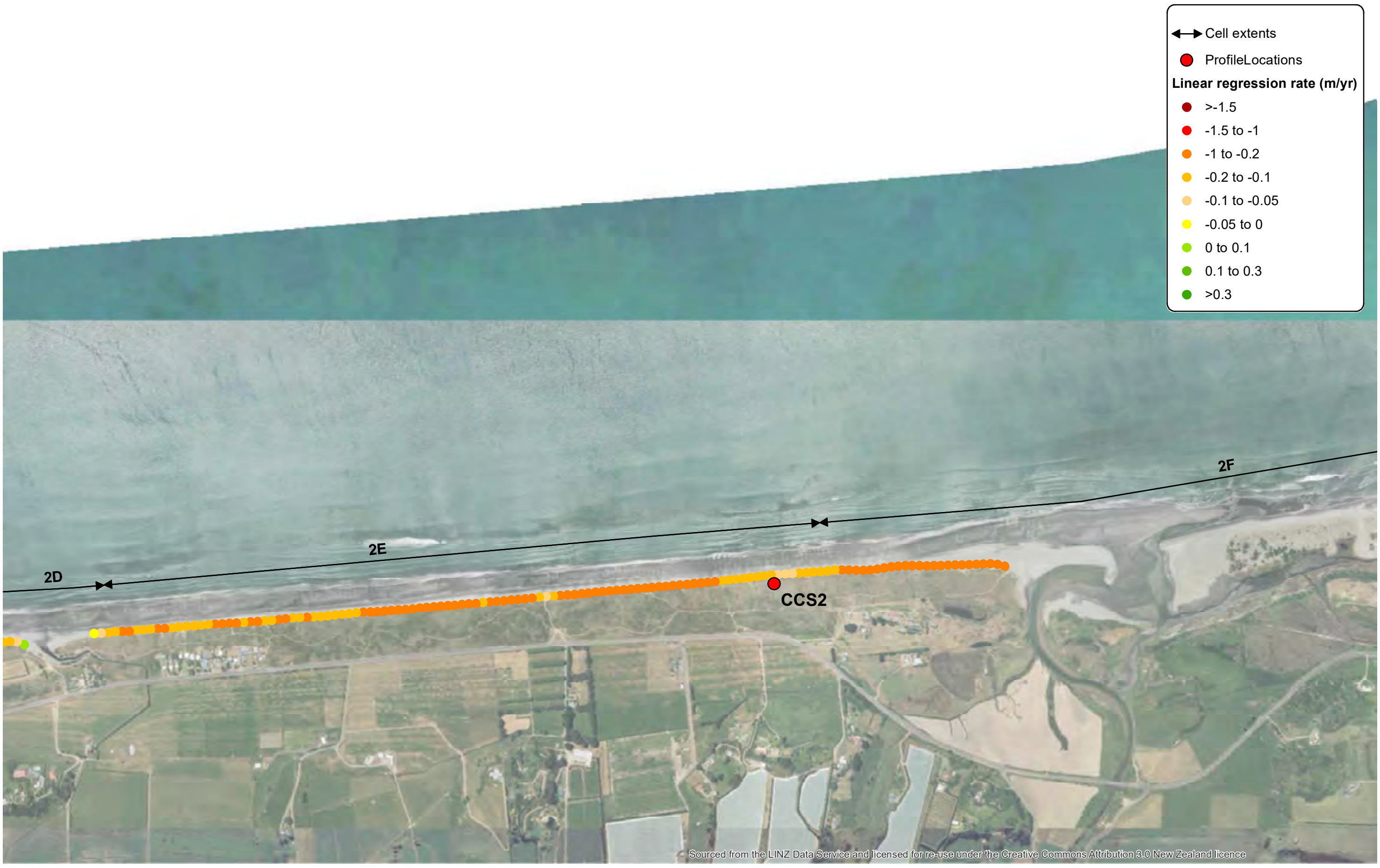

Path: T:\Tauranga\Projects\1008669\1008669.2000\WorkingMaterial\GIS\Shoreline analysis\DSAS\DSAS_Maps_2.mxd Date: 19/06/2020 Time: 6:54:25 AM

Notes: Aerial photograph (2015-2017) sourced from BOPLASS GIS server

A3 SCALE 1:10,000

0 0.1 0.2 0.3 0.4 0.5 (km)

Location Plan

Tonkin+Taylor
105 Carlton Gore Rd, Newmarket, Auckland
www.tonkintaylor.co.nz

DRAWN	RHAU	Jun.20
CHECKED		
APPROVED		

ARCFILE: DSAS_Maps_2.mxd
SCALE (AT A3 SIZE): 1:10,000
PROJECT No.: 1008669.2000

Opotiki Coastal Erosion Assessment
DSAS Analysis
Site: Hikuwai

FIGURE No. Figure 4
Rev. 0

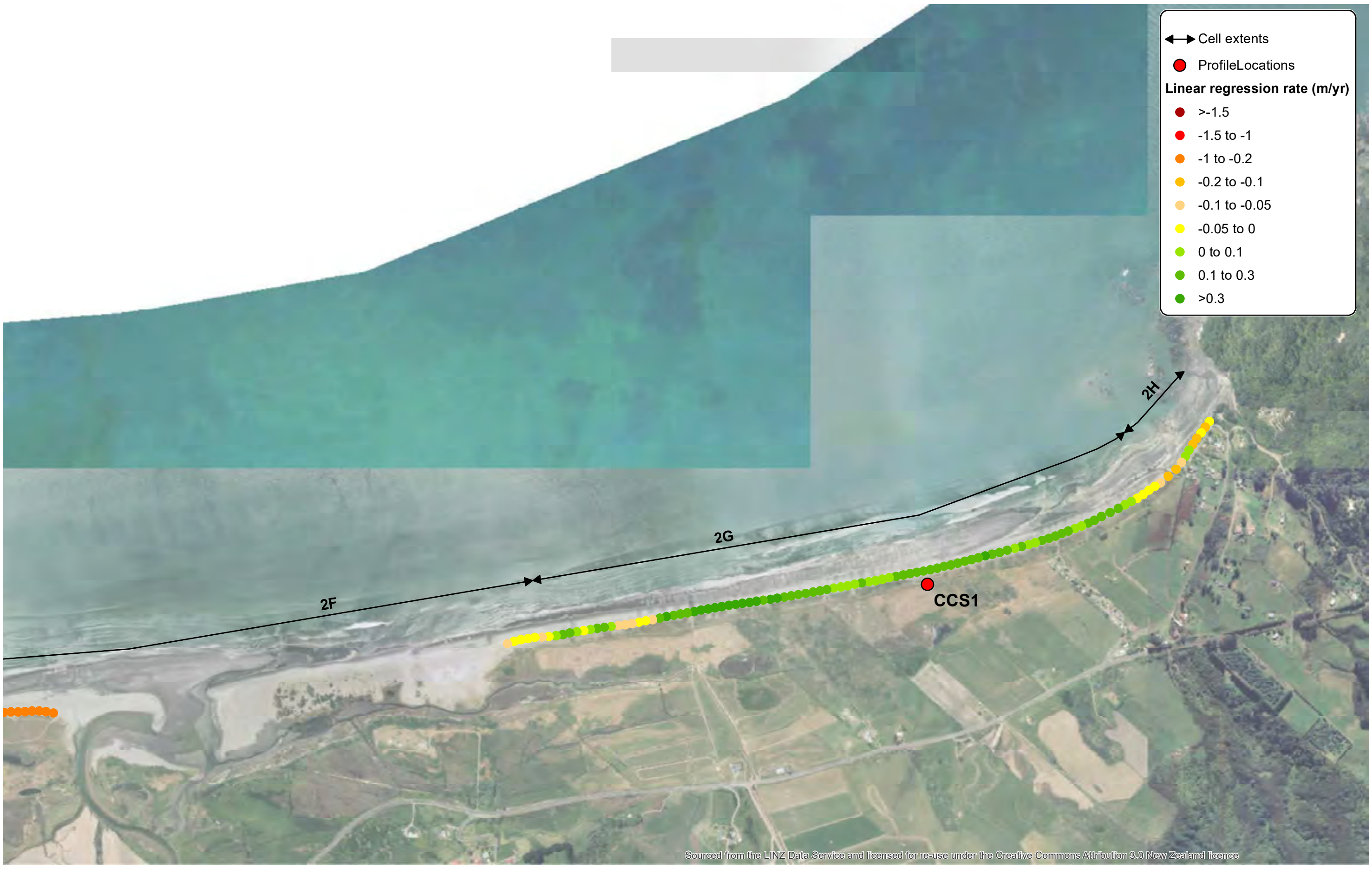

Notes: Aerial photograph (2015-2017) sourced from BOPLASS GIS server

A3 SCALE 1:10,000

0 0.1 0.2 0.3 0.4 0.5 (km)

Tonkin+Taylor
105 Carlton Gore Rd, Newmarket, Auckland
www.tonkintaylor.co.nz

DRAWN	RHAU	Jun.20
CHECKED		
APPROVED		
ARCFILE DSAS_Maps_2.mxd		
SCALE (AT A3 SIZE) 1:10,000		
PROJECT No. 1008669.2000		

Opotiki Coastal Erosion Assessment

DSAS Analysis

Site: Hikuwai

FIGURE No. Figure 5

Rev. 0

Path: T:\Tauranga\Projects\1008669\1008669.2000\WorkingMaterial\GIS\Shoreline analysis\DSAS\DSAS_Maps_2.mxd Date: 19/06/2020 Time: 6:54:48 AM

Notes: Aerial photograph (2015-2017) sourced from BOPLASS GIS server

A3 SCALE 1:12,000

0 0.1 0.2 0.3 0.4 0.5 (km)

Location Plan

Tonkin+Taylor
105 Carlton Gore Rd, Newmarket, Auckland
www.tonkintaylor.co.nz

DRAWN	RHAU	Jun.20
CHECKED		
APPROVED		
ARCFILE DSAS_Maps_2.mxd		
SCALE (AT A3 SIZE) 1:12,000		
PROJECT No. 1008669.2000		

Opotiki Coastal Erosion Assessment

DSAS Analysis

Site: Torere

FIGURE No. Figure 6

Rev. 0

Path: T:\Tauranga\Projects\1008669\1008669.2000\WorkingMaterial\GIS\Shoreline analysis\DSAS\DSAS_Maps_2.mxd Date: 19/06/2020 Time: 7:07:02 AM

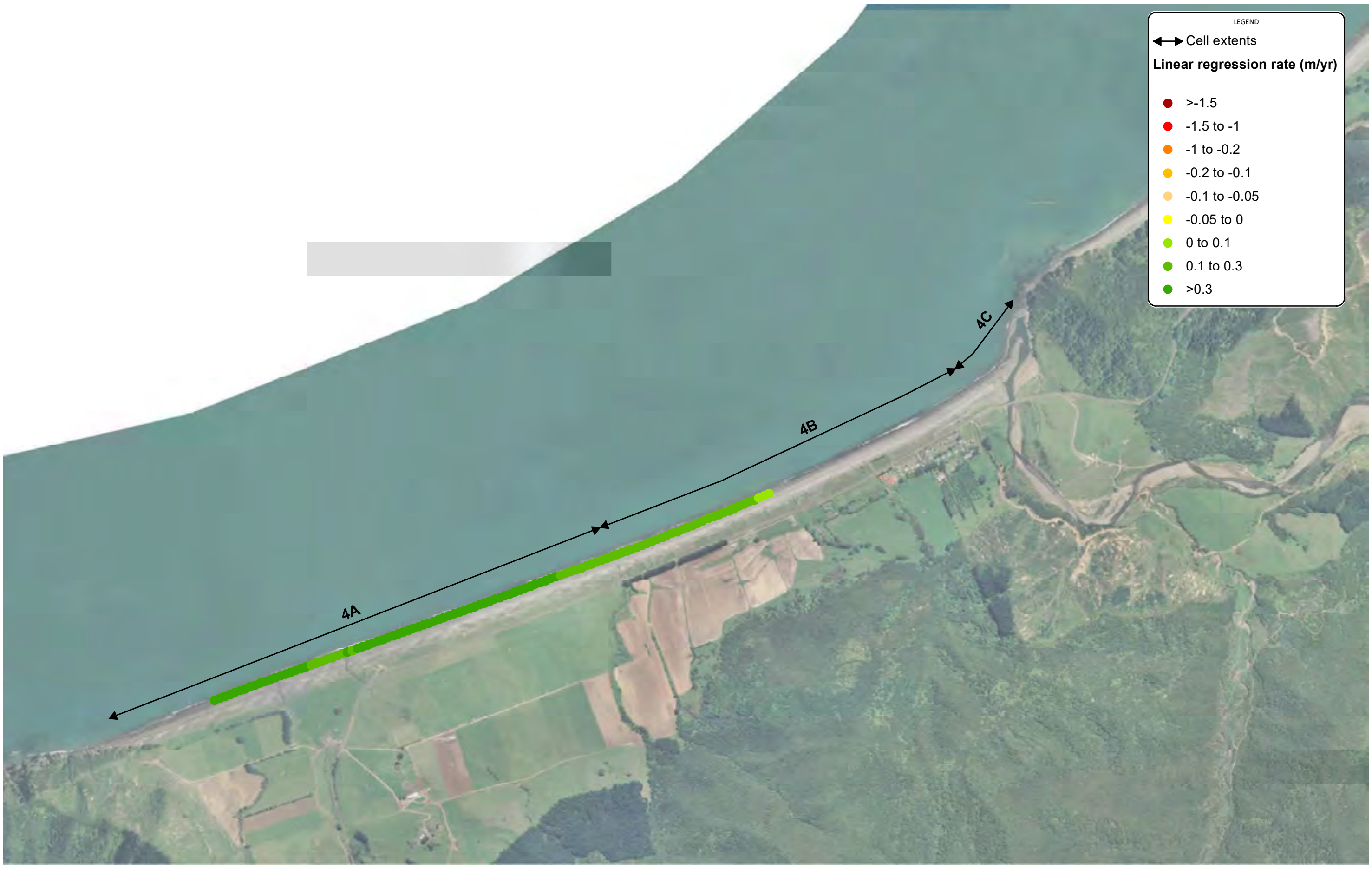

Path: T:\Tauranga\Projects\1008669\1008669.2000\WorkingMaterial\GIS\Shoreline analysis\DSAS\DSAS_Maps_2.mxd Date: 19/06/2020 Time: 7:26:46 AM

Notes: Aerial photograph (2015-2017) sourced from BOPLASS GIS server

Tonkin+Taylor
105 Carlton Gore Rd, Newmarket, Auckland
www.tonkintaylor.co.nz

DRAWN	RHAU	Jun.20
CHECKED		
APPROVED		
ARCFILE DSAS_Maps_2.mxd		
SCALE (AT A3 SIZE) 1:13,000		
PROJECT No. 1008669.2000		

Opotiki Coastal Erosion Assessment
DSAS Analysis
Site: Hawai

FIGURE No. Figure 7

Rev. 0

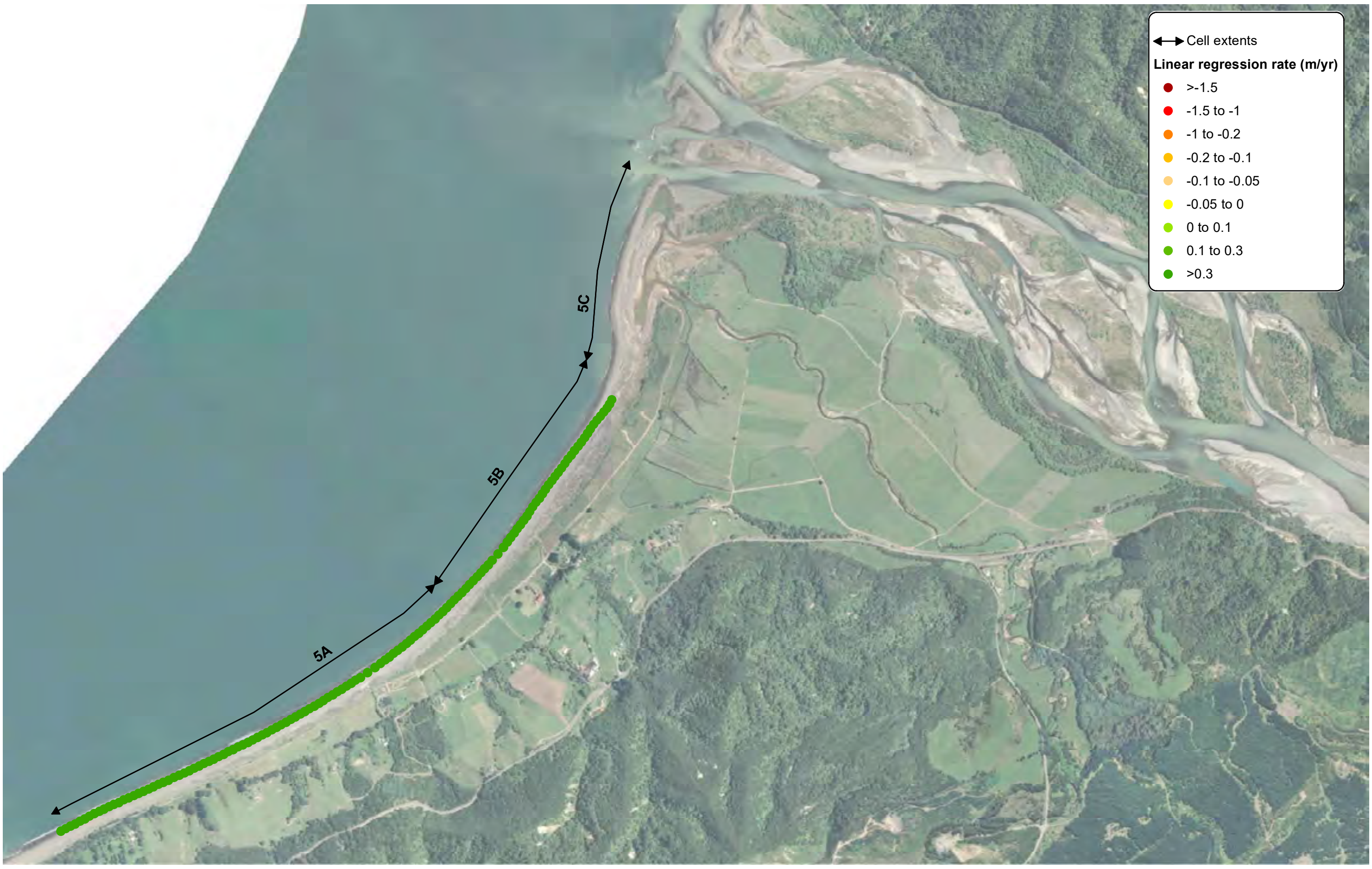

Notes: Aerial photograph (2015-2017) sourced from BOPLASS GIS server

A3 SCALE 1:13,000

0 0.15 0.3 0.45 0.6 0.75 (km)

N

Tonkin+Taylor
105 Carlton Gore Rd, Newmarket, Auckland
www.tonkintaylor.co.nz

DRAWN	RHAU	Jun.20
CHECKED		
APPROVED		
ARCFILE DSAS_Maps_2.mxd		
SCALE (AT A3 SIZE) 1:13,000		
PROJECT No. 1008669.2000		

Opotiki Coastal Erosion Assessment
DSAS Analysis
Site: Houpoto

FIGURE No. Figure 8

Rev. 0

Path: T:\Tauranga\Projects\1008669\1008669.2000\WorkingMaterial\GIS\Shoreline analysis\DSAS\DSAS_Maps_2.mxd Date: 19/06/2020 Time: 7:33:17 AM

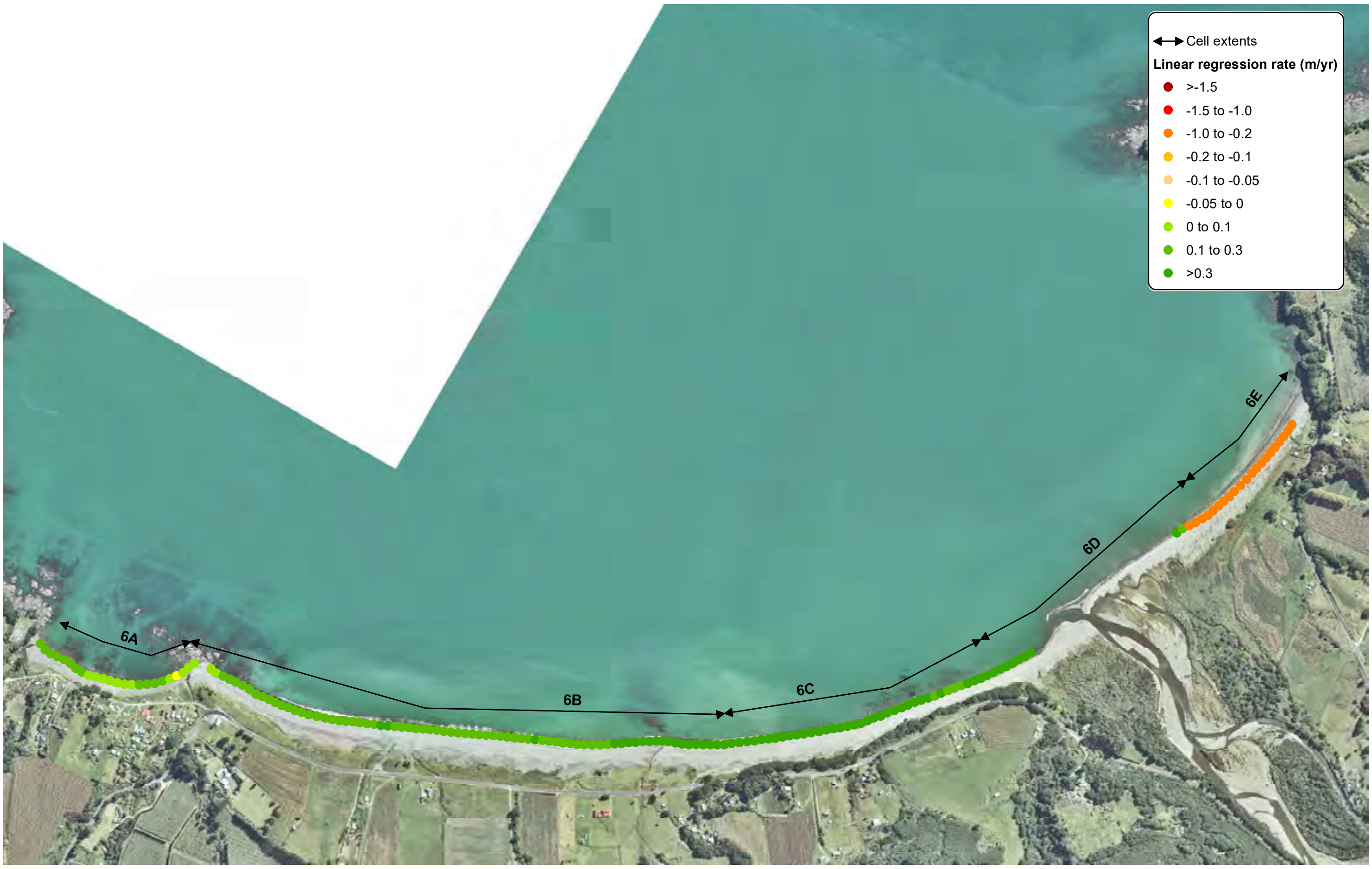

Notes: Aerial photograph (2019) sourced from LINZ Data Service

A3 SCALE 1:10,000

Location Plan

Tonkin+Taylor
105 Carlton Gore Rd, Newmarket, Auckland
www.tonkintaylor.co.nz

DRAWN	RHAU	Jul.20
CHECKED		
APPROVED		
ARCFILE DSAS_Maps.mxd		
SCALE (AT A3 SIZE) 1:10,000		
PROJECT No. 1008669.2000		

Opotiki Coastal Erosion Assessment
DSAS Analysis
Site: Omaio

FIGURE No. Figure 9

Rev. 0

Path: T:\Tauranga\Projects\1008669\1008669.2000\WorkingMaterial\GIS\Shoreline analysis\DSAS_Maps.mxd Date: 1/07/2020 Time: 8:42:13 AM

Path: T:\Tauranga\Projects\1008669\1008669.2000\WorkingMaterial\GIS\Shoreline analysis\DSAS_Maps2.mxd Date: 1/07/2020 Time: 8:54:07 AM

Notes: Aerial photograph (2019) sourced from LINZ Data Service

A3 SCALE 1:6,000
0 0.065 0.13 0.195 0.26 0.325 (km)

Location Plan

Tonkin+Taylor
105 Carlton Gore Rd, Newmarket, Auckland
www.tonkintaylor.co.nz

DRAWN	RHAU	Jul.20
CHECKED		
APPROVED		
ARCFILE DSAS_Maps2.mxd		
SCALE (AT A3 SIZE) 1:6,000		
PROJECT No. 1008669.2000		

Opotiki Coastal Erosion Assessment
DSAS Analysis
Site: Maraetai Bay and Wharekura

FIGURE No. Figure 10

Rev. 0

Notes: Aerial photograph (2019) sourced from LINZ Data Service

A3 SCALE 1:11,000

0 0.1 0.2 0.3 0.4 0.5 (km)

Tonkin+Taylor
105 Carlton Gore Rd, Newmarket, Auckland
www.tonkintaylor.co.nz

DRAWN	RHAU	Jul.20
CHECKED		
APPROVED		
ARCFILE DSAS_Maps2.mxd		
SCALE (AT A3 SIZE) 1:11,000		
PROJECT No. 1008669.2000		

Opotiki Coastal Erosion Assessment
DSAS Analysis
Site: Papatea

FIGURE No. Figure 11 Rev. 0

Path: T:\Tauranga\Projects\1008669\1008669.2000\WorkingMaterial\GIS\Shoreline analysis\DSAS_Maps2.mxd Date: 1/07/2020 Time: 9:28:14 AM

Notes: Aerial photograph (2019) sourced from LINZ Data Service

A3 SCALE 1:5,000

0 0.055 0.11 0.165 0.22 0.275 (km)

Tonkin+Taylor
105 Carlton Gore Rd, Newmarket, Auckland
www.tonkintaylor.co.nz

DRAWN	RHAU	Jul.20
CHECKED		
APPROVED		
ARCFILE DSAS_Maps2.mxd		
SCALE (AT A3 SIZE) 1:5,000		
PROJECT No. 1008669.2000		

Opotiki Coastal Erosion Assessment
DSAS Analysis
Site: Orauiti Beach

FIGURE No. Figure 12 Rev. 0

Path: T:\Tauranga\Projects\1008669\1008669.2000\WorkingMaterial\GIS\Shoreline analysis\DSAS_Maps2.mxd Date: 1/07/2020 Time: 11:38:42 AM

Notes: Aerial photograph (2019) sourced from LINZ Data Service

A3 SCALE 1:8,000

0 0.09 0.18 0.27 0.36 0.45 (km)

Location Plan

Tonkin+Taylor

105 Carlton Gore Rd, Newmarket, Auckland

www.tonkintaylor.co.nz

DRAWN	RHAU	Jul.20
CHECKED		
APPROVED		
ARCFILE DSAS_Maps2.mxd		
SCALE (AT A3 SIZE) 1:8,000		
PROJECT No. 1008669.2000		

Opotiki Coastal Erosion Assessment

DSAS Analysis

Site: Whangaparaoa

FIGURE No. Figure 13

Rev. 0

Path: T:\Tauranga\Projects\1008669\1008669.2000\WorkingMaterial\GIS\Shoreline analysis\DSAS_Maps2.mxd Date: 1/07/2020 Time: 11:47:06 AM

Appendix E: Beach profiles

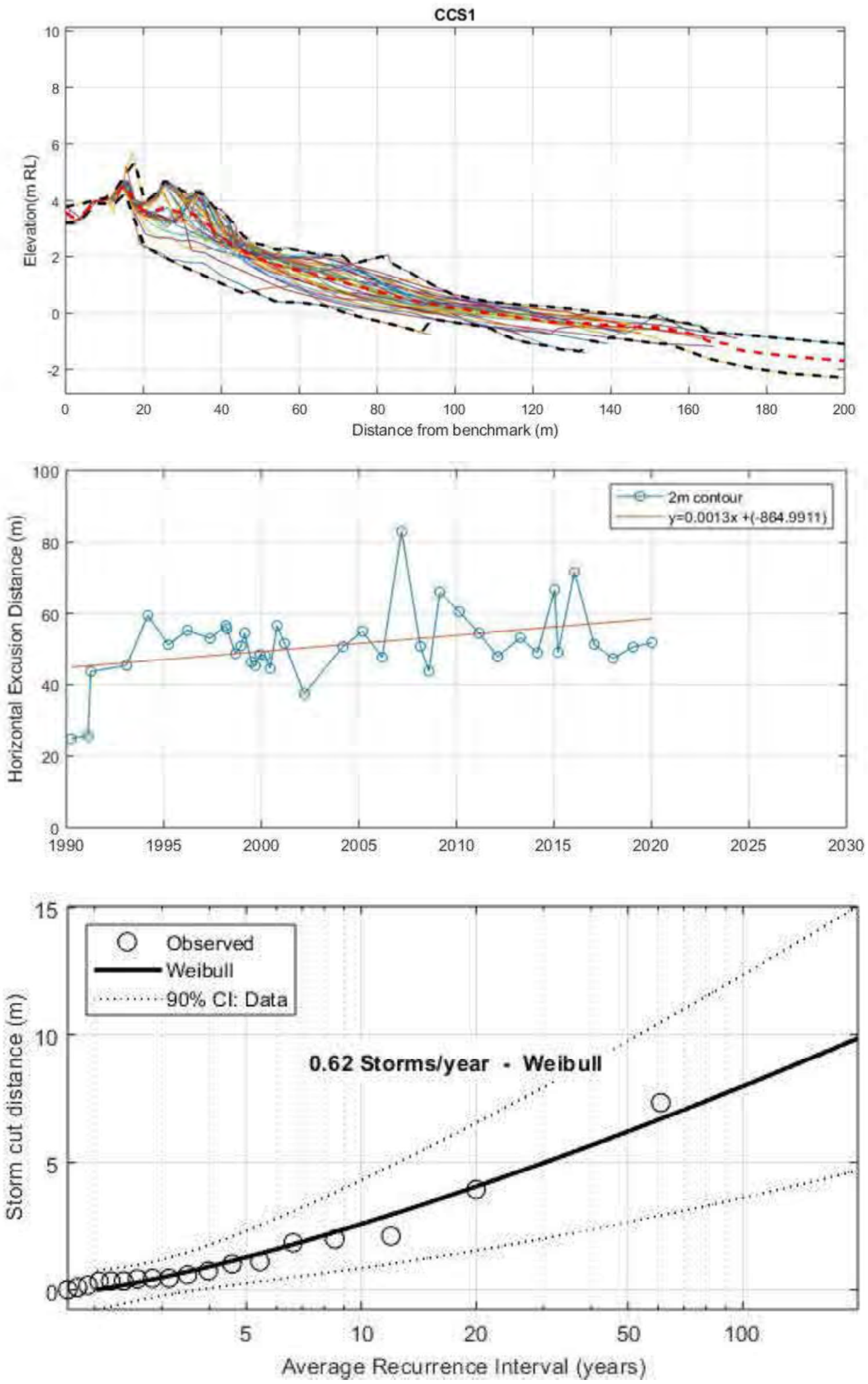

Figure C.1: (Top) Beach profiles for CCS1 for the monitoring period 1990 to 2019. Black dashed lines show the minimum and maximum profile envelopes. Red dashed line shows the average profile. (Middle) linear regression analysis. (Bottom) Extreme value analysis of inter-survey storm cut

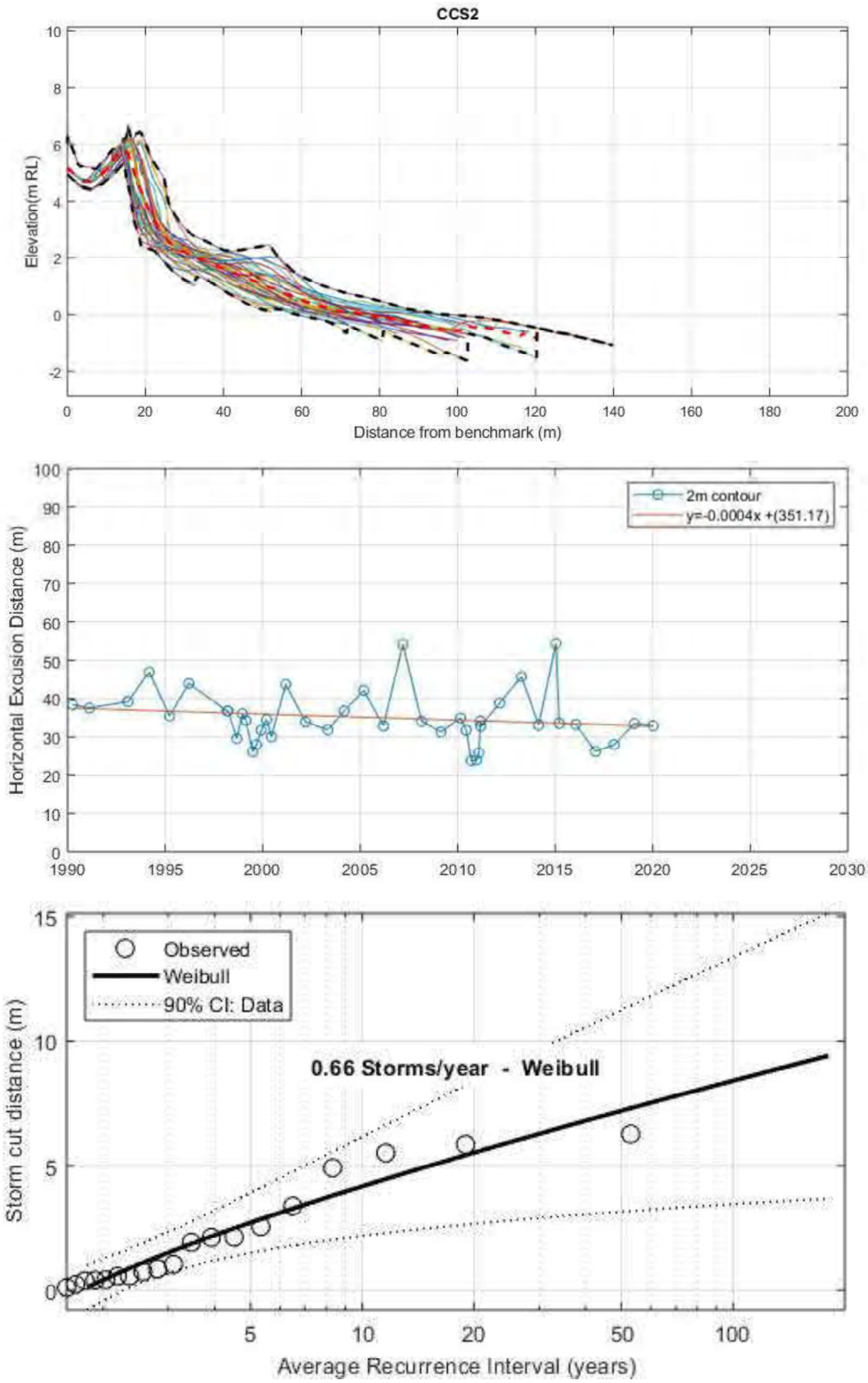

Figure C.2: (Top) Beach profiles for CCS2 for the monitoring period 1990 to 2019. Black dashed lines show the minimum and maximum profile envelopes. Red dashed line shows the average profile. (Middle) linear regression analysis. (Bottom) Extreme value analysis of inter-survey storm cut

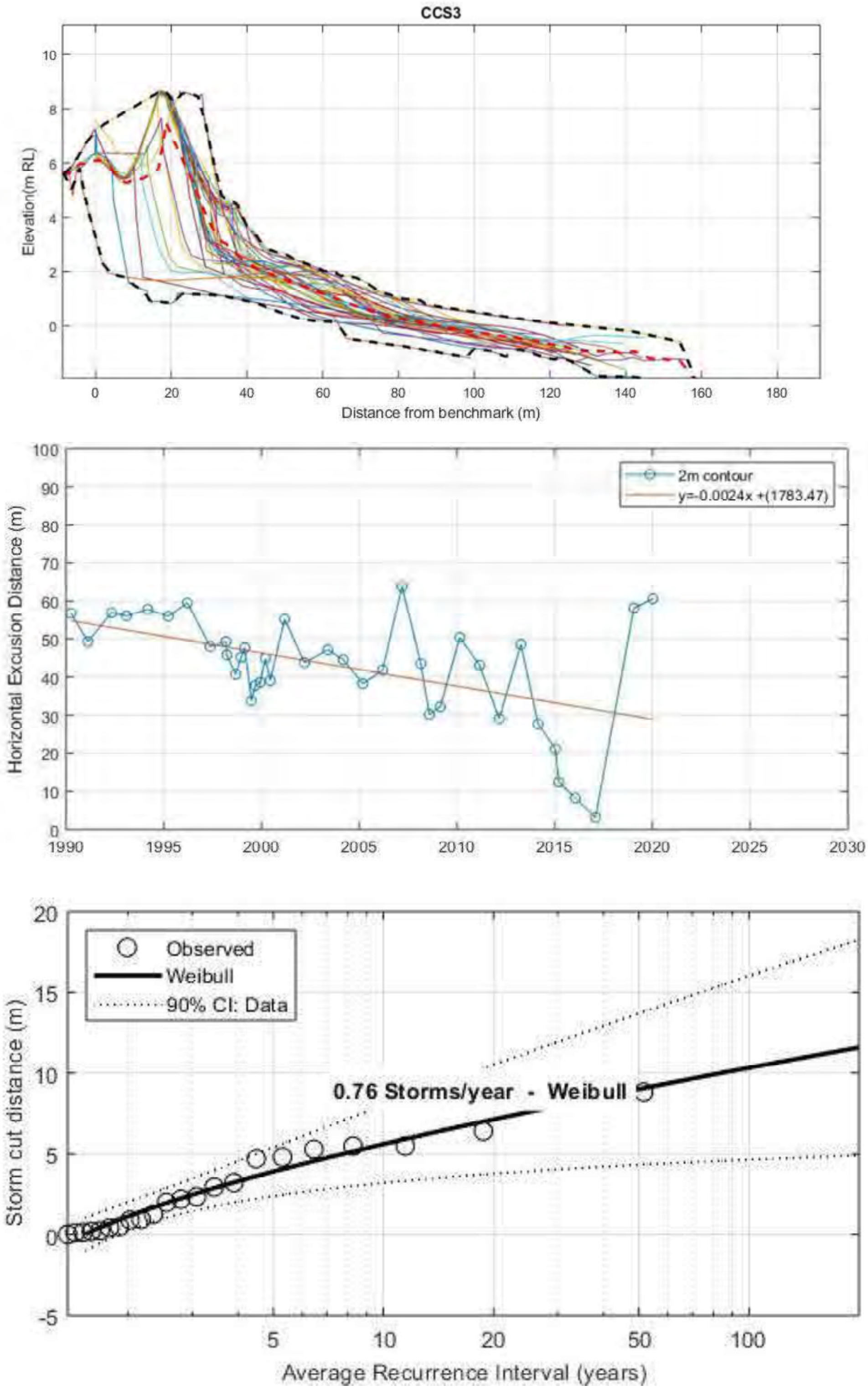

Figure C.3: (Top) Beach profiles for CCS3 for the monitoring period 1990 to 2019. Black dashed lines show the minimum and maximum profile envelopes. Red dashed line shows the average profile. (Middle) linear regression analysis. (Bottom) Extreme value analysis of inter-survey storm cut

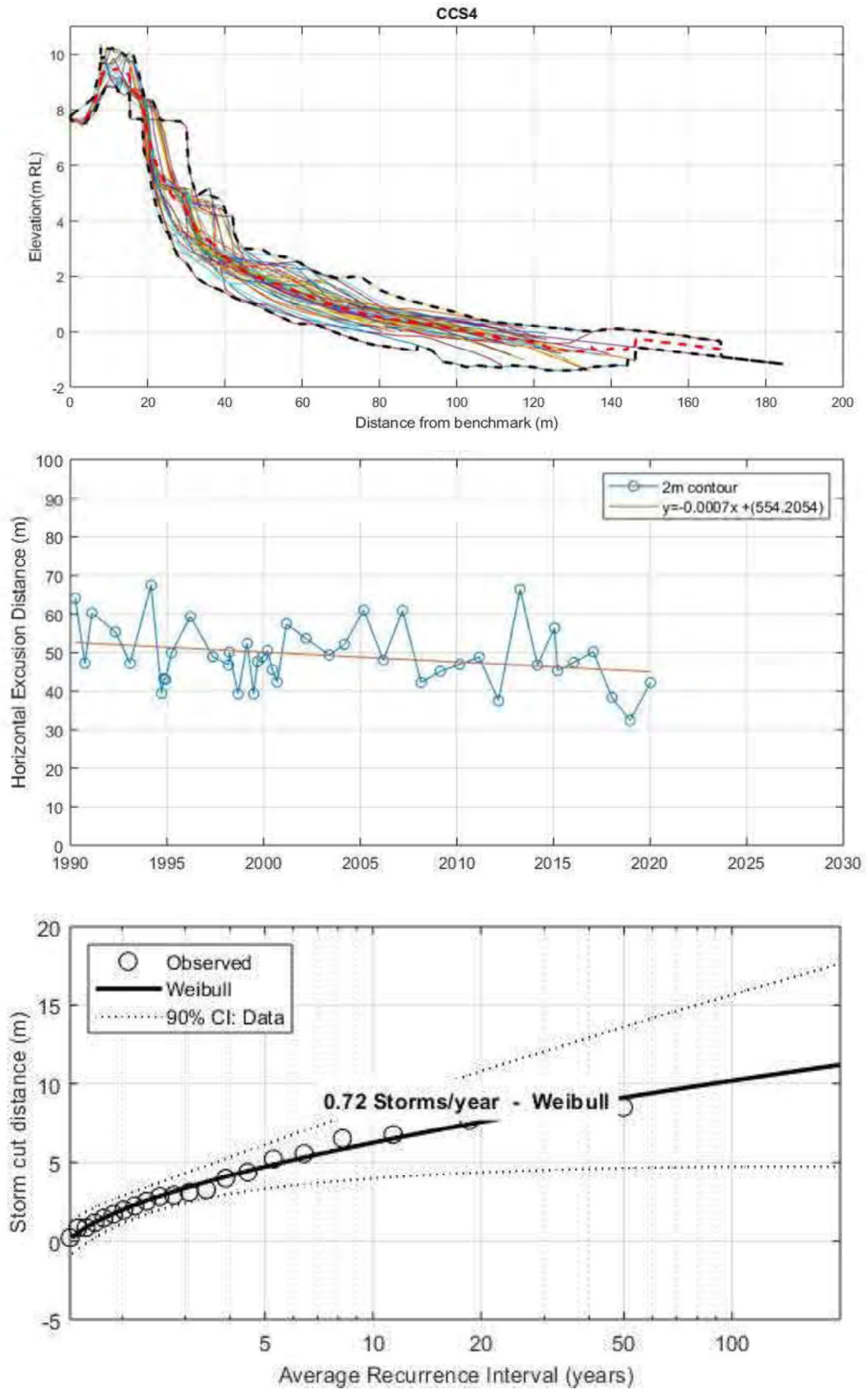

Figure C.4: (Top) Beach profiles for CCS4 for the monitoring period 1990 to 2019. Black dashed lines show the minimum and maximum profile envelopes. Red dashed line shows the average profile. (Middle) linear regression analysis. (Bottom) Extreme value analysis of inter-survey storm cut

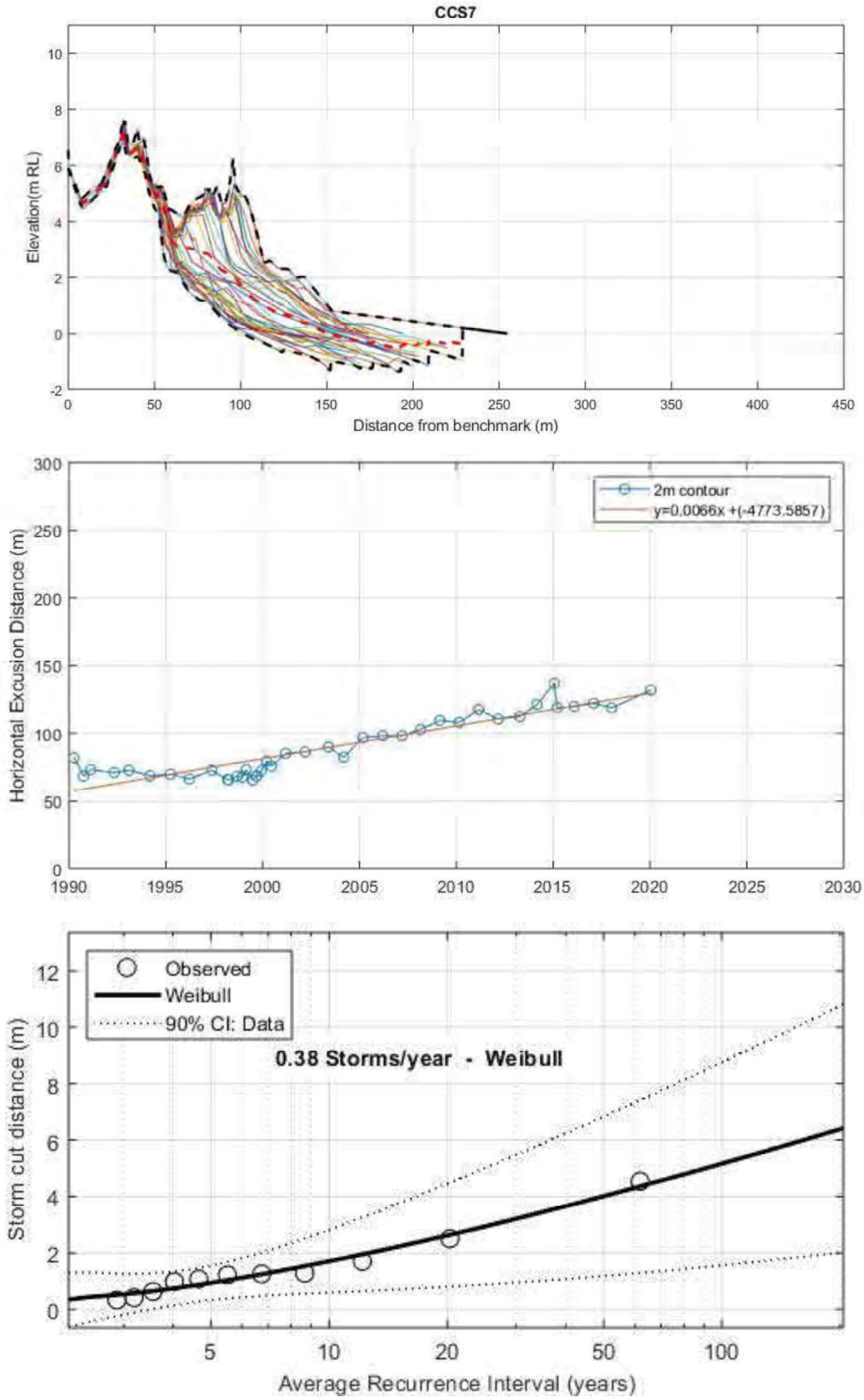

Figure C.5: (Top) Beach profiles for CCS7 for the monitoring period 1990 to 2019. Black dashed lines show the minimum and maximum profile envelopes. Red dashed line shows the average profile. (Middle) linear regression analysis. (Bottom) Extreme value analysis of inter-survey storm cut

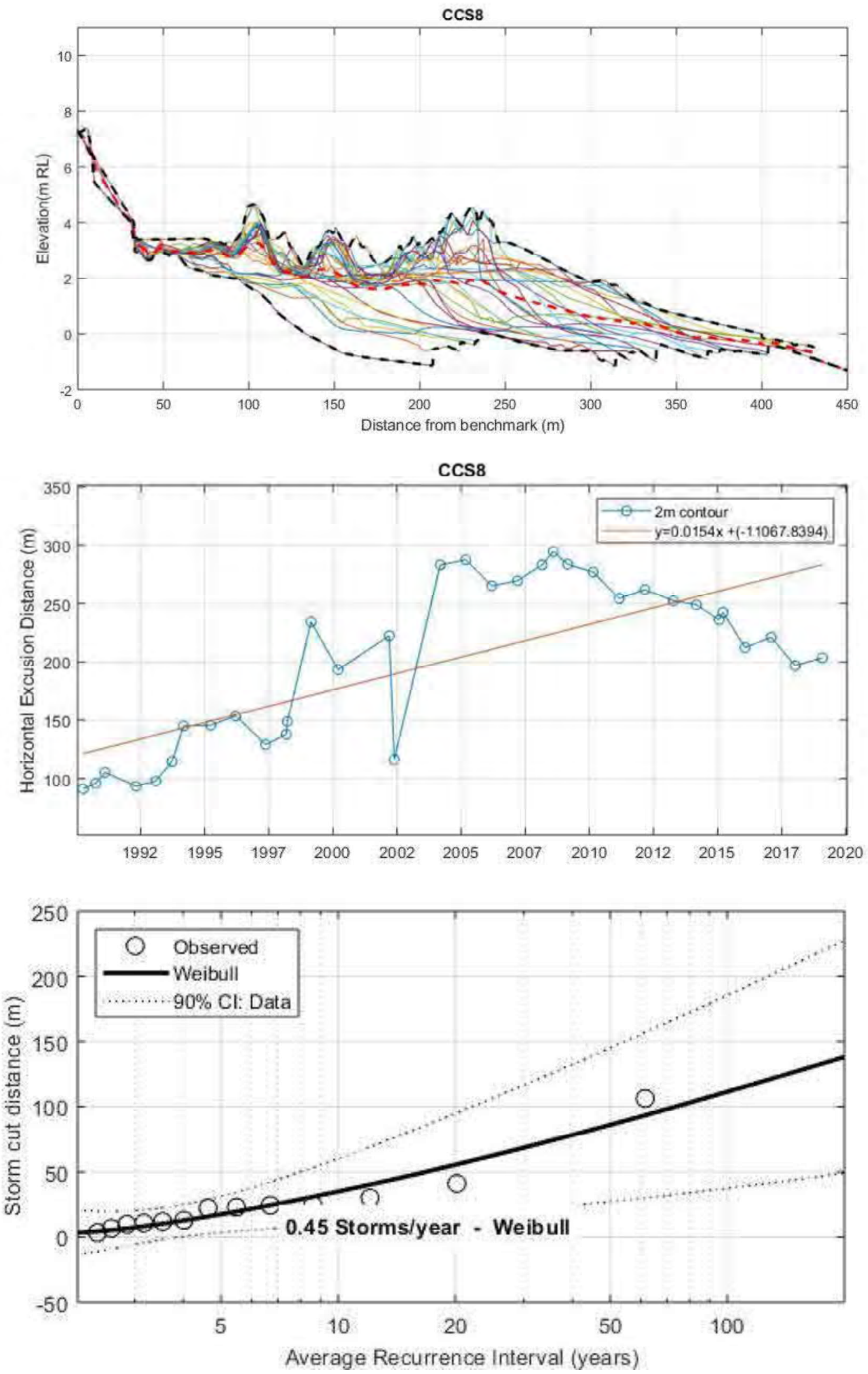

Figure C.6: (Top) Beach profiles for CCS8 for the monitoring period 1990 to 2019. Black dashed lines show the minimum and maximum profile envelopes. Red dashed line shows the average profile. (Middle) linear regression analysis. (Bottom) Extreme value analysis of inter-survey storm cut

Appendix F: Extreme water levels - memo

Tonkin+Taylor

Memo

To:	**Mark Ivamy and Peter Blackwood**	**Job No:**	**1008669.2000**
From:	**Rebekah Haughey and Eddie Beetham**	**Date:**	**12 May 2020**
cc:	**Tom Shand, Jonathan Clarke, Katalin Maltai**		
Subject:	**Ōpōtiki District erosion hazard assessment - Extreme water levels**		

1 Introduction

The present day hazard zone on a gravel beach can be described as the 'dynamic zone' that is exposed to morphodynamic change during an extreme event. Our adopted method to identify this zone requires simulating hydrodynamic processes and profile response in XBeach-G, using input water levels and wave heights that represent different average return interval (ARI) events.

To calculate a dynamic zone associated with different likelihoods, we require input water levels and offshore wave heights associated with 5 year, 50 year and 200 year ARI events. BOPRC agreed to supply T+T with joint probability combinations of water level and wave height for these three ARI scenarios, from the NIWA Coastal Calculator outputs. The Calculator provides 15 combinations of wave height and water level that are associated with each ARI scenario, and for each location. In total this constituted over 400 different sets of hydrodynamic conditions.

Joint probability combinations range from very small wave heights and high water levels, to very large waves and low water levels. The Coastal Calculator output highlights a 'peak runup' scenario based on empirical calculations of wave setup and runup. This peak runup scenario is an estimate that does not fully take in to account the local offshore bathymetry, depth limiting effects and wave setup in front of a gravel beach. The proposed method using XBeach-G simulates wave setup and runup directly by resolving the dynamic free-surface as waves interact with the actual beach profile at each site.

In order to calculate the potential dynamic zone in XBeach-G it is necessary to define which of the 15 joint probability wave height and water level combinations produces the maximum morphological change. Modelling every combination for each ARI event at all locations was considered outside the scope of this work. The preferred approach discussed with BOPRC was to conduct a sensitivity analysis. This memo outlines the sensitivity analysis with a recommendation on the joint probability combinations to be adopted for the Ōpōtiki District erosion assessment.

2 Sensitivity analysis

Rather than running all 15 scenarios to determine the appropriate storm tide and wave height combination it was agreed with Peter Blackwood (BOPRC) to run 3 different scenarios:

- The line with maximum SWRU ("pink highlight")
- The 12^{th} line
- The 7^{th} line (half way line)

An example of selecting these scenarios is provided in Figure 2.1 for Whangaparaoa for a 50 year joint probability event.

Storm tide (m)	Wave height (m)	Wave length (m)	Wave run up (including setup)	Wave setup (m)	Storm tide + wave setup	Storm tide + runup (incl s
0.27	10.12	214	4.14	1.55	1.82	4.41
0.90	10.03	212	4.11	1.53	2.43	5.00
0.99	9.75	206	3.99	1.49	2.48	4.98
1.06	9.38	198	3.84	1.43	2.50	4.90
1.14	9.04	191	3.70	1.38	2.52	4.84
1.20	8.62	183	3.53	1.32	2.52	4.73
1.27	8.12	174	3.34	1.25	2.51	4.61
1.33	7.81	165	3.20	1.19	2.52	4.53
1.39	7.27	155	2.99	1.12	2.51	4.38
1.47	6.94	148	2.85	1.06	2.53	4.32
1.56	6.72	143	2.76	1.03	2.59	4.32
1.63	6.36	133	2.58	0.97	2.59	4.21
1.69	5.95	124	2.42	0.90	2.59	4.10
1.74	5.20	109	2.11	0.79	2.53	3.85
1.78	0.10	2	0.04	0.02	1.79	1.82

Highlighted row illustrates the maximum combined storm tide and wave runup elevation.

Figure 2.1: Example of coastal calculator scenarios for a 50 year joint probability event at Whangaparaoa

We understand that the maximum joint probability combinations vary in an east to west direction along the Ōpōtiki region. Therefore we have completed a sensitivity analysis for one of the western sites (Hāwai) and the most eastern site (Whangaparaoa). Morphodynamic response to each scenario was simulated for 1 hour, using the input wave height and water level, with an across shore profile generated using LiDAR elevations at the coast and LINZ nearshore bathymetry. The dynamic zone output, calculated as the distance between MHWS and the most landward point of elevation change >0.1 m, is presented in Table 2.1 and Table 2.2 with summary output figures in Appendix A.

Table 2.1: Storm tide and wave height combinations with resultant dynamic zones for different return periods at Hāwai

ARI	Storm tide (m MVD53)	Offshore wave (m)	Dynamic Zone (m)	Coastal Calculator scenario
5 year	1.26	2.91	38.2	Line 12
	1.05	4.75	39.8	Line 7 (halfway)
	0.77	5.59	39.8	Peak RU (Line 2)
50 year	1.63	5.15	50.6	Line 12
	1.26	6.23	51	Line 7 (halfway)
	0.89	7.32	50	Peak RU (Line 2)
200yr	2.19	6.06	89.8	Line 12
	1.47	7.37	78.2	Line 7 (halfway)
	1.03	8.34	78	Peak RU (Line 2)

Table 2.2: Storm tide and wave height combinations with resultant dynamic zones for different return periods at Whangaparaoa

ARI	Storm tide (m MVD53)	Offshore wave (m)	Dynamic Zone (m)	Coastal Calculator scenario
5 year	1.24	3.52	44.8	Line 12
	1.07	5.54	91.8	Line 8 (halfway)
	0.82	6.98	110.8	Peak RU (Line 3)
50 year	1.63	6.36	149.6	Line 12
	1.27	8.12	157.6	Line 7 (halfway)
	0.9	10.03	151.6	Peak RU (Line 2)
200yr	2.19	7.9	199.8	Line 12
	1.57	9.95	172.2	Line 7 (halfway)
	1.04	11.82	182.2	Peak RU (Line 2)

Results from the sensitivity analysis at Hāwai show that the 5 year ARI scenarios produced consistent dynamic zone distances between 38-40m (Appendix A1). The 50 year scenarios at Hāwai were also similar and ranged between 50-51m (Appendix A2). The 200 year ARI combination was associated with slightly more spread in the dynamic zone distance (Appendix A3), between 78–90m. The widest dynamic zone for the 200 year scenarios was associated with the largest storm tide input of 2.19 m (1.35 m above MHWS).

The profile at Whangaparaoa is more sensitive to change because waves can surge for a significant distance landward if the still water level nears the berm crest level. Therefore, sensitivity outputs show a wider range of distances within each ARI group. For the 5 year scenarios the dynamic zone ranged between 45-111 m (Appendix A4), and the increase in distance was associated with larger offshore wave heights. The 50 year dynamic zone ranged between 150–158m, with the consistent outputs influenced by all combinations resulting in waves reaching a ridge in the backshore terrace (Appendix A5). The 200 year ARI scenarios produced dynamic zone outputs between 170-200m and were also influenced by a backshore ridge blocking landward flow (Appendix A6). The larger dynamic zone was associated with the highest storm tide scenario.

3 Conclusion

The sensitivity analysis provides important insight into how different gravel beach profiles respond to extreme wave height and water level events. Results from Hāwai indicate that the dynamic zone is typically consistent for different combinations of water level and wave height. Results from Whangaparaoa were more variable. For the higher probability events (5 year ARI) the dynamic zone increased with larger wave combinations. Whereas for the lower probability event (200 year ARI) the widest dynamic zone was associated with higher storm tide scenarios.

On the balance, we recommend that the most representative joint probability scenario is line 7. By using this scenario, water level and wave height combinations are not skewed in favour of storm tide or wave height dominant events and are therefore expected to be more representative for the purpose of assessing hazard scenarios. While the line 7 outputs is not necessarily the most extreme hazard distance associated with different ARI events, it is considered to be the most representative for a range of different ARI events and environments.

Appendix A

A1 Hāwai 5 year ARI

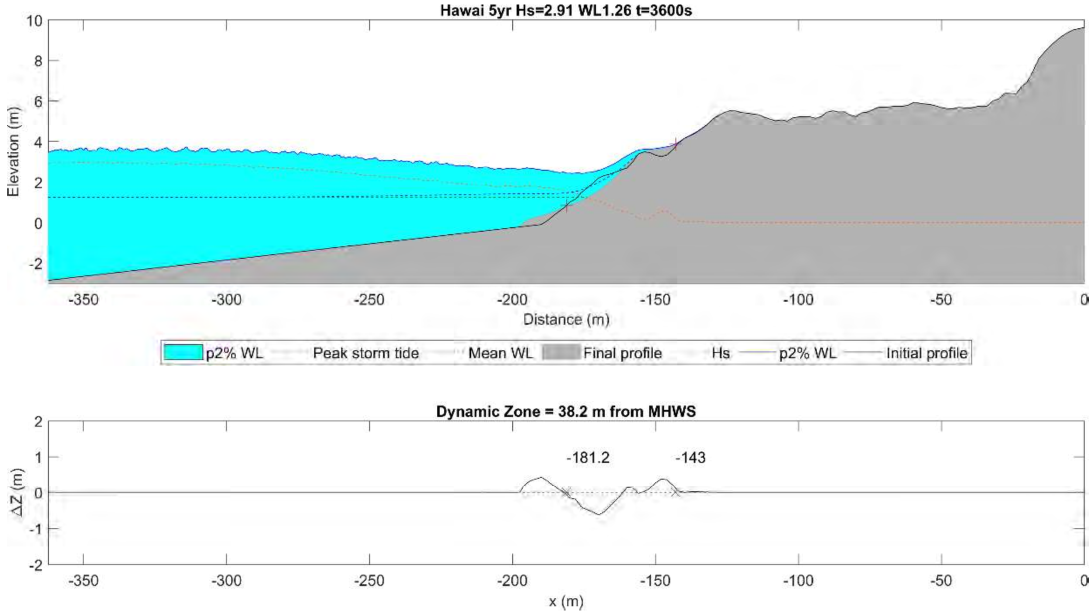

Appendix A.1: XBeach-G output showing the initial across-shore profile (black line) and final across shore profile (solid grey). The two percent exceeded water level (p2%WL) is presented (blue line) to highlight areas of flooding due to wave runup, and wave height and mean water level (influenced by wave setup). The difference between the initial and final profile is presented is presented in the lower panel and the morphodynamic zone from MHWS is identified by '+' markers in both plots.

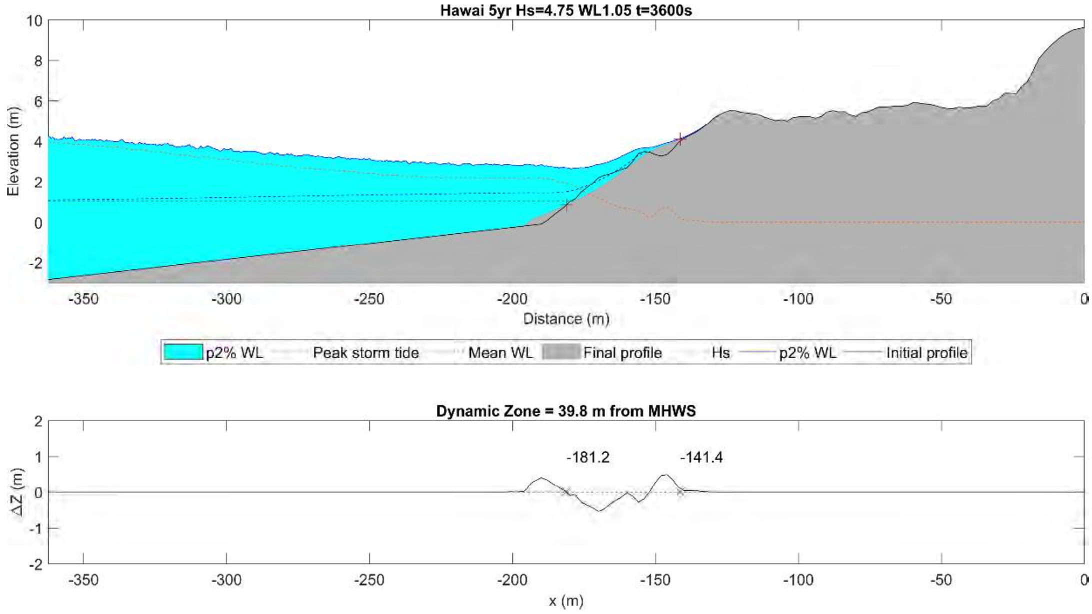

Appendix A.2: XBeach-G output showing the initial across-shore profile (black line) and final across shore profile (solid grey). The two percent exceeded water level (p2%WL) is presented (blue line) to highlight areas of flooding due to wave runup, and wave height and mean water level (influenced by wave setup). The difference between the initial and final profile is presented is presented in the lower panel and the morphodynamic zone from MHWS is identified by '+' markers in both plots.

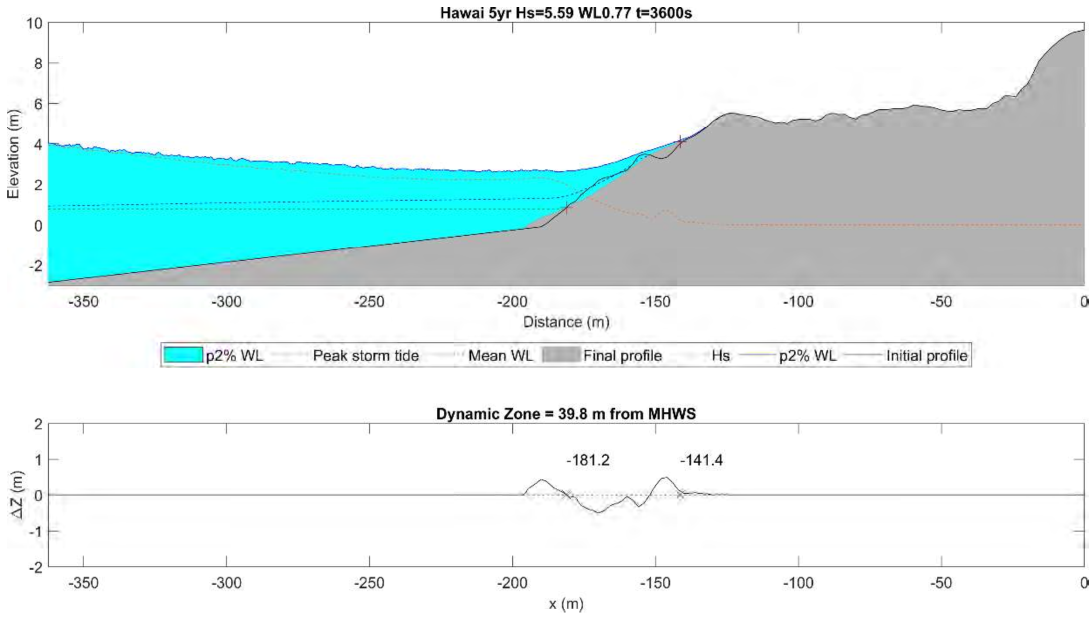

Appendix A.3: XBeach-G output showing the initial across-shore profile (black line) and final across shore profile (solid grey). The two percent exceeded water level (p2%WL) is presented (blue line) to highlight areas of flooding due to wave runup, and wave height and mean water level (influenced by wave setup). The difference between the initial and final profile is presented is presented in the lower panel and the morphodynamic zone from MHWS is identified by '+' markers in both plots.

A2 Hāwai 50 year ARI

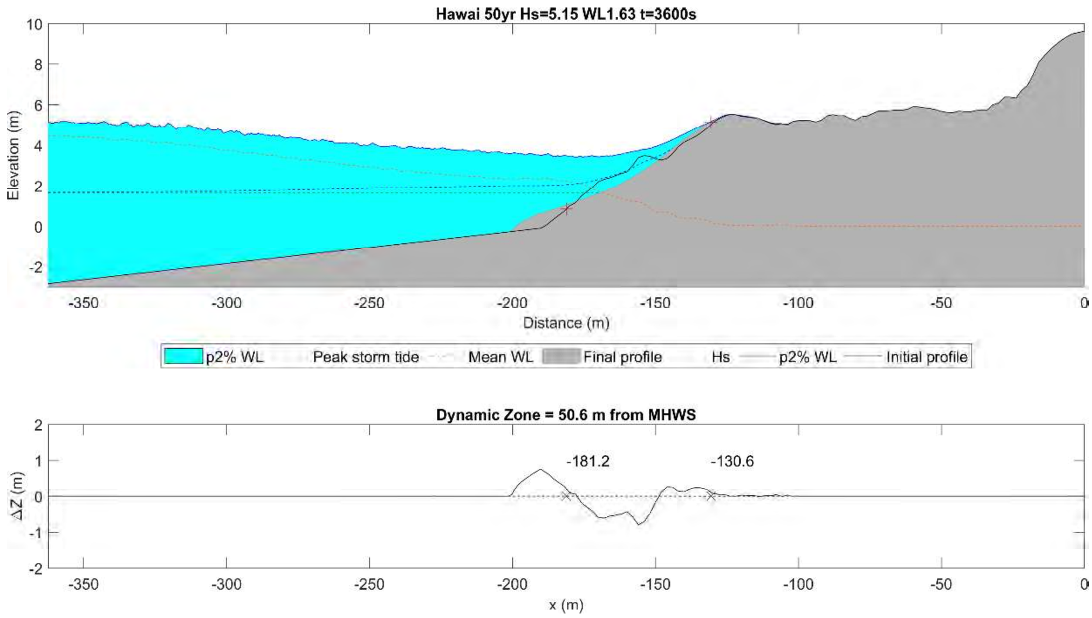

Appendix A.4: XBeach-G output showing the initial across-shore profile (black line) and final across shore profile (solid grey). The two percent exceeded water level (p2%WL) is presented (blue line) to highlight areas of flooding due to wave runup, and wave height and mean water level (influenced by wave setup). The difference between the initial and final profile is presented is presented in the lower panel and the morphodynamic zone from MHWS is identified by '+' markers in both plots.

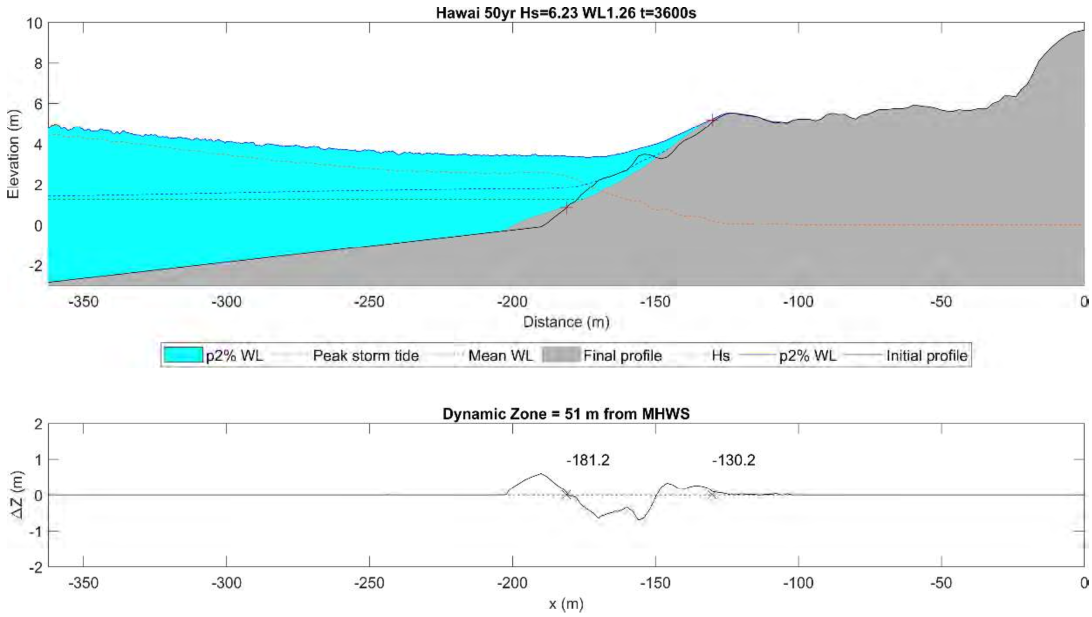

Appendix A.5: XBeach-G output showing the initial across-shore profile (black line) and final across shore profile (solid grey). The two percent exceeded water level (p2%WL) is presented (blue line) to highlight areas of flooding due to wave runup, and wave height and mean water level (influenced by wave setup). The difference between the initial and final profile is presented is presented in the lower panel and the morphodynamic zone from MHWS is identified by '+' markers in both plots.

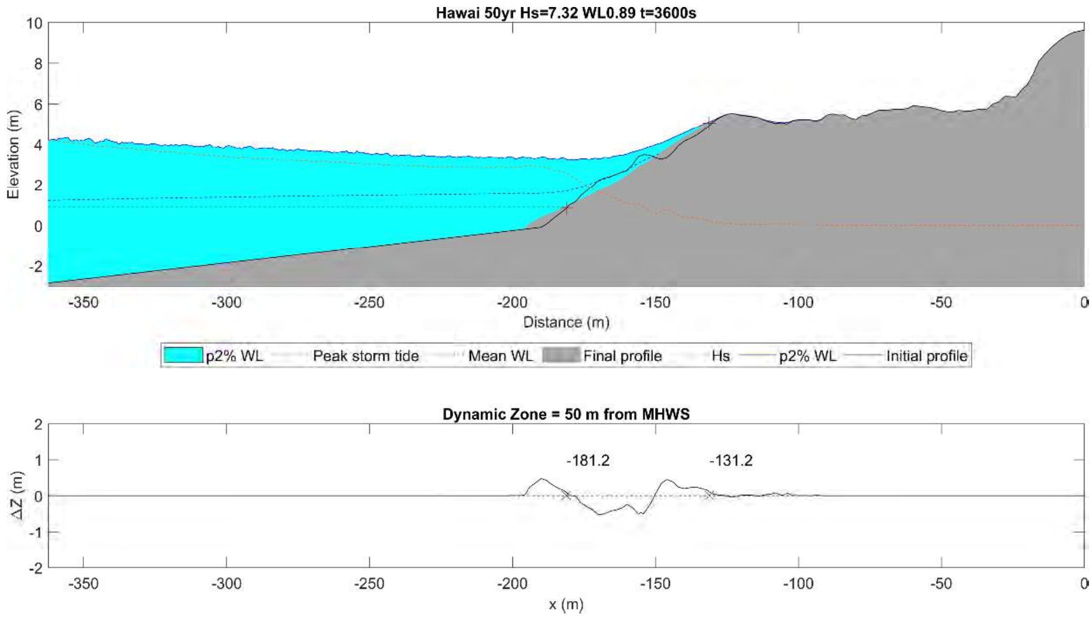

Appendix A.6: XBeach-G output showing the initial across-shore profile (black line) and final across shore profile (solid grey). The two percent exceeded water level (p2%WL) is presented (blue line) to highlight areas of flooding due to wave runup, and wave height and mean water level (influenced by wave setup). The difference between the initial and final profile is presented is presented in the lower panel and the morphodynamic zone from MHWS is identified by '+' markers in both plots.

A3 Hāwai 200 year ARI

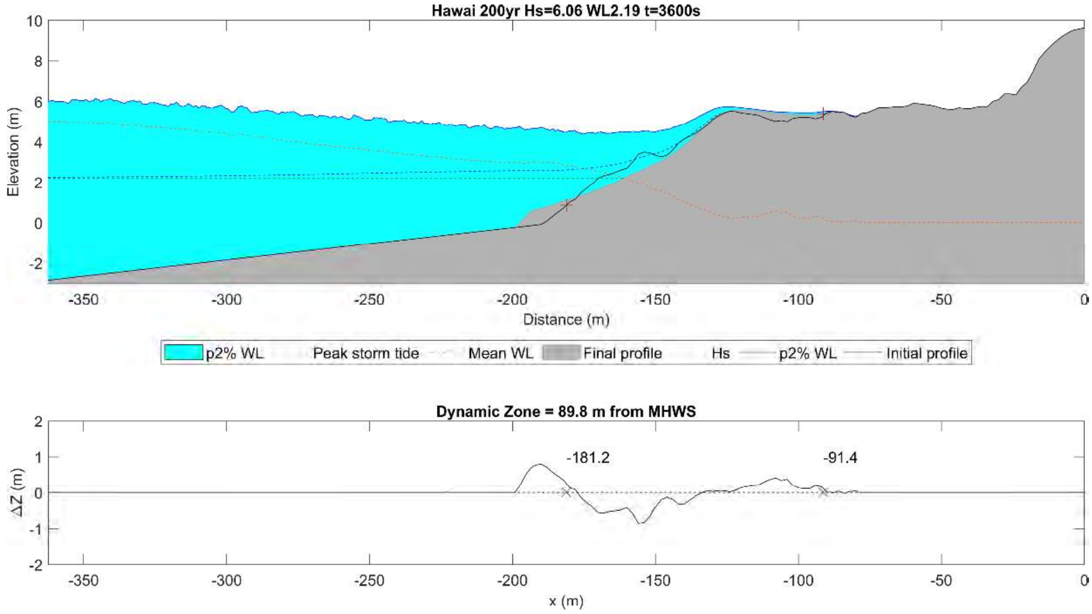

Appendix A.7: XBeach-G output showing the initial across-shore profile (black line) and final across shore profile (solid grey). The two percent exceeded water level (p2%WL) is presented (blue line) to highlight areas of flooding due to wave runup, and wave height and mean water level (influenced by wave setup). The difference between the initial and final profile is presented is presented in the lower panel and the morphodynamic zone from MHWS is identified by '+' markers in both plots.

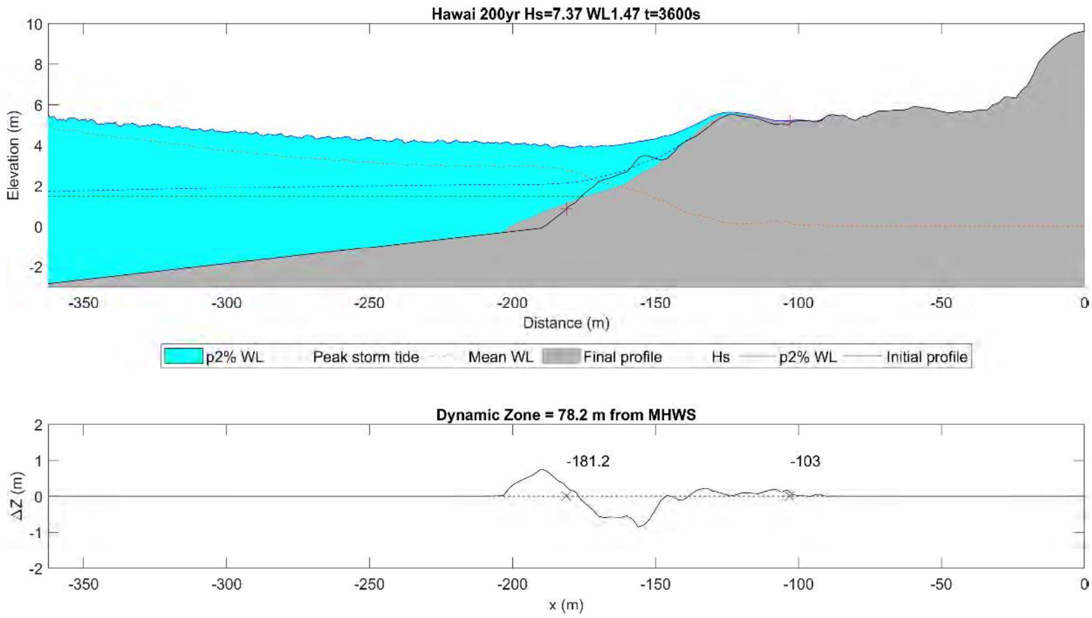

Appendix A.8: XBeach-G output showing the initial across-shore profile (black line) and final across shore profile (solid grey). The two percent exceeded water level (p2%WL) is presented (blue line) to highlight areas of flooding due to wave runup, and wave height and mean water level (influenced by wave setup). The difference between the initial and final profile is presented is presented in the lower panel and the morphodynamic zone from MHWS is identified by '+' markers in both plots.

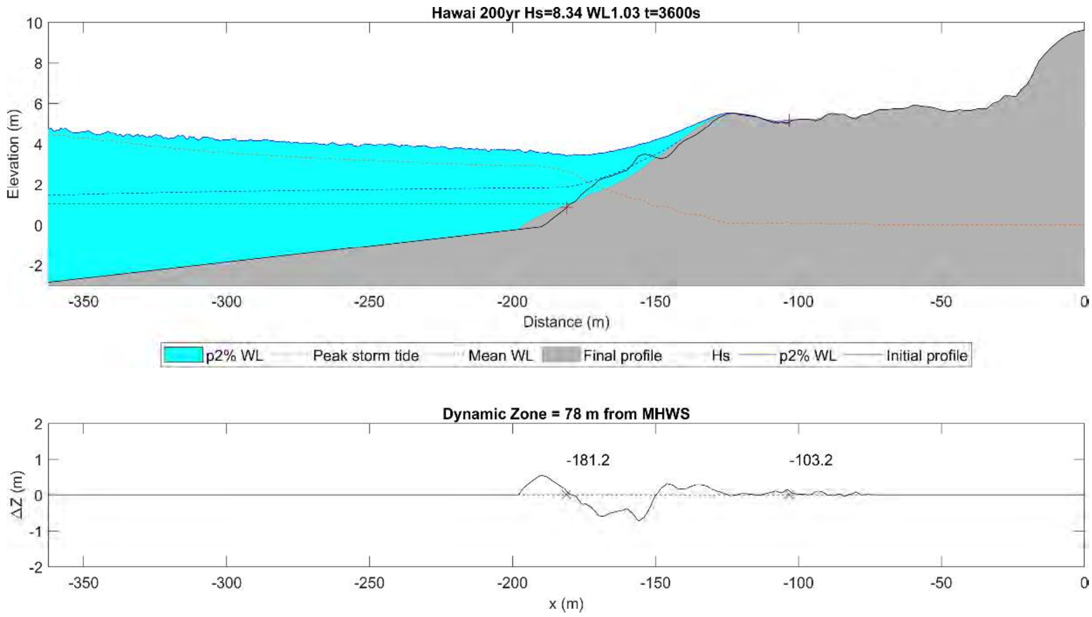

Appendix A.9: XBeach-G output showing the initial across-shore profile (black line) and final across shore profile (solid grey). The two percent exceeded water level (p2%WL) is presented (blue line) to highlight areas of flooding due to wave runup, and wave height and mean water level (influenced by wave setup). The difference between the initial and final profile is presented is presented in the lower panel and the morphodynamic zone from MHWS is identified by '+' markers in both plots.

A4 Whangaparaoa 5 year ARI

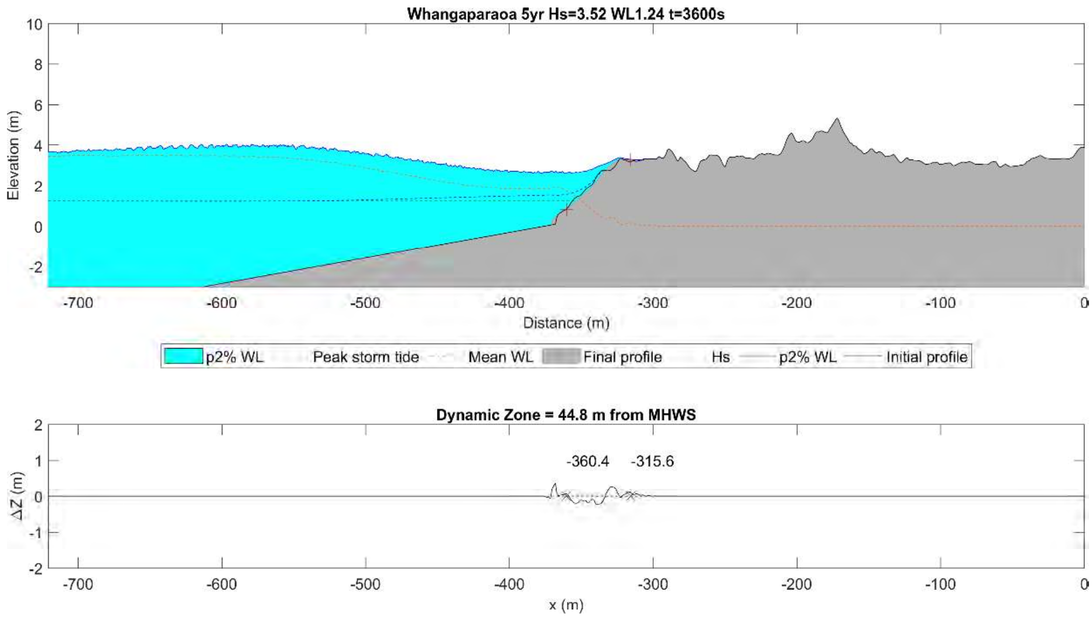

Appendix A.10: XBeach-G output showing the initial across-shore profile (black line) and final across shore profile (solid grey). The two percent exceeded water level (p2%WL) is presented (blue line) to highlight areas of flooding due to wave runup, and wave height and mean water level (influenced by wave setup). The difference between the initial and final profile is presented is presented in the lower panel and the morphodynamic zone from MHWS is identified by '+' markers in both plots.

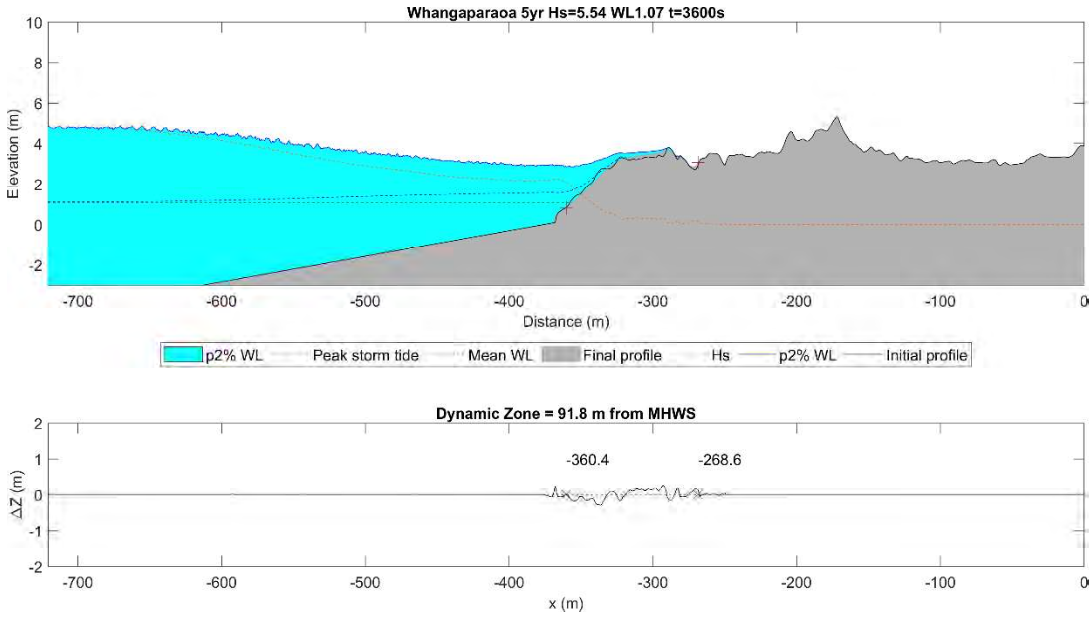

Appendix A.11: XBeach-G output showing the initial across-shore profile (black line) and final across shore profile (solid grey). The two percent exceeded water level (p2%WL) is presented (blue line) to highlight areas of flooding due to wave runup, and wave height and mean water level (influenced by wave setup). The difference between the initial and final profile is presented is presented in the lower panel and the morphodynamic zone from MHWS is identified by '+' markers in both plots.

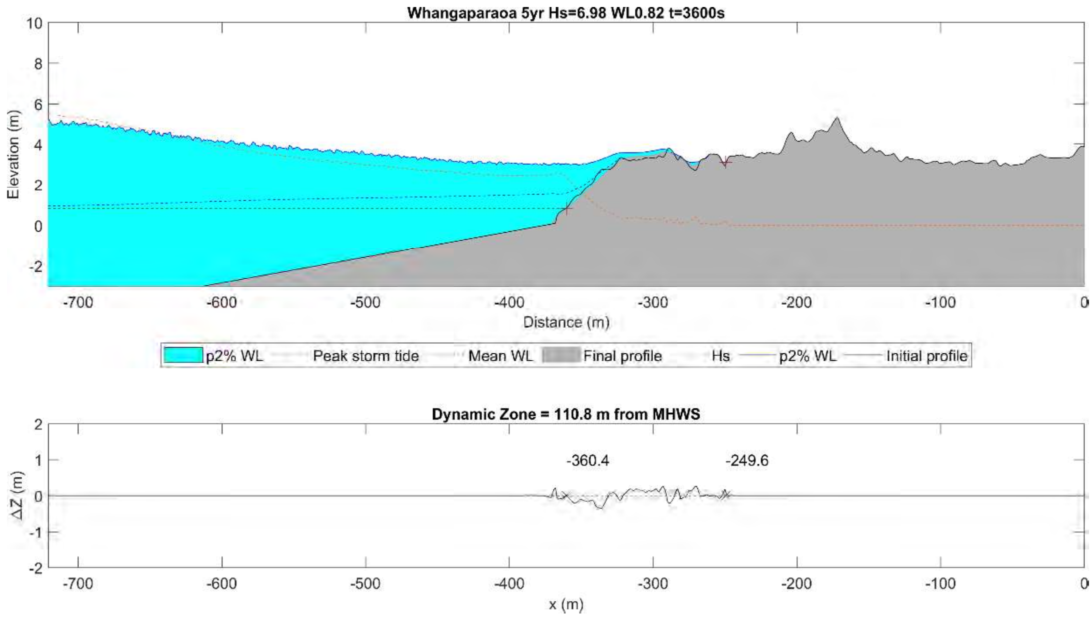

Appendix A.12: XBeach-G output showing the initial across-shore profile (black line) and final across shore profile (solid grey). The two percent exceeded water level (p2%WL) is presented (blue line) to highlight areas of flooding due to wave runup, and wave height and mean water level (influenced by wave setup). The difference between the initial and final profile is presented is presented in the lower panel and the morphodynamic zone from MHWS is identified by '+' markers in both plots.

A5 Whangaparaoa 50 year ARI

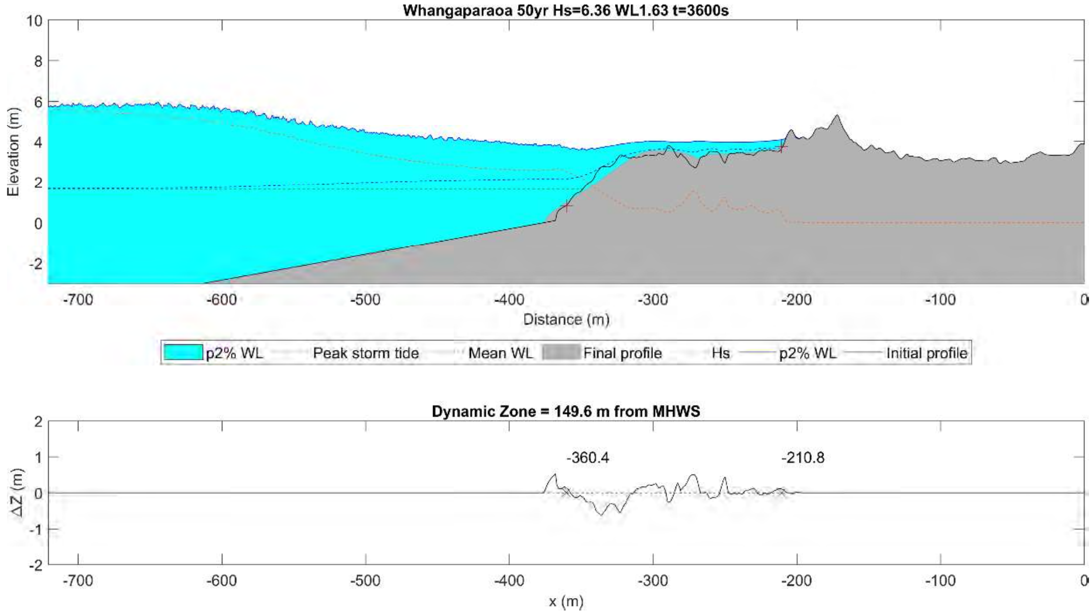

Appendix A.13: XBeach-G output showing the initial across-shore profile (black line) and final across shore profile (solid grey). The two percent exceeded water level (p2%WL) is presented (blue line) to highlight areas of flooding due to wave runup, and wave height and mean water level (influenced by wave setup). The difference between the initial and final profile is presented is presented in the lower panel and the morphodynamic zone from MHWS is identified by '+' markers in both plots.

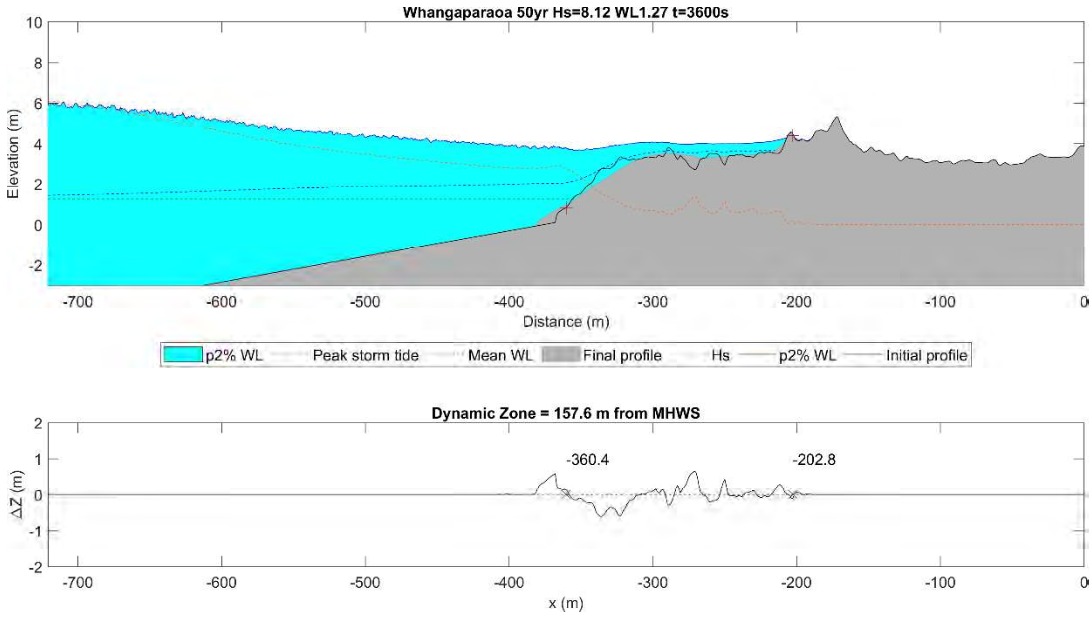

Appendix A.14: XBeach-G output showing the initial across-shore profile (black line) and final across shore profile (solid grey). The two percent exceeded water level (p2%WL) is presented (blue line) to highlight areas of flooding due to wave runup, and wave height and mean water level (influenced by wave setup). The difference between the initial and final profile is presented is presented in the lower panel and the morphodynamic zone from MHWS is identified by '+' markers in both plots.

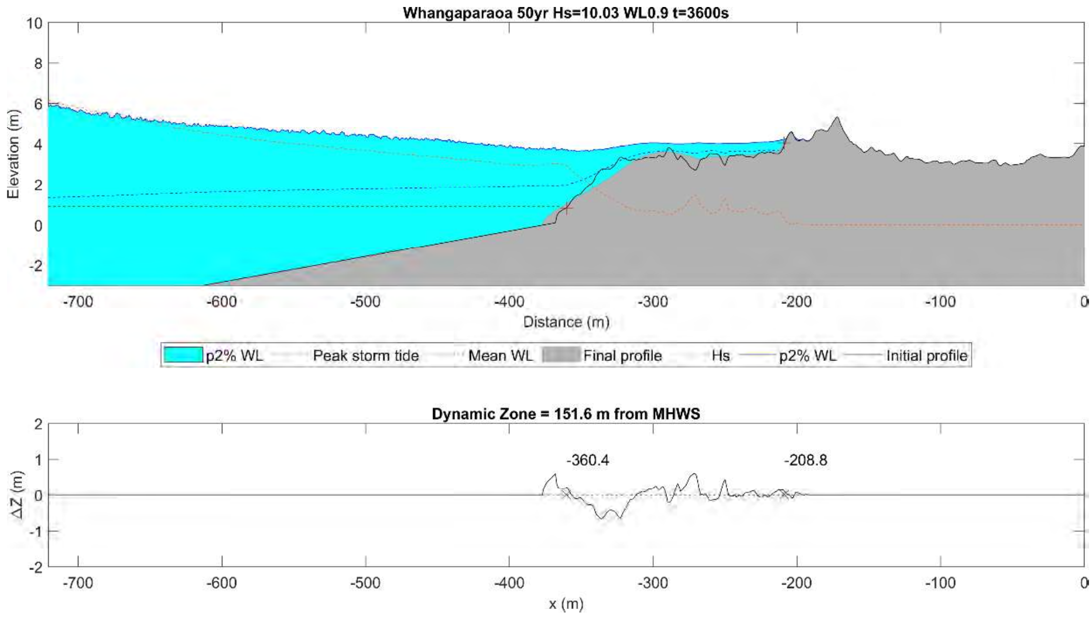

Appendix A.15: XBeach-G output showing the initial across-shore profile (black line) and final across shore profile (solid grey). The two percent exceeded water level (p2%WL) is presented (blue line) to highlight areas of flooding due to wave runup, and wave height and mean water level (influenced by wave setup). The difference between the initial and final profile is presented is presented in the lower panel and the morphodynamic zone from MHWS is identified by '+' markers in both plots.

A6 Whangaparaoa 200 year ARI

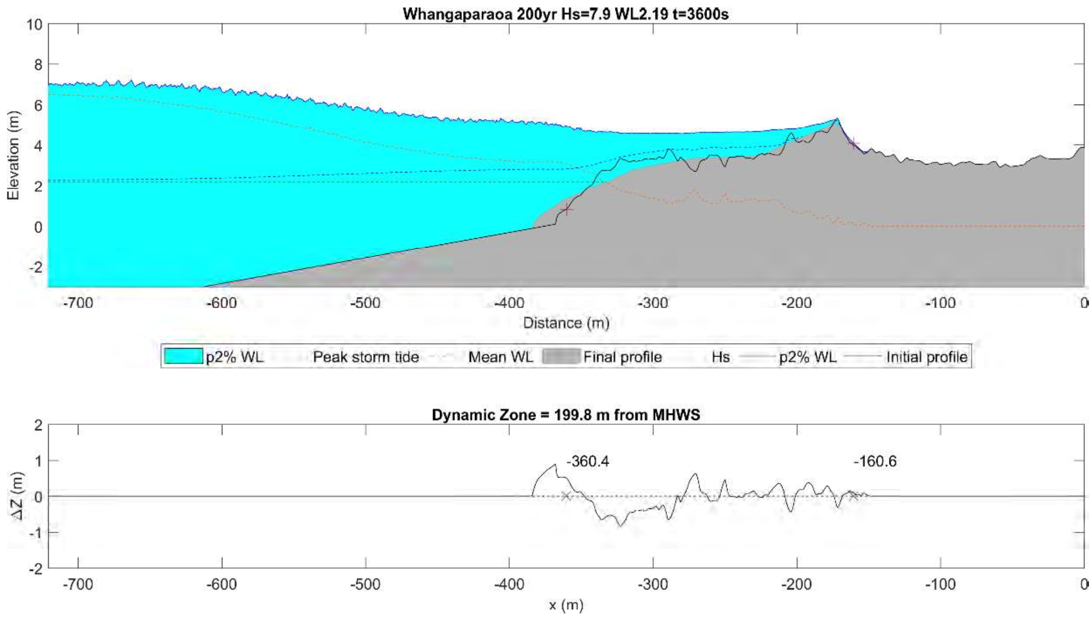

Appendix A.16: XBeach-G output showing the initial across-shore profile (black line) and final across shore profile (solid grey). The two percent exceeded water level (p2%WL) is presented (blue line) to highlight areas of flooding due to wave runup, and wave height and mean water level (influenced by wave setup). The difference between the initial and final profile is presented is presented in the lower panel and the morphodynamic zone from MHWS is identified by '+' markers in both plots.

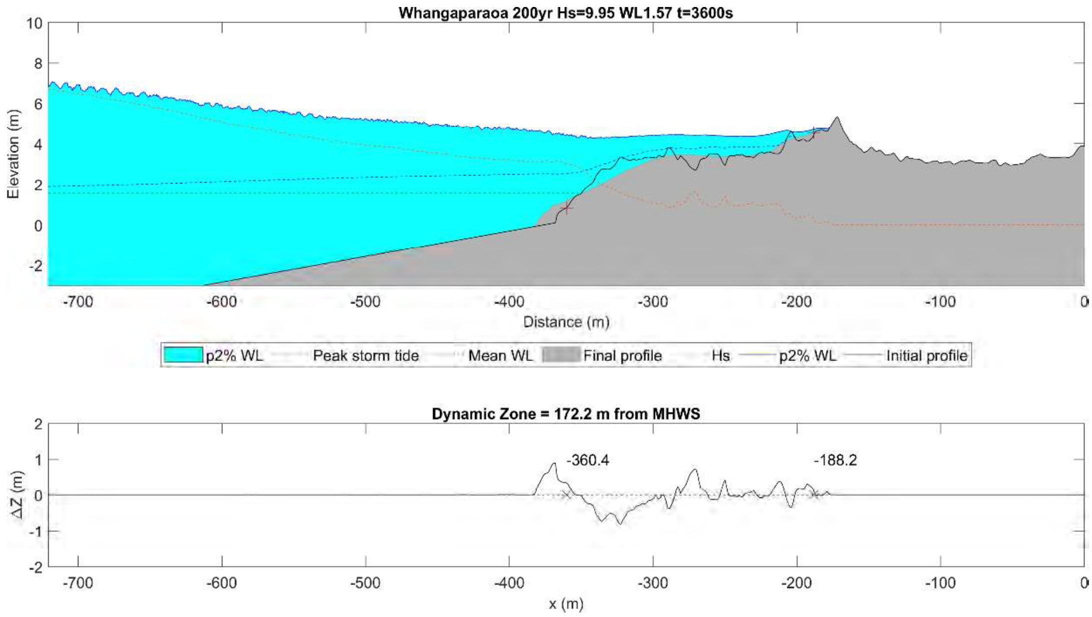

Appendix A.17: XBeach-G output showing the initial across-shore profile (black line) and final across shore profile (solid grey). The two percent exceeded water level (p2%WL) is presented (blue line) to highlight areas of flooding due to wave runup, and wave height and mean water level (influenced by wave setup). The difference between the initial and final profile is presented is presented in the lower panel and the morphodynamic zone from MHWS is identified by '+' markers in both plots.

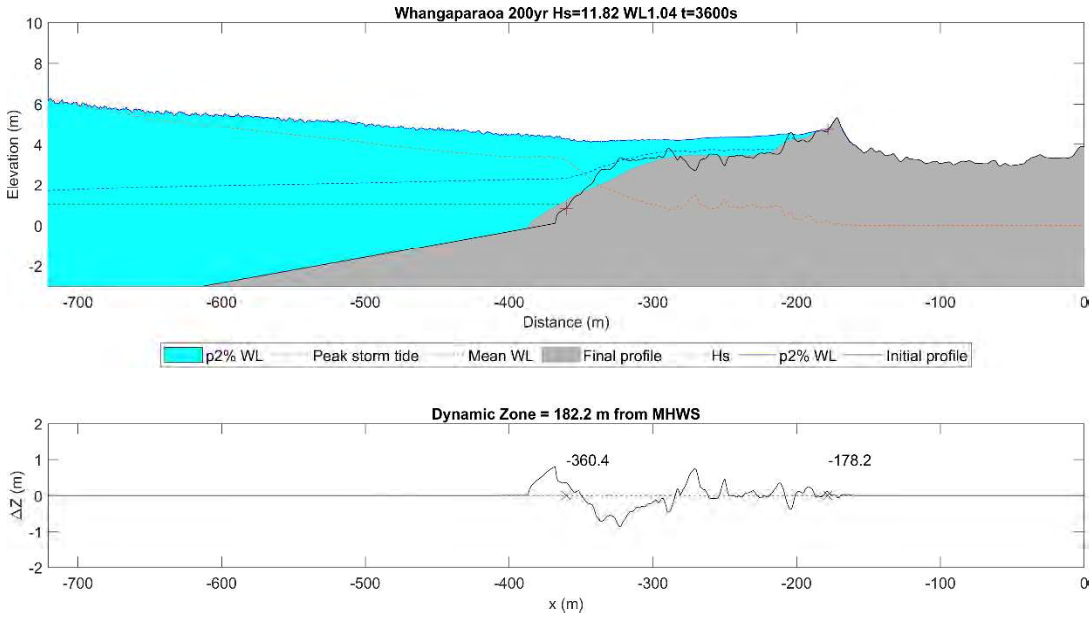

Appendix A.18: XBeach-G output showing the initial across-shore profile (black line) and final across shore profile (solid grey). The two percent exceeded water level (p2%WL) is presented (blue line) to highlight areas of flooding due to wave runup, and wave height and mean water level (influenced by wave setup). The difference between the initial and final profile is presented is presented in the lower panel and the morphodynamic zone from MHWS is identified by '+' markers in both plots.

15-Jul-20
p:\1008669\1008669.2000\workingmaterial\report\r20200429.memo_extremewl.docx

Appendix G: CEHA Histograms

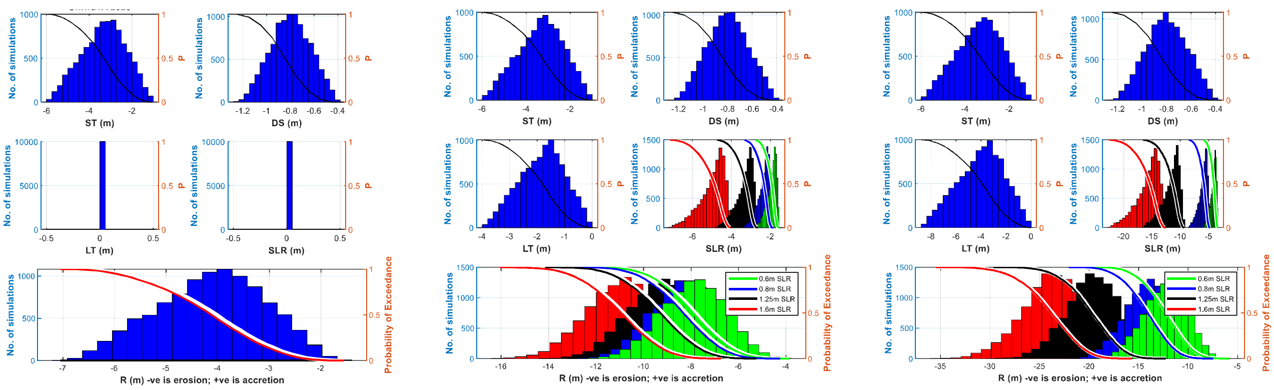

Figure G.1 Histograms and cumulative distribution functions of parameter samples and resultant CEHA distances for Cell 1A within the current, 2070 and 2130 timeframes

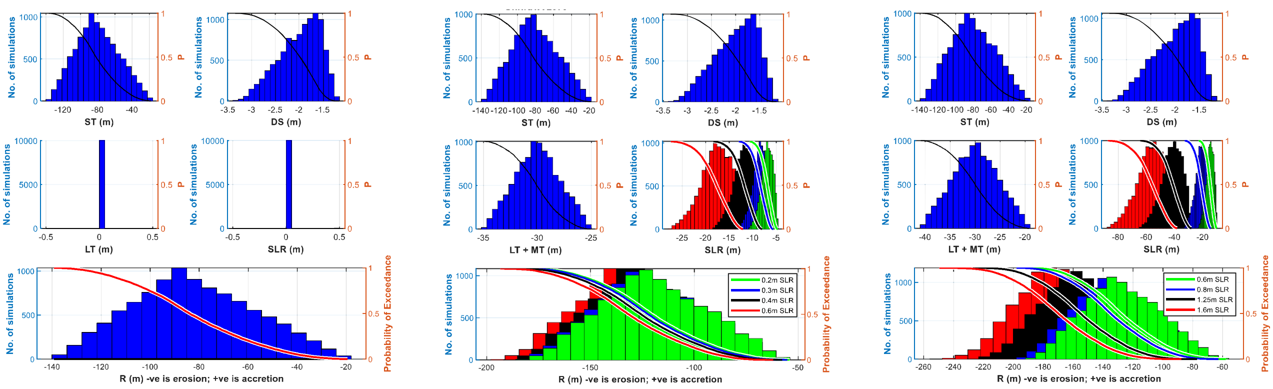

Figure G.2 Histograms and cumulative distribution functions of parameter samples and resultant CEHA distances for Cell 1B within the current, 2070 and 2130 timeframes

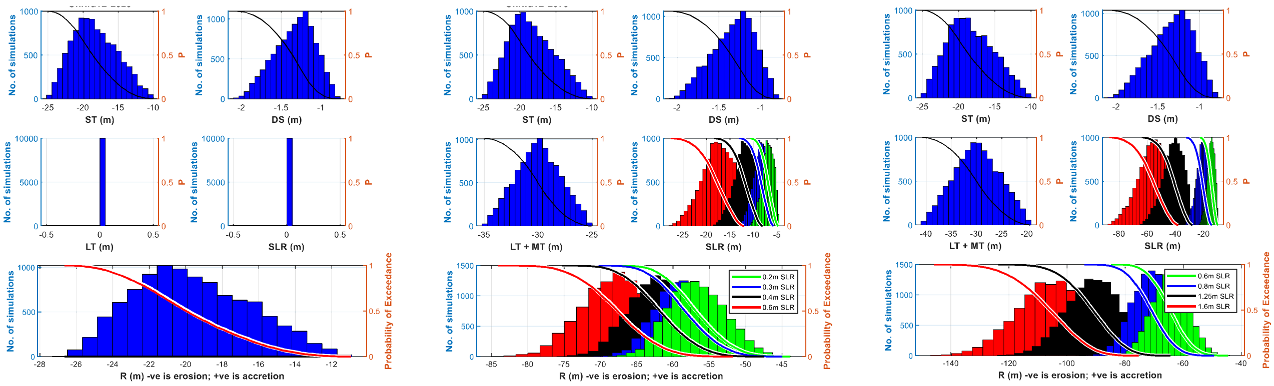

Figure G 3 Histograms and cumulative distribution functions of parameter samples and resultant CEHA distances for Cell 1C within the current, 2070 and 2130 timeframes

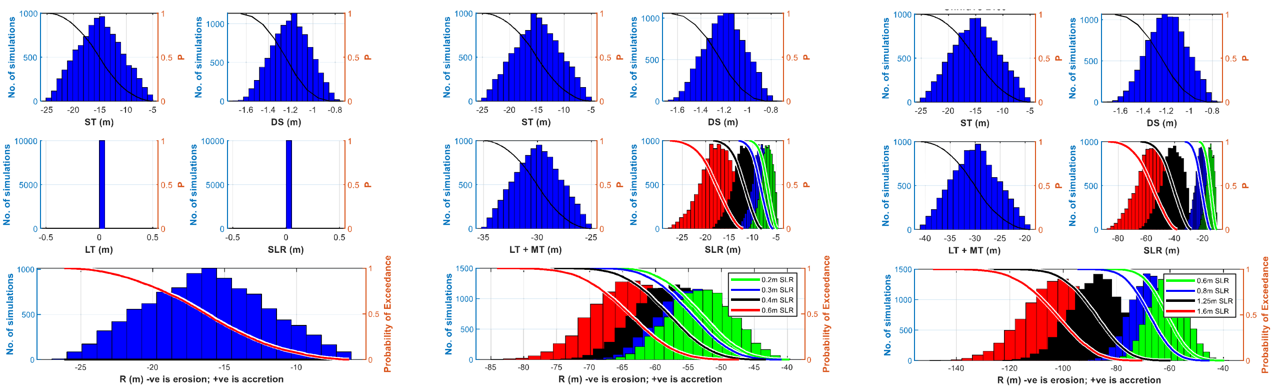

Figure G.4 Histograms and cumulative distribution functions of parameter samples and resultant CEHA distances for Cell 1D within the current, 2070 and 2130 timeframes

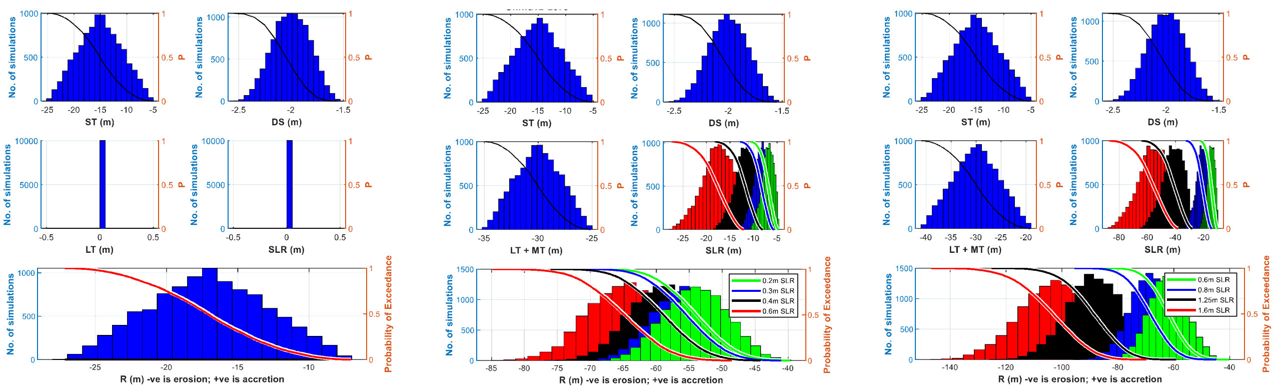

Figure G.5 Histograms and cumulative distribution functions of parameter samples and resultant CEHA distances for Cell 1E within the current, 2070 and 2130 timeframes

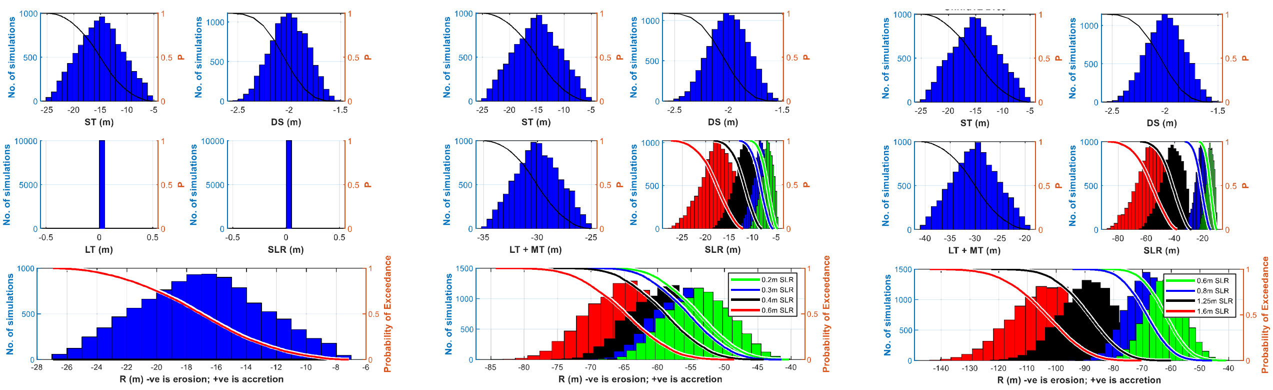

Figure G.6 Histograms and cumulative distribution functions of parameter samples and resultant CEHA distances for Cell 1F within the current, 2070 and 2130 timeframes

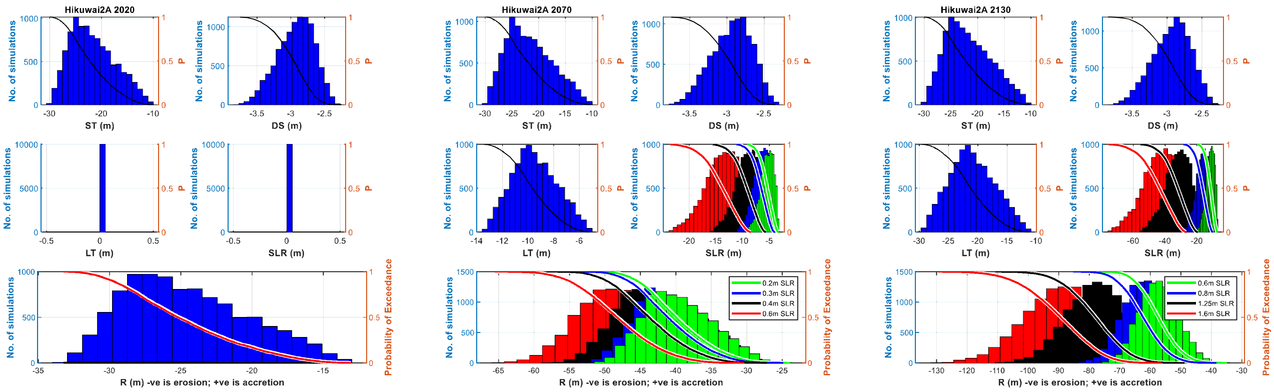

Figure G.7 Histograms and cumulative distribution functions of parameter samples and resultant CEHA distances for Cell 2A within the current, 2070 and 2130 timeframes

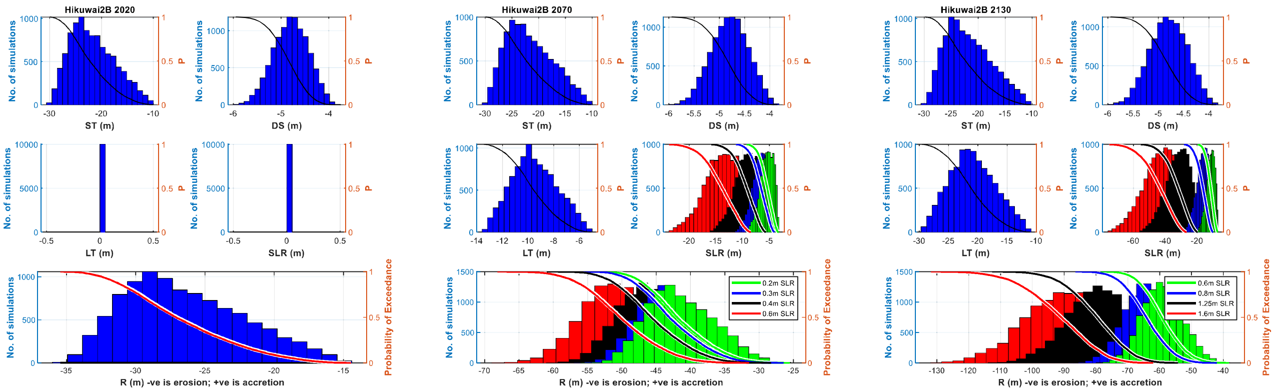

Figure G.8 Histograms and cumulative distribution functions of parameter samples and resultant CEHA distances for Cell 2B within the current, 2070 and 2130 timeframes

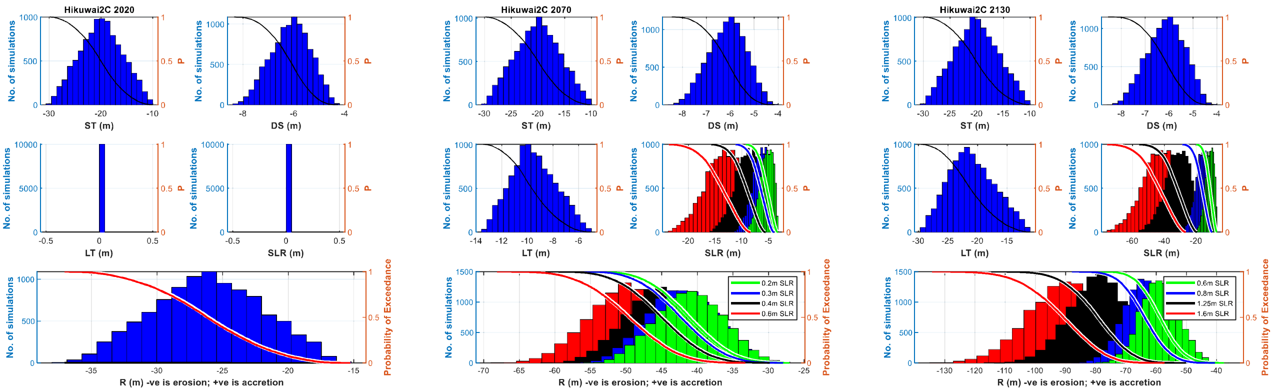

Figure G.9 Histograms and cumulative distribution functions of parameter samples and resultant CEHA distances for Cell 2C within the current, 2070 and 2130 timeframes

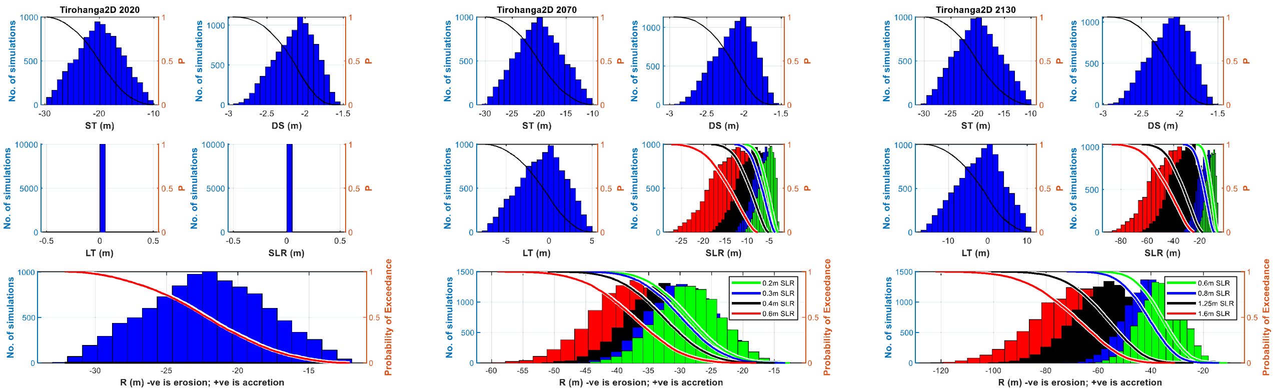

Figure G.10 Histograms and cumulative distribution functions of parameter samples and resultant CEHA distances for Cell 2D within the current, 2070 and 2130 timeframes

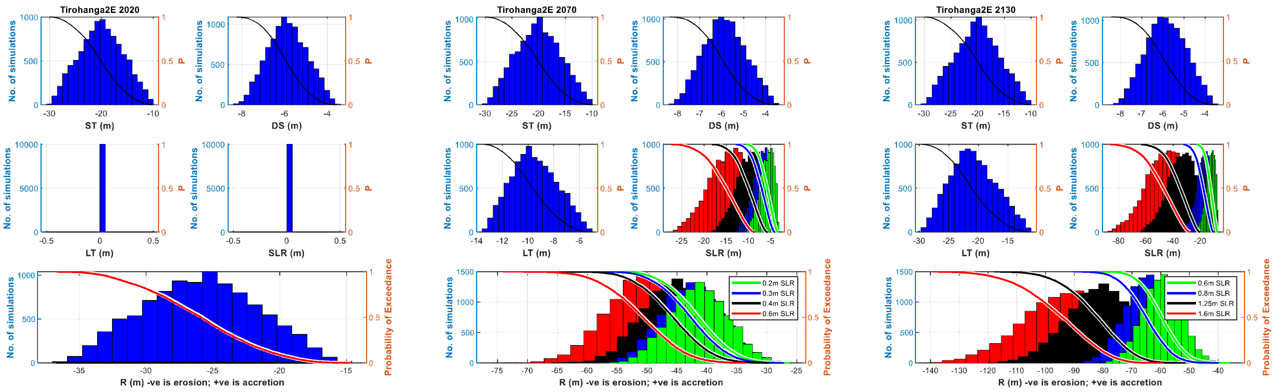

Figure G.11 Histograms and cumulative distribution functions of parameter samples and resultant CEHA distances for Cell 2E within the current, 2070 and 2130 timeframes

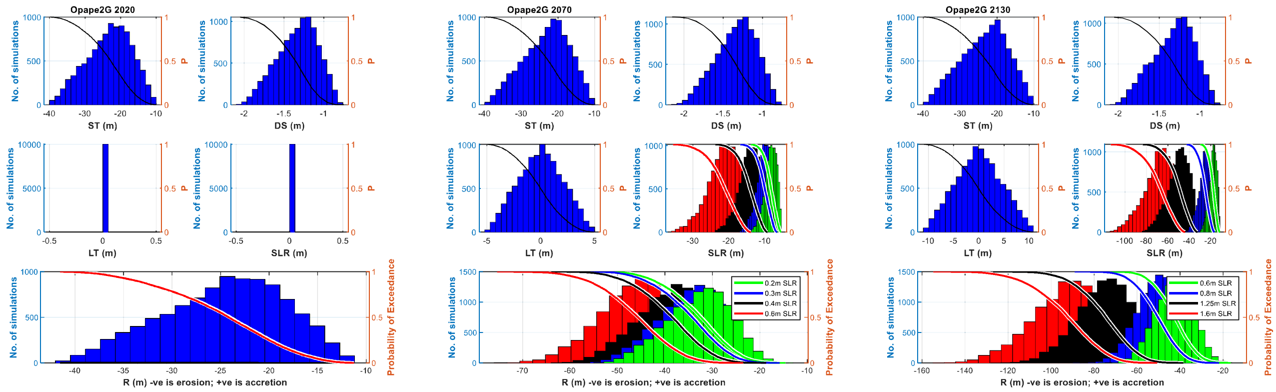

Figure G.12 Histograms and cumulative distribution functions of parameter samples and resultant CEHA distances for Cell 2G within the current, 2070 and 2130 timeframes

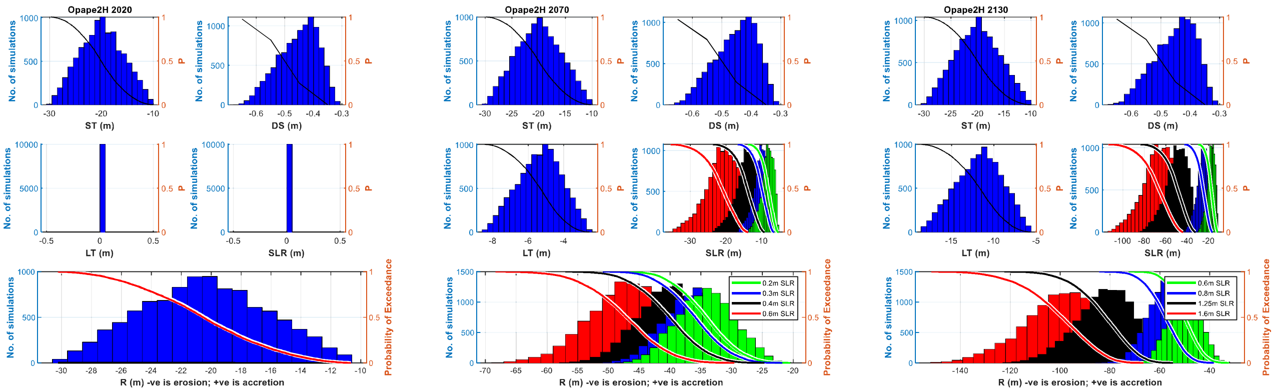

Figure G.13 Histograms and cumulative distribution functions of parameter samples and resultant CEHA distances for Cell 2H within the current, 2070 and 2130 timeframes

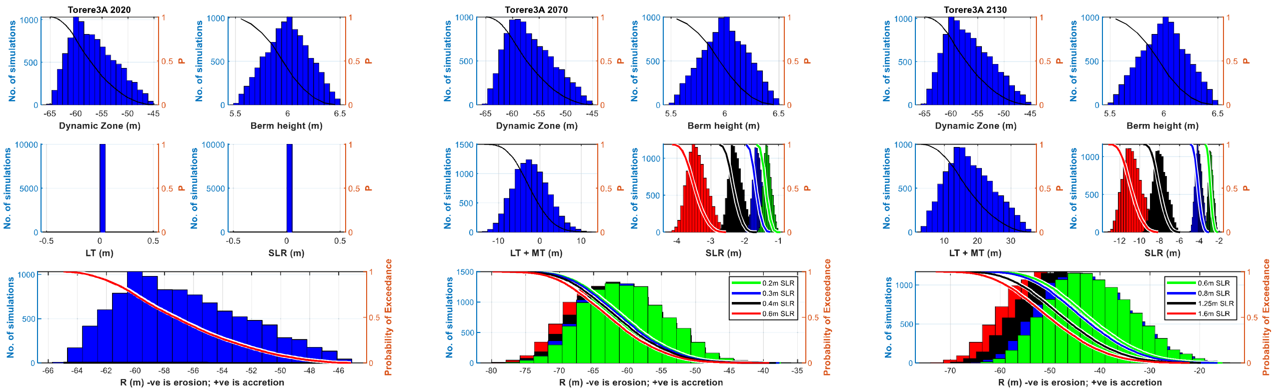

Figure G.14 Histograms and cumulative distribution functions of parameter samples and resultant CEHA distances for Cell 3A within the current, 2070 and 2130 timeframes

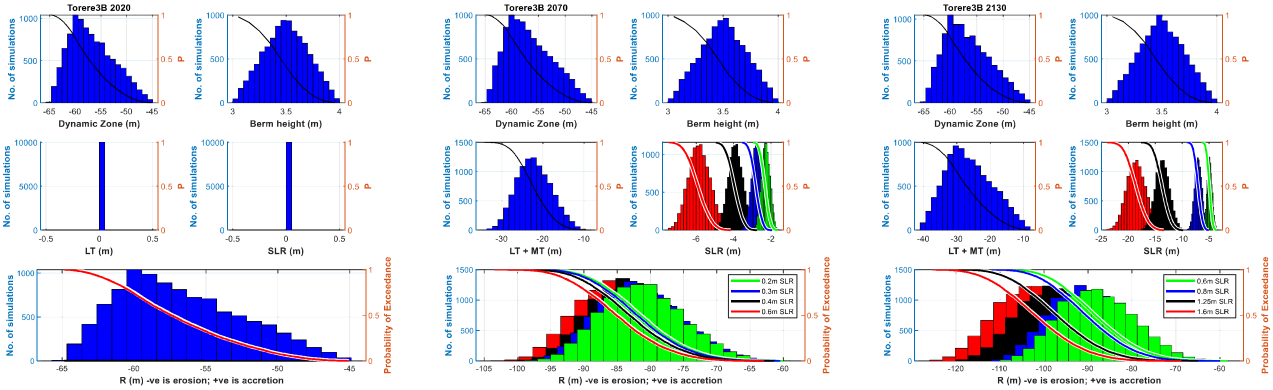

Figure G.15 Histograms and cumulative distribution functions of parameter samples and resultant CEHA distances for Cell 3B within the current, 2070 and 2130 timeframes

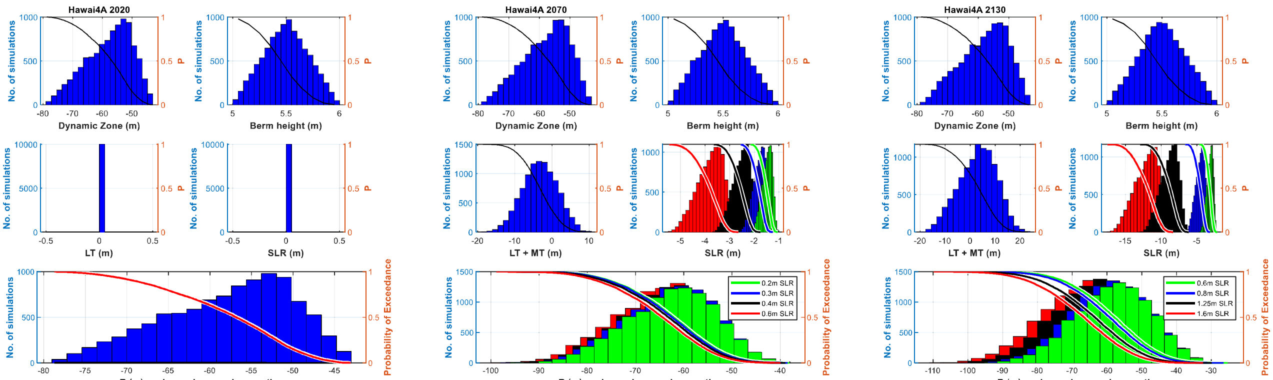

Figure G.16 Histograms and cumulative distribution functions of parameter samples and resultant CEHA distances for Cell 4A within the current, 2070 and 2130 timeframes

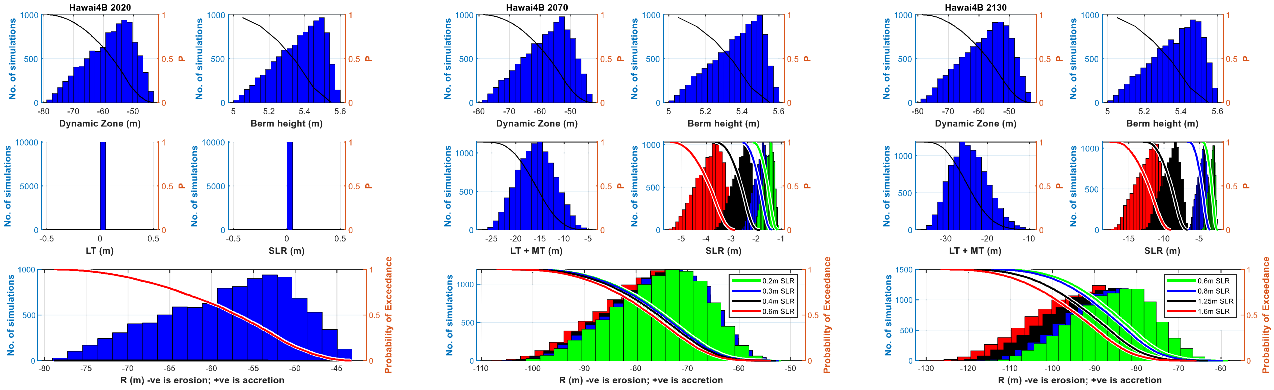

Figure G.17 Histograms and cumulative distribution functions of parameter samples and resultant CEHA distances for Cell 4B within the current, 2070 and 2130 timeframes

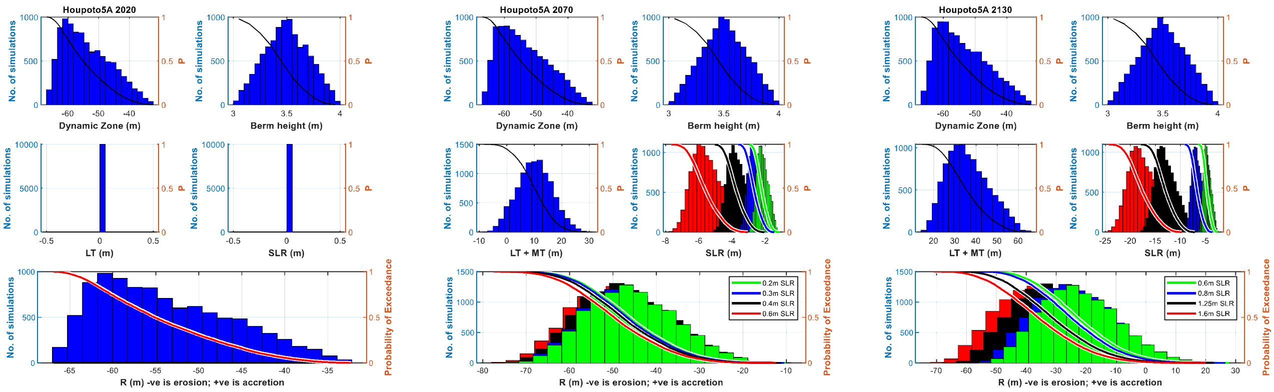

Figure G.18 Histograms and cumulative distribution functions of parameter samples and resultant CEHA distances for Cell 5A within the current, 2070 and 2130 timeframes

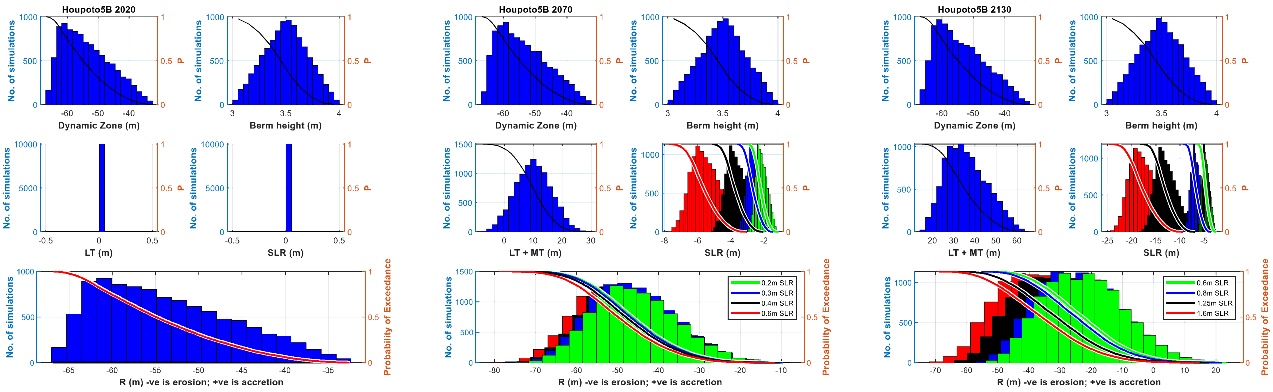

Figure G.19 Histograms and cumulative distribution functions of parameter samples and resultant CEHA distances for Cell 5B within the current, 2070 and 2130 timeframes

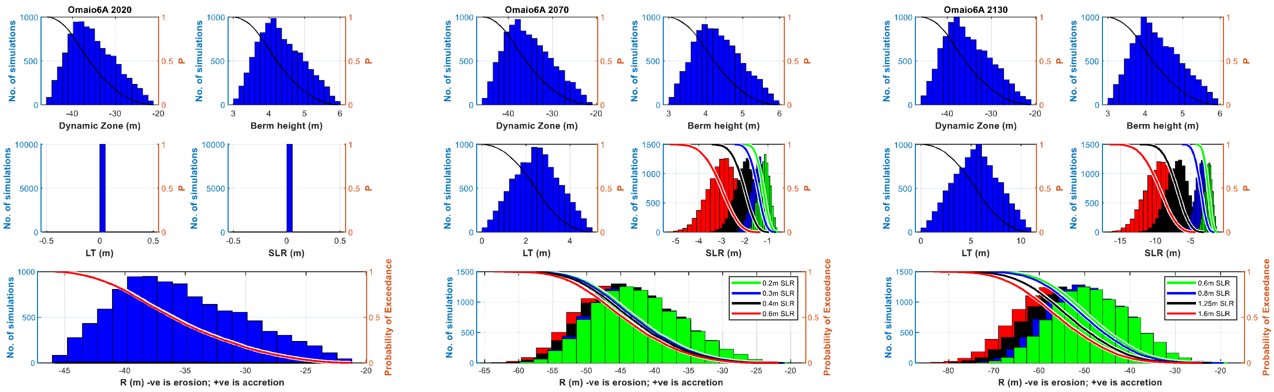

Figure G.20 Histograms and cumulative distribution functions of parameter samples and resultant CEHA distances for Cell 6A within the current, 2070 and 2130 timeframes

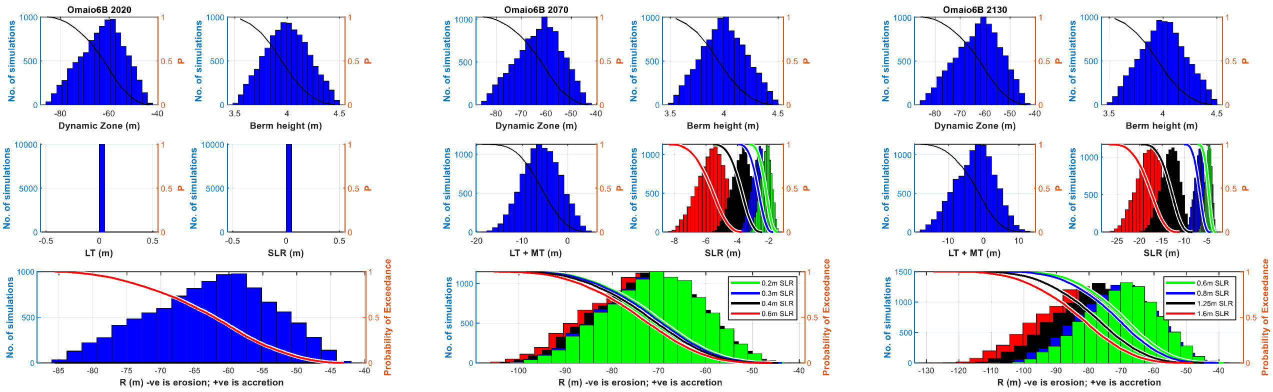

Figure G.21 Histograms and cumulative distribution functions of parameter samples and resultant CEHA distances for Cell 6B within the current, 2070 and 2130 timeframes

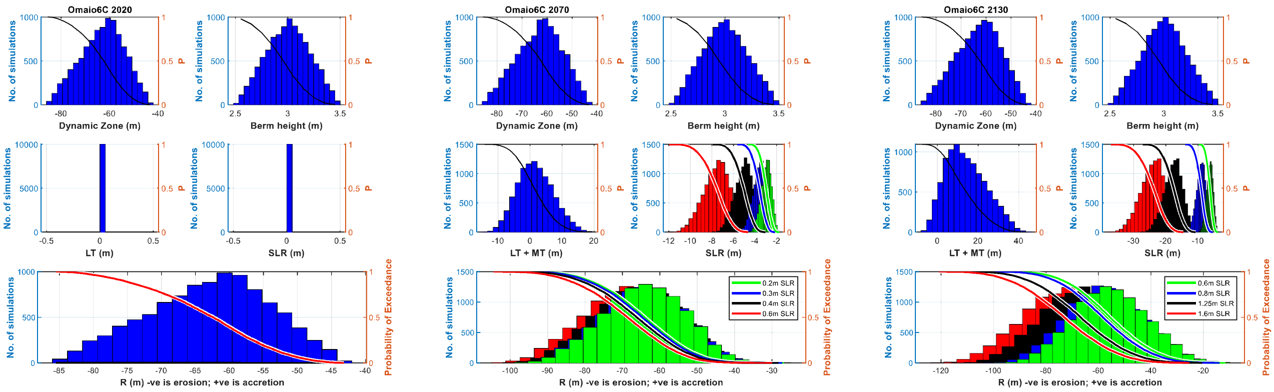

Figure G.22 Histograms and cumulative distribution functions of parameter samples and resultant CEHA distances for Cell 6C within the current, 2070 and 2130 timeframes

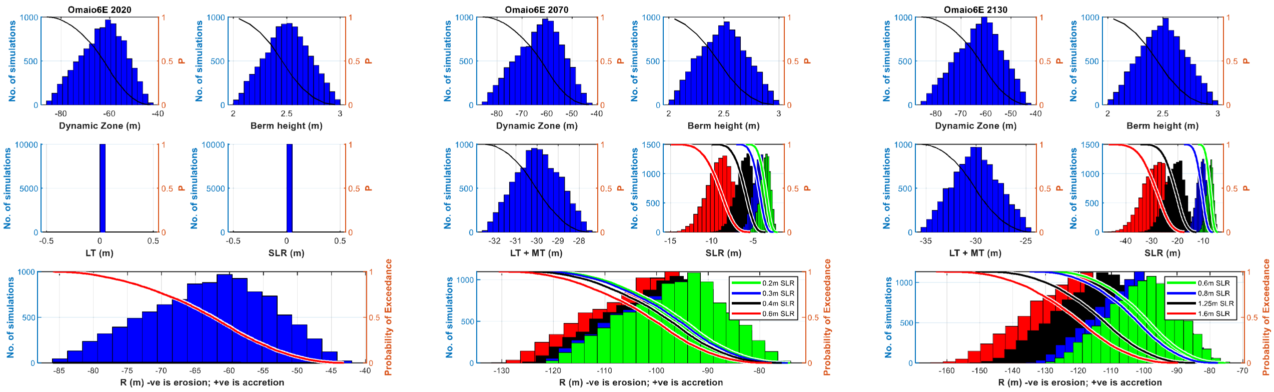

Figure G.23 Histograms and cumulative distribution functions of parameter samples and resultant CEHA distances for Cell 6E within the current, 2070 and 2130 timeframes

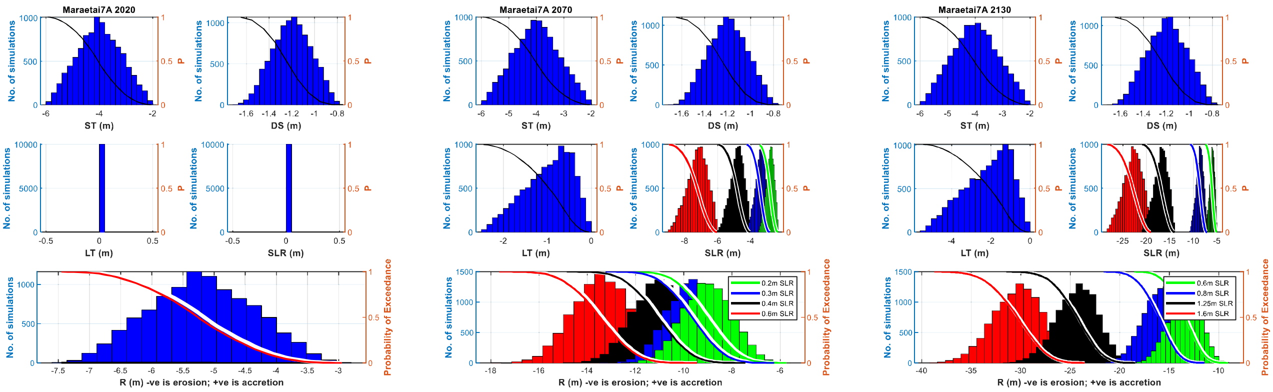

Figure G.24 Histograms and cumulative distribution functions of parameter samples and resultant CEHA distances for Cell 7A within the current, 2070 and 2130 timeframes

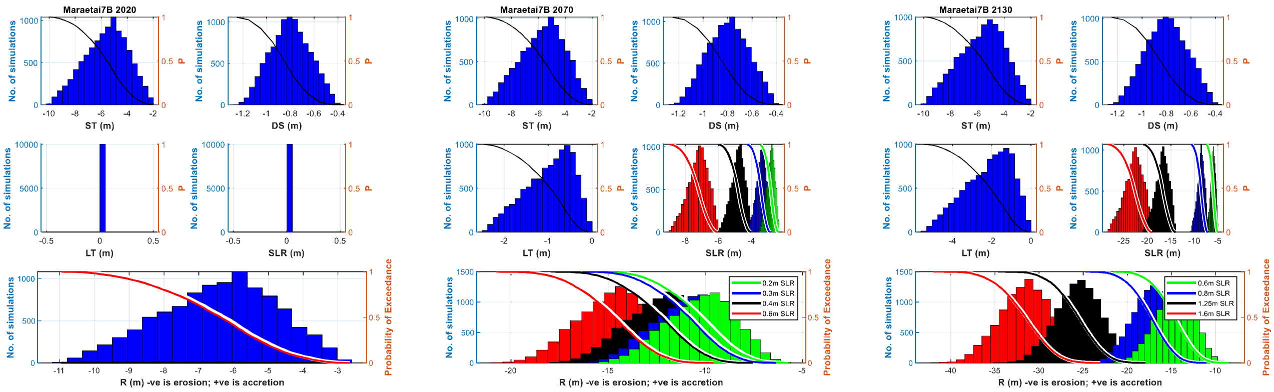

Figure G.25 Histograms and cumulative distribution functions of parameter samples and resultant CEHA distances for Cell 7B within the current, 2070 and 2130 timeframes

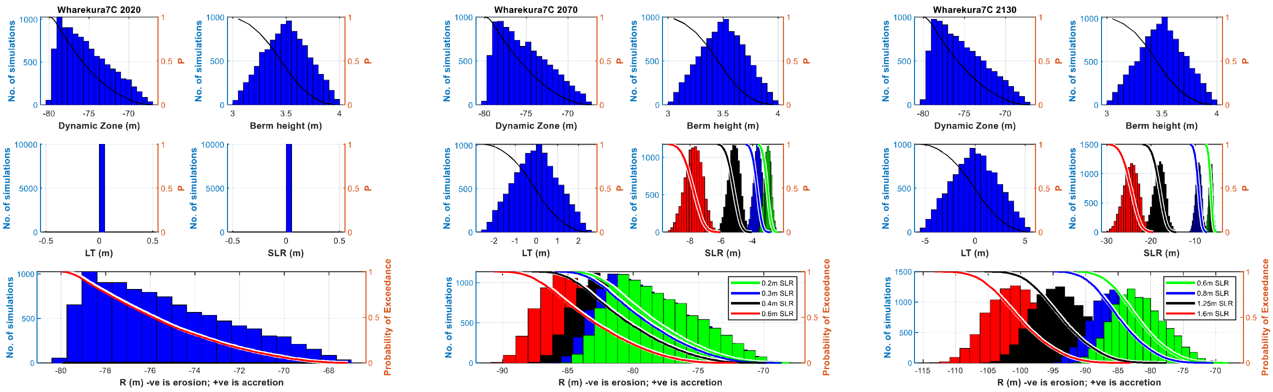

Figure G.26 Histograms and cumulative distribution functions of parameter samples and resultant CEHA distances for Cell 7C within the current, 2070 and 2130 timeframes

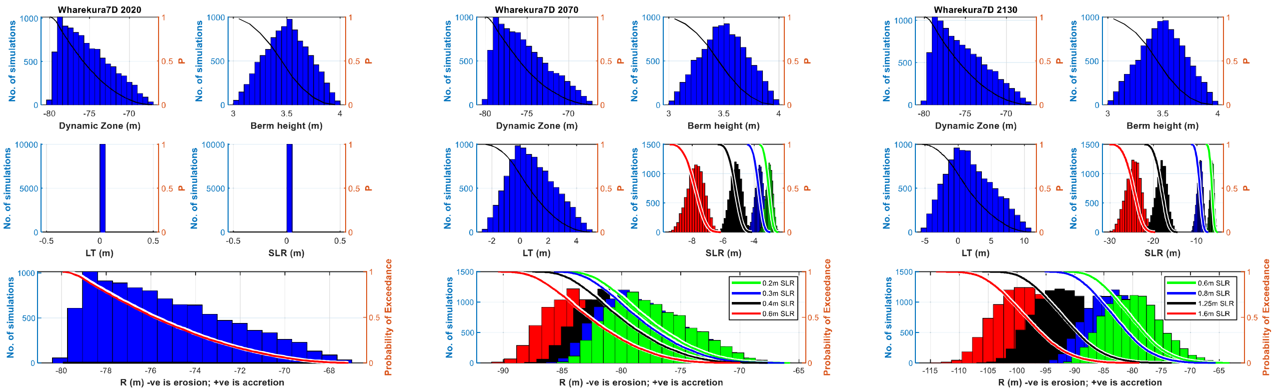

Figure G.27 Histograms and cumulative distribution functions of parameter samples and resultant CEHA distances for Cell 7D within the current, 2070 and 2130 timeframes

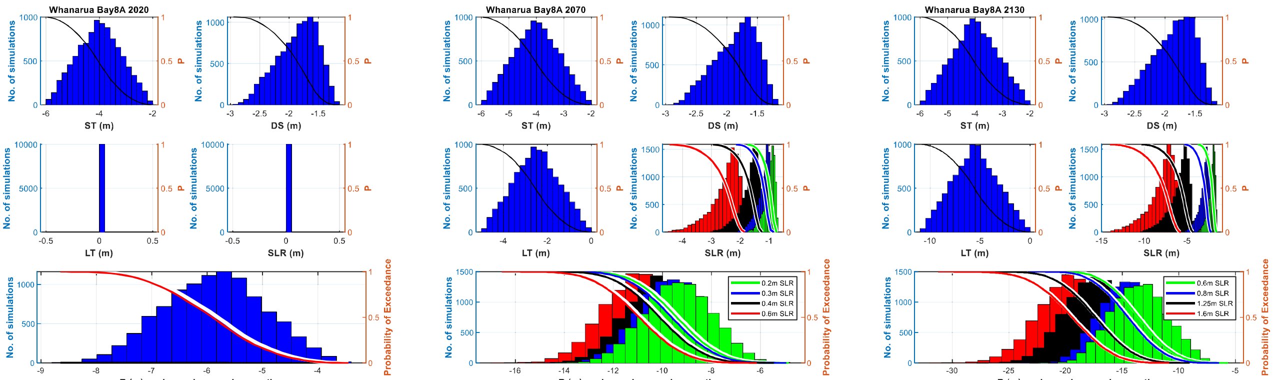

Figure G.28 Histograms and cumulative distribution functions of parameter samples and resultant CEHA distances for Cell 8A within the current, 2070 and 2130 timeframes

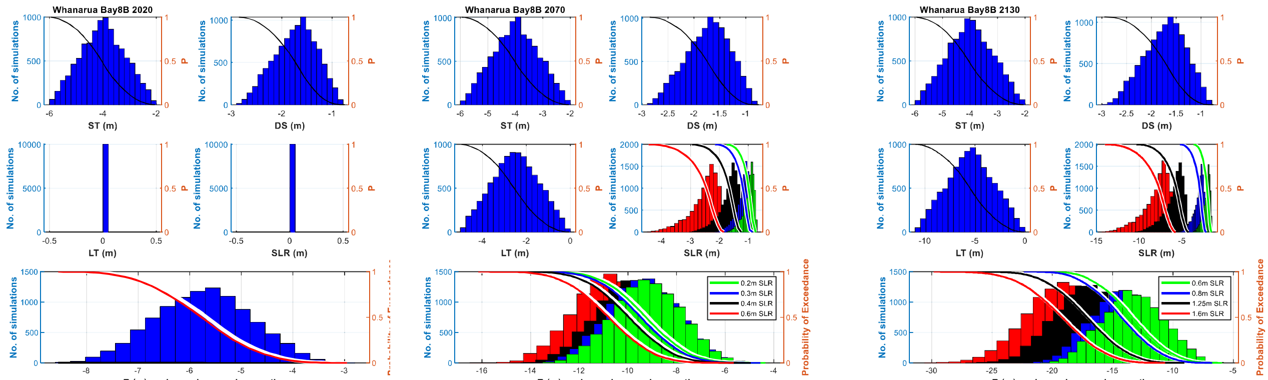

Figure G.29 Histograms and cumulative distribution functions of parameter samples and resultant CEHA distances for Cell 8B within the current, 2070 and 2130 timeframes

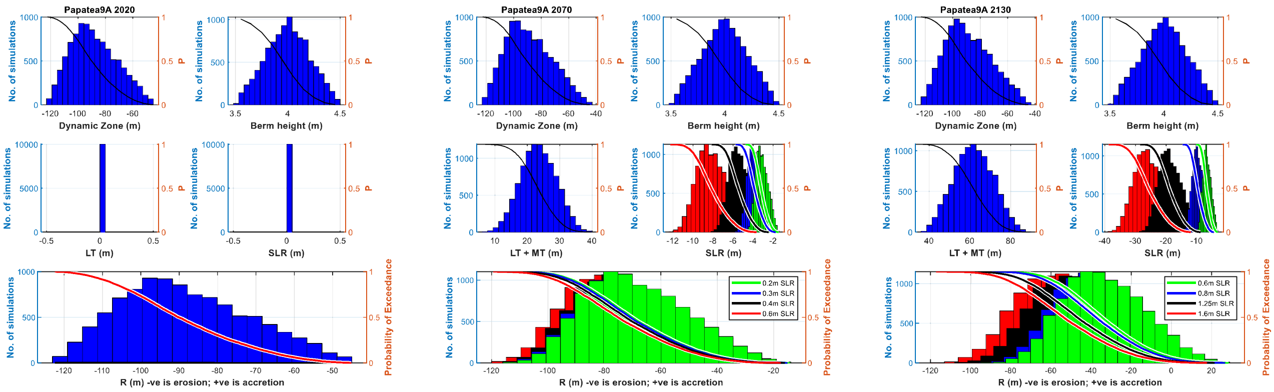

Figure G.30 Histograms and cumulative distribution functions of parameter samples and resultant CEHA distances for Cell 9A within the current, 2070 and 2130 timeframes

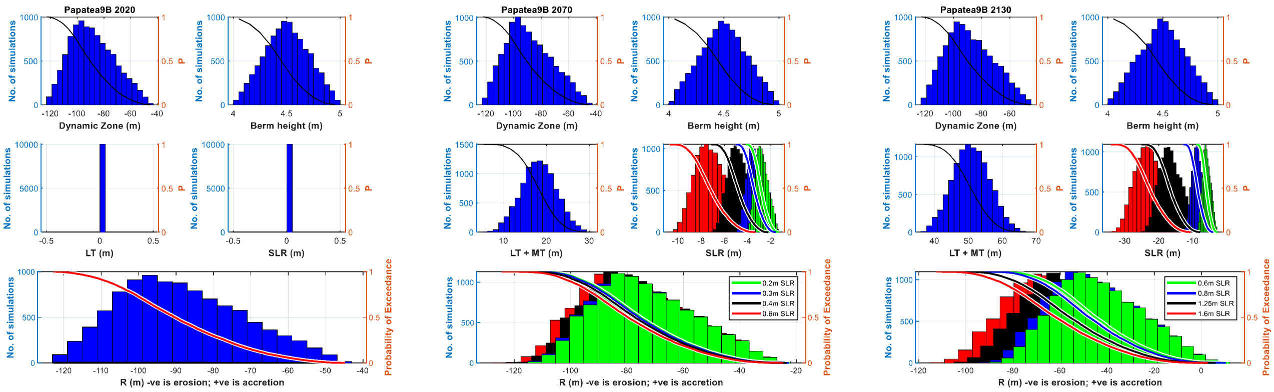

Figure G.31 Histograms and cumulative distribution functions of parameter samples and resultant CEHA distances for Cell 9B within the current, 2070 and 2130 timeframes

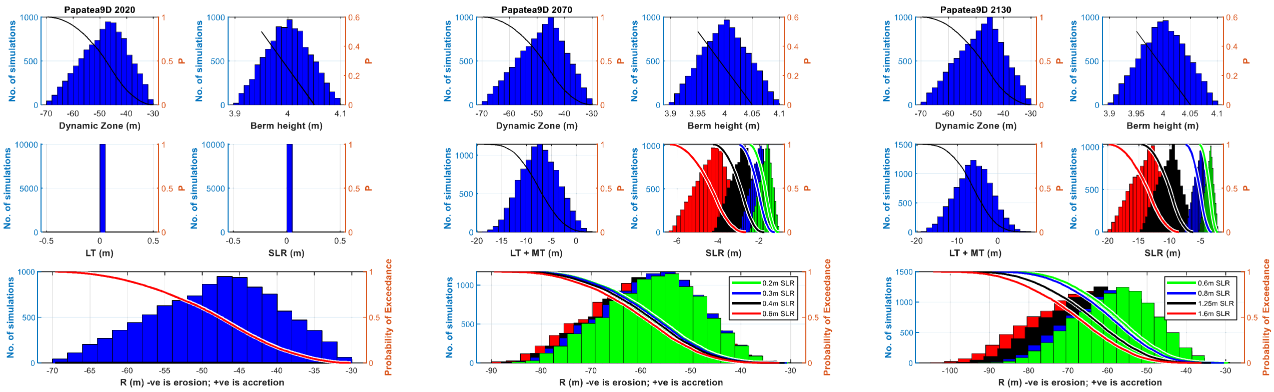

Figure G.32 Histograms and cumulative distribution functions of parameter samples and resultant CEHA distances for Cell 9D within the current, 2070 and 2130 timeframes

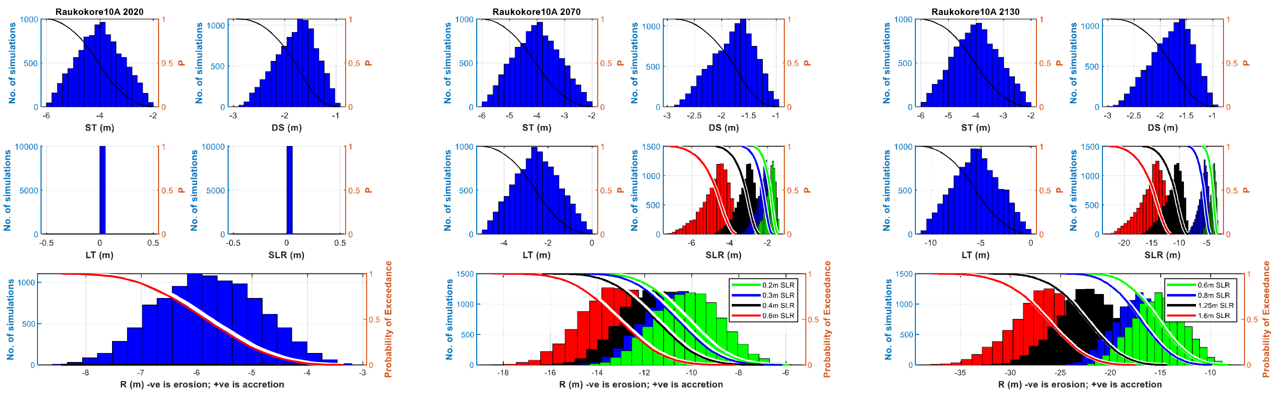

Figure G.33 Histograms and cumulative distribution functions of parameter samples and resultant CEHA distances for Cell 10A within the current, 2070 and 2130 timeframes

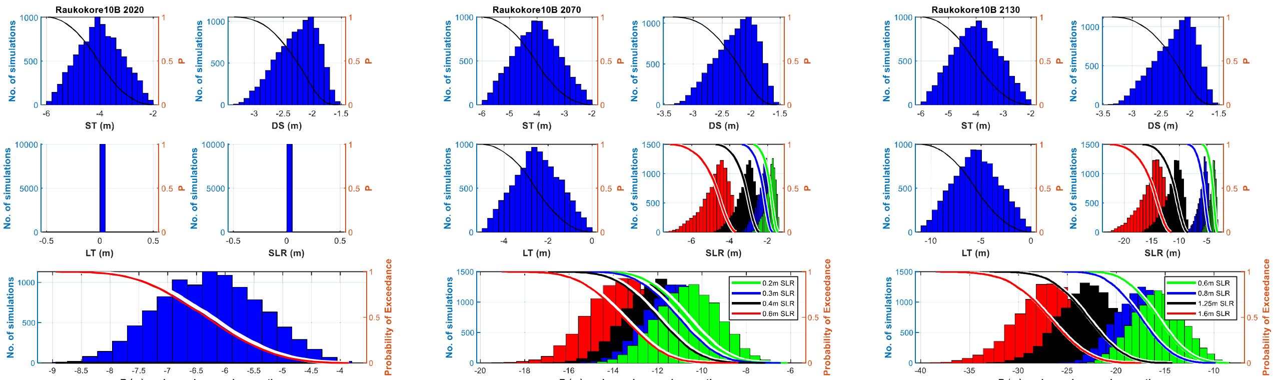

Figure G.34 Histograms and cumulative distribution functions of parameter samples and resultant CEHA distances for Cell 10B within the current, 2070 and 2130 timeframes

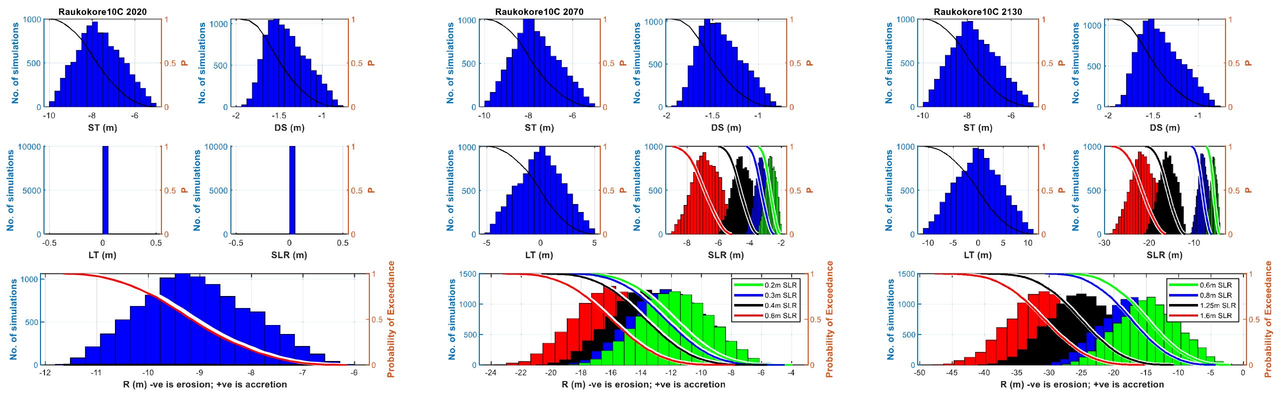

V

Figure G.35 Histograms and cumulative distribution functions of parameter samples and resultant CEHA distances for Cell 10C within the current, 2070 and 2130 timeframes

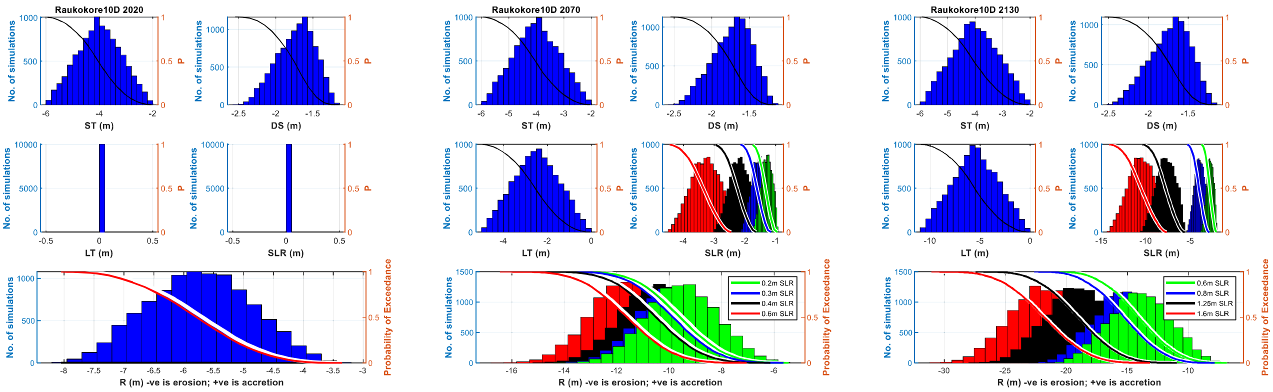

Figure G.36 Histograms and cumulative distribution functions of parameter samples and resultant CEHA distances for Cell 10D within the current, 2070 and 2130 timeframes

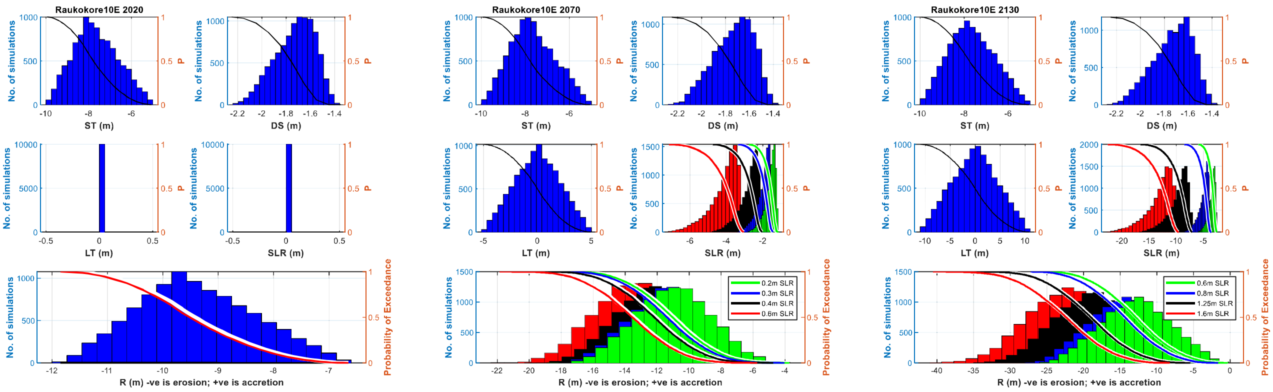

Figure G.37 Histograms and cumulative distribution functions of parameter samples and resultant CEHA distances for Cell 10E within the current, 2070 and 2130 timeframes

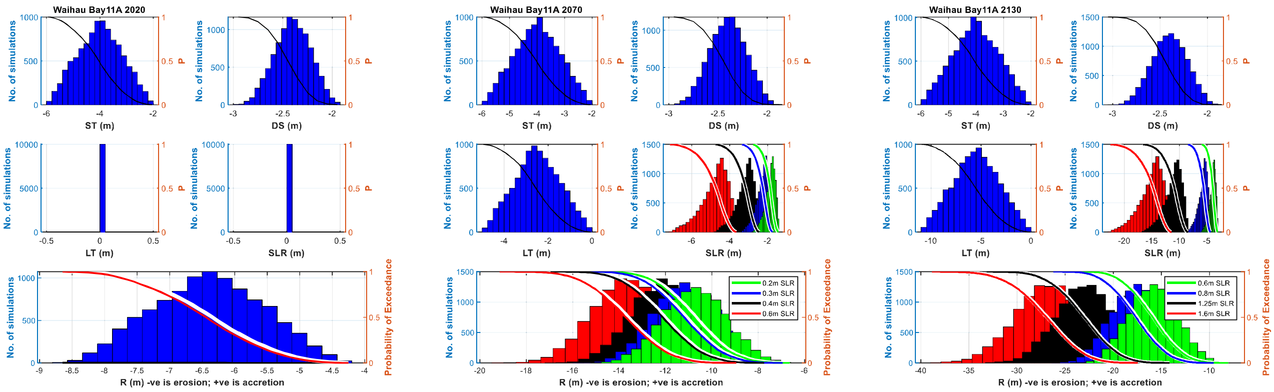

Figure G.38 Histograms and cumulative distribution functions of parameter samples and resultant CEHA distances for Cell 11A within the current, 2070 and 2130 timeframes

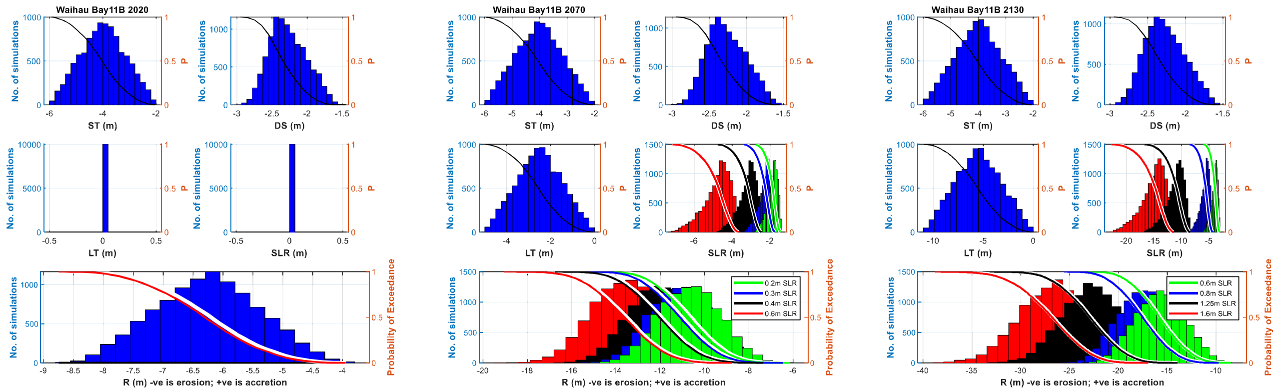

Figure G.39 Histograms and cumulative distribution functions of parameter samples and resultant CEHA distances for Cell 11B within the current, 2070 and 2130 timeframes

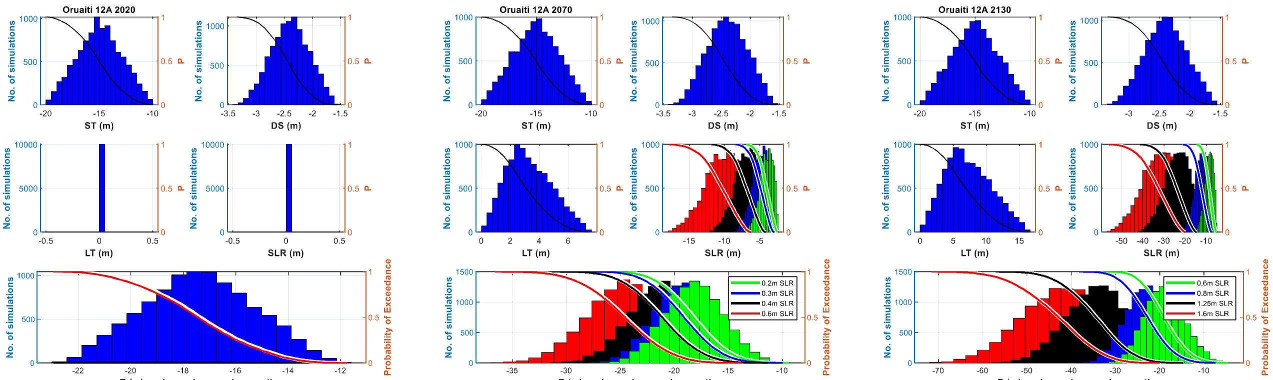

Figure G.40 Histograms and cumulative distribution functions of parameter samples and resultant CEHA distances for Cell 12A within the current, 2070 and 2130 timeframes

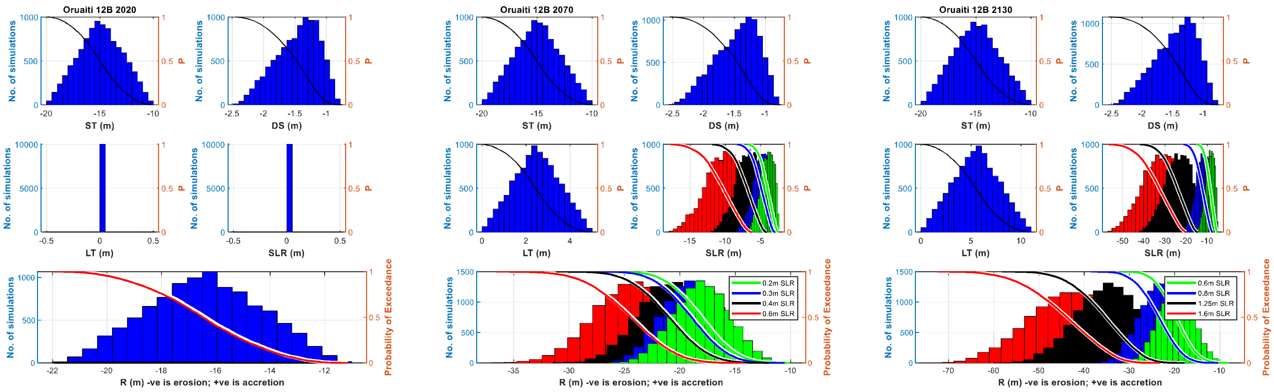

Figure G.41 Histograms and cumulative distribution functions of parameter samples and resultant CEHA distances for Cell 12B within the current, 2070 and 2130 timeframes

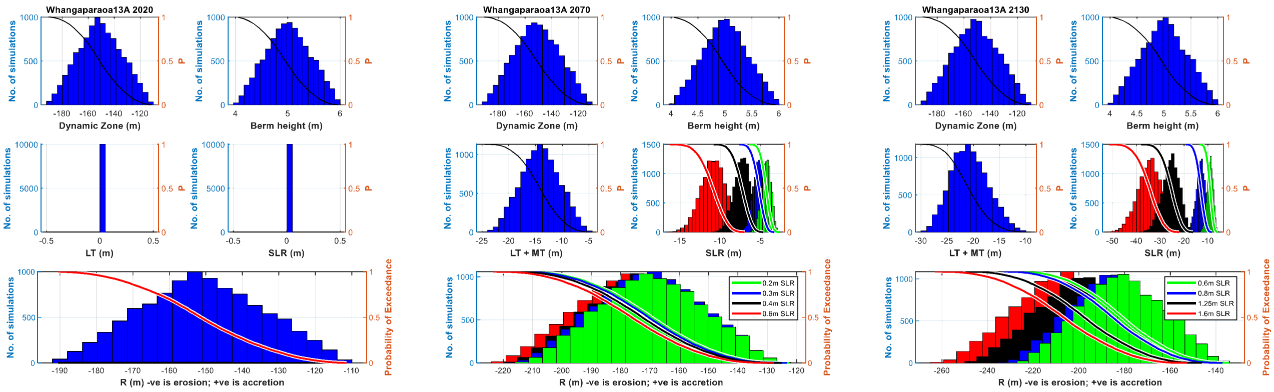

Figure G.42 Histograms and cumulative distribution functions of parameter samples and resultant CEHA distances for Cell 13A within the current, 2070 and 2130 timeframes

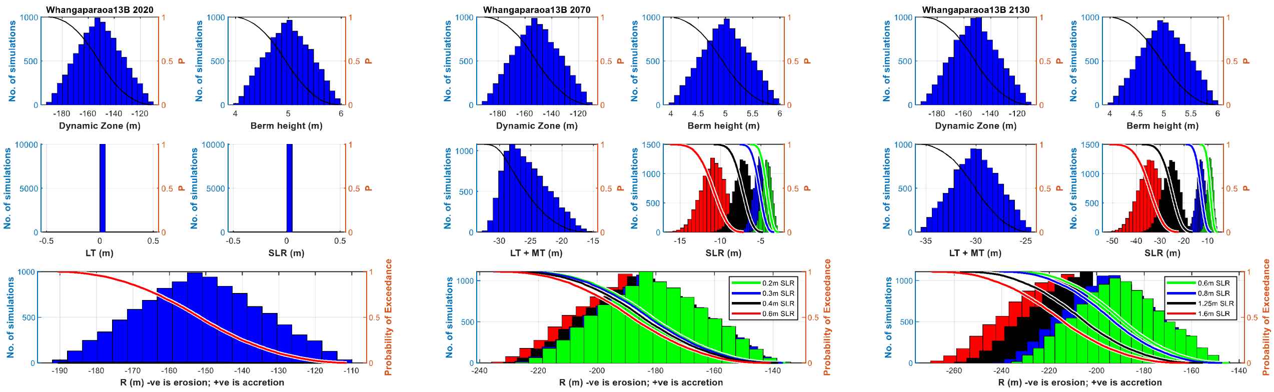

Figure G.43 Histograms and cumulative distribution functions of parameter samples and resultant CEHA distances for Cell 13B within the current, 2070 and 2130 timeframes